NUMERICAL STUDY ON THE INFLUENCE OF SUBTERRANEAN LEVELS ON THE SEISMIC RESPONSE CHARACTERISTICS OF BUILDING FRAMES

Submitted in partial fulfilment of the requirements for the award of the degree of

DOCTOR OF PHILOSOPHY

in

CIVIL ENGINEERING

by

ZELEKE LULAYEHU TADESSE

(Roll No: 719128)

Supervisor

Dr. P. HARI KRISHNA

Professor

GEOTECHNICAL ENGINEERING DIVISION

DEPARTMENT OF CIVIL ENGINEERING

NATIONAL INSTITUTE OF TECHNOLOGY

WARANGAL - 506 004 (T.S.) INDIA

AUGUST – 2023

NATIONAL INSTITUTE OF TECHNOLOGY

WARANGAL

CERTIFICATE

This is to certify that the thesis entitled "**NUMERICAL STUDY ON THE INFLUENCE OF SUBTERRANEAN LEVELS ON THE SEISMIC RESPONSE CHARACTERISTICS OF BUILDING FRAMES**" being submitted by **Mr. ZELEKE LULAYEHU TADESSE** for the award of the degree of **DOCTOR OF PHILOSOPHY** to the Faculty of Engineering and Technology of **NATIONAL INSTITUTE OF TECHNOLOGY, WARANGAL** is a record of bonafide research work carried out by him under my supervision and it has not been submitted elsewhere for the award of any degree.

Dr. P. Hari Krishna

Professor

Thesis Supervisor

Department of Civil Engineering

National Institute of Technology

Warangal (T.S.) - INDIA

APPROVAL SHEET

This Thesis entitled "**NUMERICAL STUDY ON THE INFLUENCE OF SUBTERRANEAN LEVELS ON THE SEISMIC RESPONSE CHARACTERISTICS OF BUILDING FRAMES**" by **Mr. Zeleke Lulayehu Tadesse** is approved for the degree of Doctor of Philosophy.

Examiners

_____

_____

_____

Supervisor

_____

Chairman

_____

Date: _____

DECLARATION

This is to certify that the work presented in the thesis entitled "**NUMERICAL STUDY ON THE INFLUENCE OF SUBTERRANEAN LEVELS ON THE SEISMIC RESPONSE CHARACTERISTICS OF BUILDING FRAMES**" is a bonafide work done by me under the supervision of **Prof. P. Hari Krishna** and was not submitted elsewhere for the award of any degree. I declare that this written submission represents my ideas in my own works and where others' ideas or words have been included, I have adequately cited and referenced the original sources. I also declare that I have adhered to all principles of academic honesty and integrity and have not misrepresented or fabricated or falsified any idea/data/fact/source in my submission. I understand that any violation of the above will be a cause for disciplinary action by the Institute and can also evoke penal action from the sources which have thus not been properly cited or from whom proper permission has not been taken when needed.

_____

(**ZELEKE LULAYEHU TADESSE**)

(Roll no: **719128**)

Date:

Dedication

This thesis is dedicated to my parents for their love, support, and encouragement.

ACKNOWLEDGEMENTS

The completion of the research in this thesis would not have been possible without the support of many individuals to whom I would like to express my sincere gratitude.

First and foremost, I would like to express my deep sense of gratitude to my thesis supervisor **Dr. P. Hari Krishna**, Professor, Department of Civil Engineering for his continuous monitoring, moral support, encouragement, and timely input throughout my research work. His commitment to research work is always been a source of inspiration for the rest of my life.

I would like to extend my gratitude to my Doctoral Scrutiny Committee: Chairman **Dr. G. Rajesh Kumar**, Professor, Department of Civil Engineering, and members **Dr. P. Rathish Kumar**, Professor, Department of Civil Engineering, **Dr. V. Ramana Murty**, Professor, Department of Civil Engineering, **Dr. T D Gunneswara Rao**, Professor and Head, Department of Civil Engineering, and **Dr. A. Venu Gopal**, Professor, Department of Mechanical Engineering for their continuous monitoring, keen interest, insightful comments, and encouragement.

I am also thankful to **Dr. G Kalyan Kumar**, **Dr. M. Heeralal**, **Dr. Arif Ali Baig Moghal**, and **Dr. G. V. Ramana**, the faculty members of the Department of Civil Engineering, NITW for the moral support given during the period of research work.

I wish to express my sincere thanks to **Dr. Venkata R. P. Koteswara**, Associate professor, Department of Civil Engineering, Vardhaman College of Engineering, Hyderabad, for offering me inspirational discussions, helpful comments, and thoughtful advice during the research.

I would like to thank all my friends and colleagues for their constant support in both my life and research. I gratefully acknowledge the financial support provided by the **Government of the Federal Democratic Republic of Ethiopia**.

A very special debt of deep gratitude is offered to my parents. Their love and support provided me with the energy to attain my study.

Finally, I thank everyone, who contributed either directly or indirectly to the successful completion of this work.

- Zeleke Lulayehu Tadesse

ABSTRACT

The seismic interaction of the structures with compliant soil has been the subject of various experimental and numerical studies assuming the elastic or inelastic behavior of both structure and foundation soil. These coupled interactions are complex and significantly important in understanding and interpreting the real performance. The seismic performance of building structures is often influenced by the interaction between various integrated components such as superstructure, foundation, subterranean levels, and the supporting and surrounding soil deposit with the effects of dynamic filtering, which is widely referred to in the literature as soil-structure interaction (SSI). The seismic SSI analysis can be helpful in realistically predict the deformation characteristics, seismic response force demand, and the behaviour of the entire system by incorporating the soil strata as a single integral compatible structural component.

Many studies have been carried out in recent decades with a strong emphasis on seismic SSI. Most investigations to far have focused on buildings with shallow and deep foundations, including piles. Because of fast urbanization or infrastructural growth, as well as a lack of space in cities, the majority of buildings in metropolitan areas are often planned with one or more subterranean levels for parking and other amenities. Very limited experimental and numerical studies have been presented on the building frame with subterranean levels. However, numerous issues remain concerning the effects of the subterranean levels on the design and seismic response parameters of multi-storey buildings. In the present study, several novel objectives are identified and investigated.

(1) to evaluate the influence of subterranean levels on foundation input motion (FIM); (2) to appraise the applicability of theoretical solutions to predict the FIM in comparison to the nonlinear numerical model incorporating the kinematic SSI effect; (3) assess the influence of different modeling approaches and subterranean levels on the seismic response history analysis of the superstructure; and (4) investigate the effect of subterranean levels and their embedment depth on the seismic response of building frame considering SSI. As a result, to effectively address these issues, realistic numerical models are developed and used in a practical manner. These models encompass a wide range of soil types and soil-structure system (SSS) under the influence of various earthquake ground motions.

A 15-storey medium-rise reinforced concrete moment resisting frame (RC-MRF) building with subterranean levels resting on a raft foundation was adopted as a reference for various investigations in the present study. Three deep homogenous subsoil conditions underlain by bedrock were adopted: soil types C, D, and E, denoting dense, medium, and soft soil deposits, respectively. Three alternative base conditions, five different models, and seven earthquake input motions have been considered. The comprehensive numerical studies was conducted utilizing the finite element method (FEM) by ABAQUS software to address the above-mentioned issues. Several indicators for both soil and structural response are established in terms of response spectral acceleration, transfer functions with respect to free-field motion (FFM), and seismic response demands such as lateral displacements and drifts. According to the investigation conducted in the present study, the major findings are given below.

From the numerical analyses, there is in general a reduction of the motion at the subterranean level of a building as the subterranean level depth increases, whereas in contrast more intense than the FFM revealed especially at lower periods and for profounder depths of embedment, predominantly in soil type E (soft soil). Similarly, the effect of soil properties on foundation input motion (FIM) exhibits the same characteristics as the stiffness of the soil properties decreases from medium-dense to soft soil. These results demonstrate clearly how the embedded stiff subterranean level existence in different subsoil conditions causes the high frequencies to be filtered or the reduction of FIM with respect to FFM.

The applicability range of theoretical transfer function models was also compared with numerical model results. The models properly anticipate a constant transfer function value for higher periods, which is consistent with the numerical analyses, whereas the divergence is more significant, especially within a small time range. Variations between analytical and numerical transfer function models could also be due to the underlying assumptions applied to build theoretical models. It can be seen that the numerical models can estimate more consistently taking into account the effects of embedment depths and soil nonlinearity. Nevertheless, the analytical models fail to account for certain crucial features such as subterranean levels flexibility, nonlinear behavior of soil deposit, and frequency-dependent amplification of foundation level motion relative to the FFM.

From the major findings of the numerical investigations in the present work, the interaction between the superstructure, subterranean levels, foundation, and subsoil conditions plays a substantial role in altering the seismic response behavior of the building. It is observed that the superstructure seismic response demands in terms of storey level relative lateral displacement and inter-storey drift ratio (DR) values are intensified when incorporating the subterranean levels and SSI, as well as due to the variation of soil density. The influence is more considerable predominantly in the case of flexible-base models resting in medium and soft soil. On the other hand, generally, when the embedment depth of the subterranean levels increases the storey level lateral displacements and DR values are decreased.

Based on the undertaken investigations, it can be concluded that the nonlinear seismic design of an RC-MRF building structure excluding the substructure level and SSI is not adequate to assure structural safety. Also, various modeling strategies often used for the analysis of the seismic response of building structures considerably alter the seismic response characteristic and demand of the superstructure. Although building codes used simplified procedures where the base of the superstructure at the ground surface is assumed to be fixed and the analysis is carried out under the influence of FFM, may often be correct enough. According to the investigation in this study, however, the incorporation of the influence of subterranean levels and seismic SSI is required to predict accurately the seismic response characteristics and demands of the superstructure with great rigor, especially the building structure resting on medium and soft soil deposits with shallow embedment depths.

Table of Contents

List of Figures

List of Tables

Nomenclature

The following list gives the notations used in chapters of the thesis

Roman Symbols

a_0	dimensionless circular frequency
A	foundation area
B	width of foundation
c	viscous damping coefficient
D	foundation embedment depth
E_c	modulus of elasticity of concrete
f_{ck}	characteristic compressive strength of concrete
f_{max}	maximum frequency
G	shear modulus
G_{cyc}	cyclic shear modulus
G_{max}	shear modulus
G_{sec}	secant shear modulus
H	Total depth of soil
f_y	yielding strength of steel
I_u	translational transfer functions
I_θ	rotational transfer functions
j	index representing translational or rocking modes
$[k]$	stiffness matrix
$\bar{k}$	foundation impedance function
k_s	modulus of subgrade reaction
$[M]$	mass matrix
$[M_{soil}]$	the soil mass matrix
$[M_{structure}]$	the structure mass matrix
r	equivalent radius of a foundation
T_1	fundamental period of vibration
{u}	displacement vector

u_{FIM}	foundation input motion
u_g	free-field motion
u_h	foundation horizontal translation
$\{u_{II}\}$	inertial interaction component of the displacement vector
$\{u_{KI}\}$	kinematic interaction component of the displacement vector
$\{\ddot{u}_g\}$	input displacement vector
v_n	normal components of the velocity at the boundary
V_p	dilatational wave velocities
v_s	tangential components of the velocity at the boundary
V_s	shear wave velocity
$V_{s,30}$	average shear wave velocity of the top 30 meters of a site
w	foundation settlement

Greek Symbols

α	mass model coefficients
β	stiffness model coefficients
γ	shear strain
γ_{cyc}	cyclic shear strain
$\gamma_{textupcyc}$	shear deformation
γ_{tl}	elastic cyclic threshold shear strain
θ	foundation rotation
θ_{FIM}	foundation rocking input motion
ν	Poisson's ratio
λ	minimum wavelength of the applied signals or geometrical scaling factor
ξ	Damping ratio
ρ	soil mass density
ρ_F	foundation mass densities
ρ_s	soil mass densities

τ	shear stress
ψ	dilatancy angle
ω	angular frequency

Abbreviations

ATC	Applied Technology Council
BRM	Bedrock Motion
BS	Basement Storey
CL	Low-placticity Clays
EL	Equivalent Linear
EOM	Equations of Motion
EQ	Earthquake
FB	Fixed Base
FEM	Finite-Element Method
FFM	Free-Field Motion
FFT	Fast Fourier Transform
FIM	Foundation Input Motion
GM	Silty Gravel
II	Inertial Interaction
KI	Kinematic Interaction
NEHRP	National Earthquake Hazard Reduction Program
NIST	National Institute of Standards and Technology
OCR	Overconsolidation Ratio
PEER	Pacific Earthquake Engineering Research Centre
PGA	Peak Ground Acceleration
PI	Plastic Index
RC-MRF	Reinforced Concrete Moment Resisting Frame
SDOF	Single-Degree-Of-Freedom
SRA	Site Response Analysis
SSI	Soil-Structure Interaction
SSS	Soil-Structure System
TF	Transfer Function
VSAB	Viscous-Spring Artificial Boundary

CHAPTER – 1

INTRODUCTION

1.1 General

Considerable advancements in the development of thorough methodologies to precisely analyse structural models and estimate the demands for different levels of earthquake ground motion has made in recent decades. However, the majority of these approaches do not explicitly incorporate the substructure system and subsoil conditions. The precise idealization of substructure components, including the foundation, soil, and their interaction, has become one of the most difficult aspects of structural modelling of building structures in recent years. Consequently, the structure is assumed to be fixed to the foundation, and the underlying soil is only taken into account by selecting appropriate ground motions compatible with the features of the soil deposit. Both research and practical experience have revealed that a structure with a different foundation and built on a compliant soil deposit could respond differently in comparison to a fixed base situation.

Substantial researches has been carried out on the response of building structures under the influence of various loading conditions by using in-situ and laboratory observations (Amendola et al., 2021; Celebi and Safak, 1991; Gueguen and Bard, 2005; Jakrapiyanun, 2002; Kim et al., 2014; Luco et al., 1988; Meli et al., 1998; Murià-Vila et al., 2004; Rayhani and Naggar, 2007; Sawada and Takemura, 2014; Tileylioglu et al., 2011; Wei et al., 2017; Yamahara, 1970), simplified discrete model and analytical studies (Maravas et al., 2014; Stewart et al., 1999; Triantafyllidis, 1986; Veletsos and Meek, 1974; Vrettos, 1999), and also numerical studies (Casciati and Borja, 2004; Güllü and Jaf, 2016; Nguyen et al., 2017; Rayhani and Naggar, 2008; Tabatabaiefar and Massumi, 2010; Torabi and Rayhani, 2014). Among the whole methods, analytical and numerical methods are the first preferred ones as the other methods are found to be either economically not viable or time consuming.

The studies have revealed that the incorporation of a soil-structure system (SSS) in the seismic response analysis of structures constructed on deformable soils causes a significant influence on the seismic response of structures in comparison to the same structures with an

idealized fixed base at the ground surface. The influence is primarily exerted through modifying the seismic force demands (i.e., storey shear and bending moment) and deformation characteristics (i.e., fundamental natural period, storey drift, etc.) of the structure and its near-field soil component. Among the major causes for this change is that a part of the vibrational energy of the structure placed on a compliant foundation is dissipated by hysteretic action and the spreading of stress waves in the supporting soil deposit (Tabatabaiefar et al., 2013). The flexible base is shown to be a suitable solution for reducing the seismic force demand of structures due to an increase in the period of vibration and effective damping of the structure's entire system (Bilotta et al., 2015; Scarfone et al., 2020; Visuvasam and Chandrasekaran, 2019).

Although these studies are valuable in predicting the behavior of structural systems reasonably, advanced models are required to understand the structural system behavior more accurately, especially in the case of building structures resting on compliant subsoil conditions under major earthquake excitation. The behavior of building structure varies with the stiffness of subsoil conditions, substructure system, and characteristics of earthquake motions. Furthermore, the problem is complicated by the various scenarios of foundation embedment in soil (Anwar et al., 2019). For getting the accurate behavior of building structures, one has to comprehend the complex interactions among the different components in a SSS. In the seismic response analysis of any specific issue, numerical methods have a high competency of incorporating the effects of nonlinearity arising from the changes in geometries and material behaviour, interface conditions, nonhomogeneous material properties, stress anisotropy, as well as radiation and material damping changes. Given the benefits of using numerical approaches over other methods, as well as the need for rigorous and realistic results, numerical methods for seismic response evaluation are strongly recommended (Bowles, 1997; Dutta and Roy, 2002).

However, in the conventional seismic resistance analysis and design practice of building structures, the process is normally carried out assuming fixed-base support for the targeted structure at the ground surface under excitation of free-field motion (FFM), which is the earthquake motion on the ground surfaces in the absence of any structure or excavation. Essentially, this assumption is acceptable for two cases. The first case is for lightweight low-rise buildings since the induced inertial-driven forces are negligible; thus, the effects of interaction among soil-structure are insignificant. The second case is relatively heavy building structures that

rest on a shallow foundation in stiff soil or rock; on the one hand, kinematic effects are indeed negligible since the FFM is approximately equal to the foundation input motion (FIM) of the structure. FIM is the motion of the embedded foundation that accounts for the geometry and stiffness of the base slab. However, depending on both soil deformability and the structure's slenderness ratio, inertial effects can be very strong in structures resting on shallow foundations (Veletsos and Meek, 1974). Moreover, it has been recognized in recent decades that the idealization of fixed bases and ignoring the compliant foundation-soil effect, particularly for buildings built on soft soils with shallow and deep foundations, could result in unsafe design (Anwar et al., 2019; Fatahi and Tabatabaiefar, 2014; Krawinkler et al., 2003; Wolf, 1985). As a result, the effect of compliant foundation soil alters the seismic response characteristics of a structural system due to the stiffness of the structure and soil flexibility. Furthermore, current practices and design procedures are inadequate to capture more realistic phenomena of the interaction between the structure and soil (Sharma et al., 2018).

Building frames are one of the major components in the structure, which governs the stability of the entire structural system when subjected to different gravitational and lateral loading conditions. The response of any system including more than one element is always interdependent. The superstructure, the substructure comprising subterranean levels and foundation as well as the soil mass together form a complete system. The seismic response demands in the structural system may differ due to the coupled interaction of different components in the system. The distribution of the seismic response demands on the superstructure system varies depending on the stiffness and system of the substructure, as well as the deformation characteristics of the soil. Several authors have reported the significance of the interactive behavior on the response of the superstructure (Ali et al., 2023; Khazaei et al., 2017; Oz et al., 2020; Shen and Qian, 2019; Tabatabaiefar and Fatahi, 2014b; Wani et al., 2022; Zhang and Far, 2022a).

1.2 Soil Structure Interaction (SSI)

During the incidence of an earthquake, the seismic structural response of buildings is often influenced by the interaction between various integrated components such as superstructure, substructure, and soil, which is often termed as Soil-Structure Interaction (SSI). These interdependent interactions are intricate and considerably important in understanding the real

performance of the structural system. Thus, SSI is receiving considerable attention from many researchers and is primarily focused on practical applications.

Because of the differences in their perspectives, geotechnical engineers are often more concerned with soil properties than structural engineers. Structural engineers, on the other hand, are specifically more concerned with the structural properties of a structure, and the foundation-soil flexibility effect on structure rest is usually ignored (NIST, 2012). As a result, complex models are usually applied solely to one component of the SSI phenomena, leaving the other aspect vulnerable. So, to gratify the requirements of both geotechnical and structural engineering as well as accurately predict the seismic response history of the structure in SSI problems, the structural systems and soils must be modeled properly. Many researchers (Agha et al., 2020; Amorosi et al., 2017; Bolisetti et al., 2014; Bolisetti and Whittaker, 2015; Silva et al., 2018; Hoseny et al., 2023; Hokmabadi et al., 2014; Nguyen et al., 2020; Tahghighi and Mohammadi, 2020b; Torabi and Rayhani, 2014) also have reported the importance of SSI effects in their studies.

The seismic response characteristics and force demands of the structural system depend on the substructure components and the stiffness of the subsoil conditions. These response parameters in the superstructure may alter the pattern of load distribution among the structural elements, which causes excessive deflections and failure of the structural elements. The incorporation of soil-foundation flexibility in the structural response analysis may get intensified the displacement while reducing the seismic force demands. The general practice of seismic response analysis of building structures without SSI may result in extra cost thus the influence of SSI has to be taken into consideration for predicting the responses.

Structures imposed to deformations without causing any damage result in a substantial overall economy and enhance the serviceability of the structure. For accomplishing this, design engineers have to understand the real characteristics of the structural system under the influence of foundation-soil flexibility and earthquake loads. In addition to the foregoing, it is vital to comprehend how each component affects the others.

1.3 Method of Analysis

In the domain of seismic SSI assessment, one of the most difficult features in structural models of building structures is the appropriate idealization of subterranean components

comprising subterranean levels, foundation, nearby and foundation soil medium, their interaction, and boundary conditions in SSS. If the soil medium, soil-structure interfaces, and boundary conditions are simulated appropriately utilizing a suitable modelling approach, the seismic SSI response of the structural system can be evaluated more accurately (Raychowdhury, 2011; Yeganeh and Fatahi, 2019).

In the subject of geotechnical earthquake engineering, SSI problems can be solved by utilizing various soil domain modeling techniques depending on the part of the structure that needs to be evaluated. Studies of conceivable alternative models among SSI systems have been conducted with a focus on the physical idealization and modeling of the soil medium (Dutta and Roy, 2002). In the past few decades, researchers have developed different methods for SSI studies. The methods can be categorized into four categories, namely, the Winkler method, Lumped parameter method, the Continuum method, and the Finite Element method.

(i) The Winkler model approach or the subgrade reaction theory is the simplest model representing the linear elastic behaviour of the soil for interaction among foundations and soils to predict a vertical deformation of the foundation because of the load acting on it. This approach uses a single bed of closely spaced series of independent, and linear elastic vertical springs attached to the foundation to represent the soil medium idealization (Winkler, 1867).

(ii) A lumped parameter method idealizes the frequency-dependent SSI of a weightless foundation situated on or entrenched into an unbounded soil domain. In this approach, along three mutually perpendicular axes in the case of 3D analysis of the SSI problem, translational and rotational springs are attached at the foundation level of the structures to consider the deformable behaviour of soil. Also, dashpots are added parallelly with springs to account damping system of the soil medium (Wolf, 1994b).

(iii) The elastic continuum method is a conceptual technique of a physical idealization of the unbound soil domain for the SSI problem. The commencement of soil domain representation as a half-space elastic medium is possibly initiated from Boussinesq's study to estimate a static stresses problem in a solid medium subjected to a unit point load acting normally to its plane surface, in which for the sake of simplicity the soil domain was considered to be perfectly elastic, isotropic, homogeneous, and semi-infinite. Nevertheless,

the influence of soil stratification and anisotropy may be appropriately considered in the analysis (Harr, 1966). This method, unlike to Winkler model, gives a lot of information related to the stresses and deformations that occur inside the soil domain. It also has the significant benefit of having simple input parameters such as Poisson's ratio and Young's modulus.

(iv) Formulation of the finite elements, which discretizes both the structure and soil into finite elements, imposing appropriate boundary conditions at the interface of the soil-structure. The FEM can be utilized to analyze both simple and complex SSI problems with extensive details and is an appropriate technique for seismic response analysis to a wide variety of scenarios (Cook et al., 1989; Matinmanesh and Asheghabadi, 2011). In addition to its being proven as an effective solution tool, FEM is also vital to understand that the simulation process requires a lot of memory and time for the 2D or 3D models to provide complete results. SSI often depends on the soil model constitutive behaviour. Therefore, the selection of an effective constitutive method leads to better results in the study of SSI issues in FEM.

1.4 Scope and Objectives

The incorporation of the substructure system and the underlying soil to understand the influence on the realistic seismic response behaviour of the superstructure is crucial. Many studies have been conducted recently that have focused on the seismic response of structures while taking into account the interaction between structure and soil. However, most studies to date have been limited to building structures with shallow foundations (Dutta et al., 2004; Fatahi et al., 2016; Tabatabaiefar and Massumi, 2010; Yeganeh and Fatahi, 2019), and deep foundations (Cai et al., 2000; Cavalieri et al., 2020; Ghandil and Behnamfar, 2015; Hokmabadi et al., 2014; Kassas et al., 2022; Lee et al., 2016; Lu et al., 2004; Maheshwari et al., 2004; Tabatabaiefar et al., 2015). Because of fast urbanization or infrastructural growth, as well as a lack of space in cities, the majority of buildings in metropolitan areas are often planned with one or more subterranean levels for parking and other amenities. However, a limited number of studies have been conducted on the seismic response of building frames with subterranean levels (Anwar et al., 2019; Hoseny et al., 2022, 2023; Ganainy and Naggar, 2009; Naeim et al., 2008; Saad et al., 2012; Scarfone et al., 2020; Turan et al., 2013). The seismic response behaviour of the superstructure depends on the interaction of the building frame with the substructure system and soil. The interaction of the

superstructure with the substructure and soil needs to be considered to predict the accurate behaviour of the building frames. With this scope of the investigation, the present study is performed to study the influence of subterranean levels on the seismic response characteristics of building frames under different subsurface site conditions, substructure parameters, and selected earthquake ground motions. To assess these types of complex interaction behaviors, numerical modelling plays a significant role. FEM-based software gives realistic behavior close to that of the field response. ABAQUS is one of the software, which is based on FEM principles and in the present study, this software is widely used by several researchers for numerical analysis (Agha et al., 2020; Bahuguna and Firoj, 2022; Lagaguine and Sbartai, 2023; Miao et al., 2020; Mohammadyar and Akhtarpour, 2023; Zhang and Far, 2022a).

By considering the above factors, the following objectives are intended to accomplish for the present research study:

- Evaluate the effect of subterranean levels on the foundation input motions for seismic response analysis of building structures.
- Appraise the applicability of theoretical models for quantifying the foundation input motion in comparison to nonlinear numerical models.
- Assess the effect of SSI modeling approaches on the seismic response history analysis of building frame structures with subterranean levels.
- Investigate the effect of subterranean levels and embedment depths on the seismic response of building frames considering SSI.

According to IS 875-3 (2015), building structures are classified based on height (H) into three categories like (i) low-rise (H < 20 m), (ii) mid-rise (20 m < H < 50 m) and (iii) high-rise (H > 50 m) structures.

To achieve the above objectives, a 15-storey mid-rise RC-MRF building designed according to the Indian building code (IS 1893 (Part 1), 2016; IS 456, 2000) in a high-risk earthquake-prone zone (zone V) is considered in the present study. The width of the building is 15 m in both x and y directions and the height of the building is 45 m above ground level.

The details of different parameters considered in the present study are given below.

a) Number of storeys above ground: 15-storey.
b) Number of underground storeys: 0, 1, 3, and 5 subterranean levels designated by 0BS, 1BS, 3BS, and 5BS. Where BS is basement storeys.
c) Alternative models of building frame with subterranean levels: Five models represented by Model 1A, 1B, 2A, 2B, and 3A. Details are given in section 3.5.2.2.
d) Subsurface soil conditions: Three different soil types, which are a homogenous dense GM (Soil type - C), medium CL (Soil type - D), and soft CL (Soil type - E) soil profile underline by rigid bedrock. The soil is classified as per ASCE/SEI 7-10 (2010).
e) Input ground motions: Seven earthquake ground motions are selected consistently according to ASCE/SEI 7-16 (2018) from the PEER strong motion database (PEER).

In general, this work aims to reveal how realistic numerical models can be created and used in a practical manner to address the problems related to nonlinear seismic SSI. As far as the author is aware, the influence of subterranean levels on the seismic response of building frames has not been thoroughly studied. However, very few studies have been carried out and these works have not been comprehensively addressed. The present study introduces a novel perspective by investigating the influence of subterranean levels on the response of buildings under nonlinear seismic SSI. The results of this study demonstrate how the characteristic and magnitude of the foundation input motion of the building alters with the existence and embedded depth of subterranean levels. The study also illustrates how seismic response demands alter as modeling approaches change and the number of subterranean levels increases in varied soil profiles. This exploration contributes to a deeper understanding of the complex interplay between building structures, subsoil conditions, and seismic loads.

It is the ultimate goal to promote practice towards the incorporation of subterranean levels and seismic SSI phenomena in order to enhance the prediction of the structural response under earthquake ground motions.

1.5 Research Methodology

In the present study to achieve the above mentioned objectives, numerical studies that are planned are given in Figure 1.1.

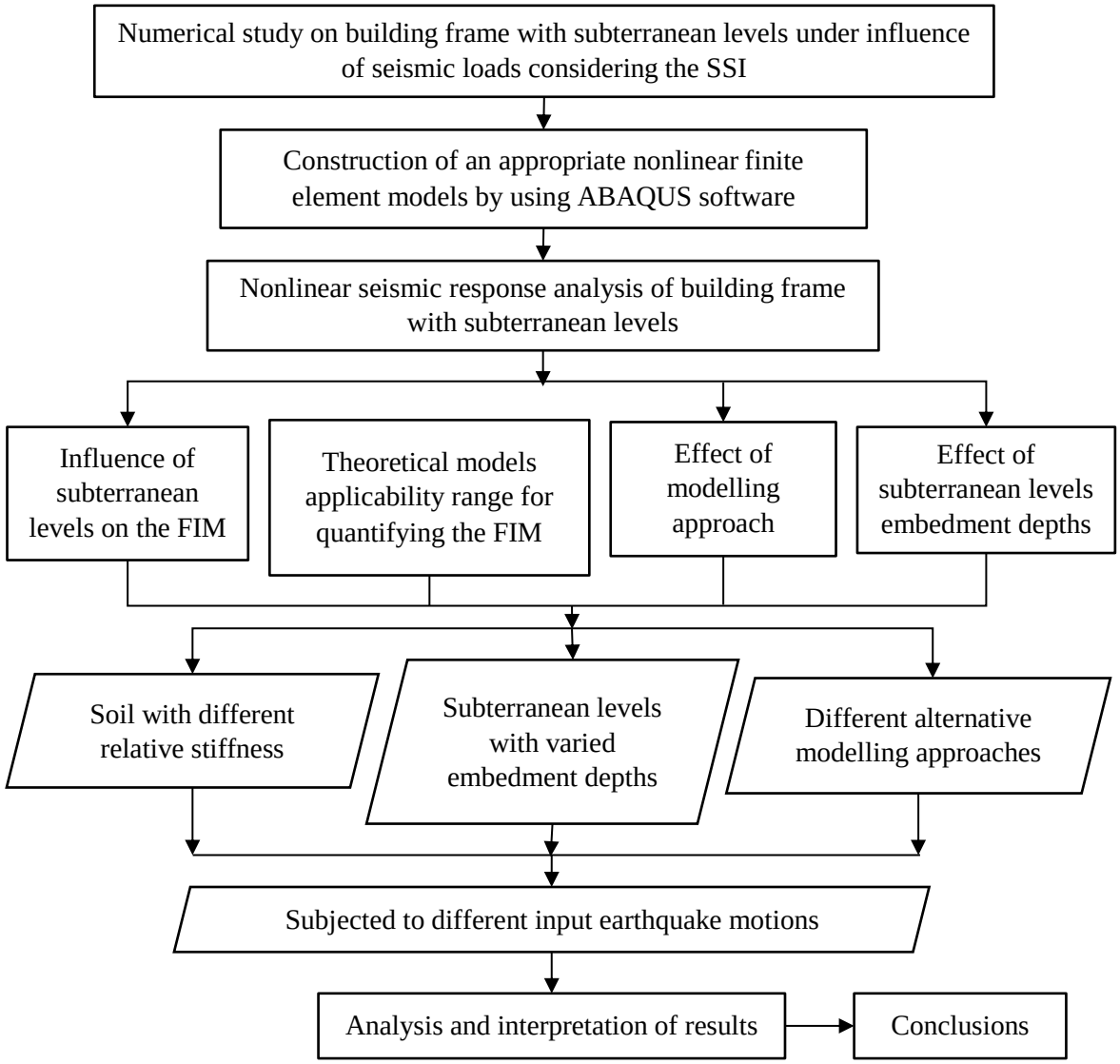

Figure 1.1 Schematic diagram of the methodology adopted for the research work.

1.6 Structure of the Thesis

The present thesis mainly deals with two closely related subjects: SSI and the seismic response of building frames with subterranean levels. To clarify the importance of integrating SSS into the building design process, the discussion of the research conducted is presented with a brief description of seismic response analysis. This thesis comprises five chapters, ranging from an introduction to the SSI and seismic response to a brief statement of its conclusions and scope for further study. The contents of the chapters are briefly described below:

Chapter 1 provides an introduction to the thesis, highlights its scope and objectives along with the research methodology adopted in the present study, and describes its structure.

Chapter 2 presents a comprehensive literature review on the seismic SSI, modeling, and analysis approaches, their effects on the seismic response of building structure, and SSI in seismic resistance design codes/guidelines. A critical appraisal of the literature is also presented in the conclusion, based on the reviewed material.

Chapter 3 provides the material used and their properties along with a detailed numerical procedure adopted for the present study. The methodology used for the study has been described in detail in this chapter. Numerical modelling by FEM-based ABAQUS software has also been explained in detail by validating the software.

Chapter 4 comprises the analysis and discussions along with the inferences on the results pertaining to the numerical analysis of the seismic response of RC-MRF building with subterranean levels under earthquake loads.

Chapter 5 summarizes the conclusions made from the present study.

CHAPTER - 2

REVIEW OF LITERATURE

2.1 General

The dynamic behaviour of structures under seismic excitation is often altered by the source of earthquake motion, earthquake travel path, local site conditions, as well as SSI effects. In particular, the seismic response characteristics and demands of structures are influenced by the flexibility of the foundation support, incorporation of the substructure system, and variations of motions between the foundation level and ground surface. As a result, a rational treatment of SSI effects may be necessary for an accurate assessment of seismic response demands in structures. This chapter elaborates on seismic response analysis of buildings featuring subterranean levels, various alternative foundation-soil modelling approaches, and criteria stipulated specified in seismic resistance design codes and related SSI procedures have been discussed. In this chapter, an attempt is made to provide a comprehensive appraisal of current studies from the last few decades. The geotechnical components that include the soil domain, subterranean structural system, and foundation are focused on, as well as the limitations & strengths of various models are also discussed.

2.2 Historical development of SSI

The study of SSI is an interdisciplinary field of work that combines structural and soil mechanics, material science, geomechanics and geophysics, earthquake engineering, structural and soil dynamics, computational and numerical methods, as well as a variety of other technical disciplines. SSI has received extensive attention internationally in recent years (Abdel et al., 2015; Bapir et al., 2023; Hoseny et al., 2022, 2023; Ghandil and Behnamfar, 2017; Hassani et al., 2018; Luo et al., 2016; Rahmani et al., 2016; Sobhi and Far, 2022; Tahghighi and Mohammadi, 2020a; Visuvasam and Chandrasekaran, 2019; Zhang and Far, 2022b, 2022a). This phenomenon is related to wave propagation in a coupled system, which includes a structure built near the surface of the soil. It began in the late 19^{th} century and gradually advanced and matured during the subsequent decades and the first half of the 20^{th} century. In the second half of the century, it advanced quickly,

primarily due to the demands of offshore industries and nuclear power, the introduction of simulation tools and powerful computers like FEM, and the requirement for improvements in seismic safety.

Kausel (2010) and Roesset (2013) presented evolutions of recent developments in field of SSI. Beginning with the fundamental solutions (generally known as Green's functions) developed by mathematicians and scientists as early as the early nineteenth century, Kausel (2010) described a chronological progression in SSI. The author reported a number of an individual who made substantial contributions to static SSI, including Boussinesq, Reissner, Steinbrenner, Hanson, and Mindlin. The theory proposed by Reissner, in 1936, laid the foundation for dynamic SSI which was further enhanced by continued development work work by Bycroft, Housner, Luco, Newmark, Veletsos, Whitman, and many others. Besides to the two primary SSI mechanisms—kinematic and inertial—that Whitman initially developed, Roesset (2013) has been discussed the substructure and direct approaches to doing SSI analysis. The author also discussed earlier studies on the dynamic stiffness of foundations, the impacts of stratified soils, embedment depths, and deep foundations.

Several publications have highlighted the SSI research status. The experiment and prototype observation, analytical method, semi-analytical (analytical-numerical) method, and numerical method are the main methods for investigating SSI in accordance with technical advancement.

2.3 Significance of SSI

The analysis of engineered structures under the influence of SSI assesses the combined response of the structure, its foundation system, and the soil beneath the foundation and sides of the subterranean levels under seismic excitation. The seismic SSI analysis will more realistically predict the deformation characteristics, seismic response force demand, and the behaviour of the entire system by incorporating the soil strata as a single integral compatible structural component. Several studies have been carried out on SSI problems to obtain more accurate solutions (Ali et al., 2023; Badry and Satyam, 2017; Far, 2019; Ghandil and Behnamfar, 2015; Medina et al., 2013). The influence of SSI has been evaluated and found that there is a redistribution of response demands in the structural system and soil mass. These interaction effects are more predominant in

loose or highly compressible soils (Agha et al., 2020; Mourlas et al., 2020; Oz et al., 2020; Requena-Garcia-Cruz et al., 2022; Tabatabaiefar and Fatahi, 2014a; Tahghighi and Mohammadi, 2020b; Wani et al., 2022). The interaction effect on the soil-foundation-structure system depends on the relative stiffness of the superstructure, and the substructure components including foundation and soil mass.

2.4 Fundamentals of Seismic SSI

Since in several sites structures are built on compliant (medium-dense and soft) soils, the conventional method of evaluating the seismic response of buildings makes the implausible assumption that a structure is rigidly supported (fixed-base condition). Thus, the incorporation of compliant soil behaviour could alter the seismic response performance of the structure in comparison to the fixed-base models. The fundamentals of seismic SSI are reviewed in this subsection. It is provided to compare the seismic response performance of fixed-base and flexible-base conditions.

2.4.1 Seismic response of structures with fixed and flexible base conditions

As illustrated in Figure 2.1, (Wolf, 1985) compared the structure seismic response performance built on a rock to that of the same structure having a rigid foundation embedded in the soil to emphasize the salient features of SSI. The substructure system comprises the side walls and the base-slab.

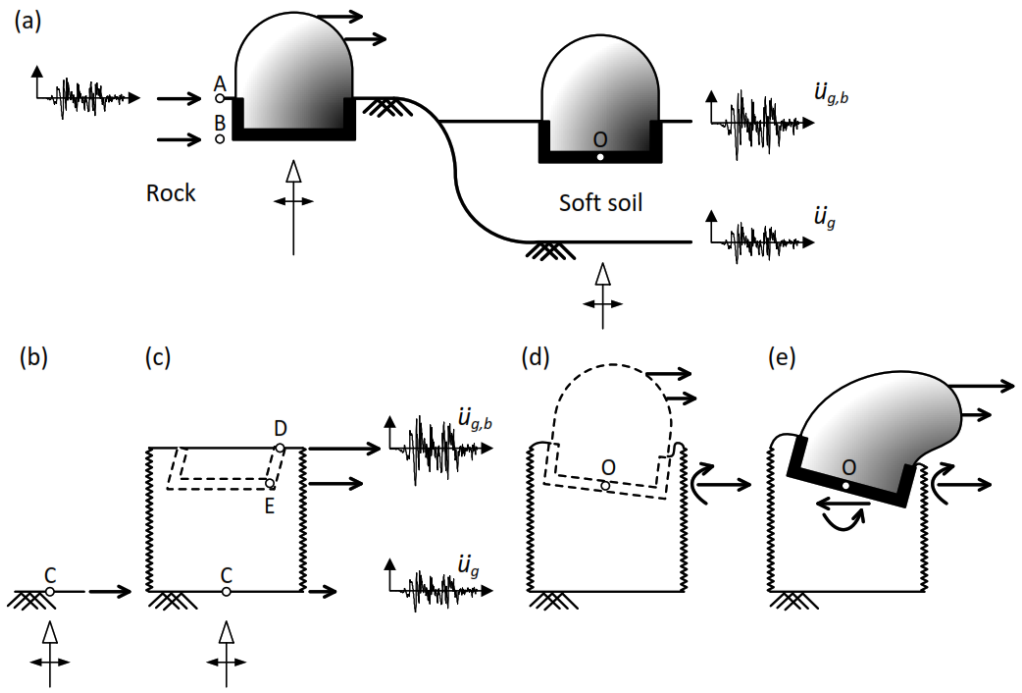

Figure 2.1 Performance of structure under seismic excitation built on rock and soil: (a) structure resting on different site conditions, (b) outcropping rock, (c) free-field motion, (d) kinematic interaction, and (e) inertial interaction (adopted after (Wolf, 1985)).

The solid arrows on the seismic wave incident diagram show that the vertical propagation of the horizontal seismic wave motions through the rock to the structure. Length of the solid arrows represents the amplitude of the motions. Point A is used as a benchmark to compare the motion to that at other sites, which is located at the rock free surface (Figure 2.1a). The horizontal motions at points A and B for the structure resting on rock are nearly same and identical to the applied horizontal seismic wave motion. This scenario is nearly identical to a fixed-base condition. As a result, it is reasonable to directly apply the motion that was captured at reference point A to the superstructure base. If the stiffness of the structural system to lateral loads is high, the induced base motion would result in horizontal acceleration. The base will consequently experience an overturning moment and a transverse shear force. Because the rock is quite inflexible, the seismic force demands of the structure at the base would rarely lead to any further ground deformation. Therefore, the rigid substructure system is attached to the rock and moves in accordance with its motion.

On the other hand, the seismic response of the structure embedded in the soil differs from that of the structure on the rock. The primary cause of this discrepancy is that the motion at point O (i.e., the base-slab center) differs from that at reference point A as a result of the following three phenomena.

i) FFM, which relates to the motion at the free surface of the site with an absence of any excavations and structures, is modified. The motion at point C ($\ddot{u}_g$), as illustrated in Figure 2.1c, which would be the same as at the benchmark if there was no soil atop the rock (Figure 2.1b), is attenuated by the soil deposit overlying the rock. The vibration caused by the wave as it travels through the soil deposit causes the FFM to either be amplified or attenuated. In most cases, the motion is amplified based on the excitations frequency content. Hence, once the structure is built, the motions at points D and E ($\ddot{u}_{g,b}$) as depicted in Figure 2.1c, which would be on the interface between the soil and the structure are different from that in point C. Therefore, a seismic site response analysis (SRA) is required for evaluations of FFM (see section 3.5.4.1).

ii) Constructing a rigid substructure system in the soil alters the foundation level motion, which could experience some rocking motion in addition to average translational displacement (Figure 2.1d). The combined response would consequently result in a variation of horizontal acceleration across the superstructure height. This is essentially a result of differences in stiffness among the surrounding soil and the substructure components and take place even when the structural system is massless. It is often known as Kinematic Interaction.

iii) The base shear force and moment caused by the inertial-driven forces will lead to further deformation in the surrounding soil, which alters the foundation level motion at point O (Figure 2.1e). This interaction process is also referred to as Inertial Interaction, which occurs between the excited structure and the surrounding soil deposit.

2.4.1.1 Kinematic interaction

Kinematic interaction (KI) is the result of the stiffness difference between the substructure components and the surrounding soil. In the absence of a structure, soil particles move according to the wave propagation pattern. If a foundation is embedded in the soil deposits and is rigid (very

stiff), it is unable to follow the pattern of free-field displacement. As a result, the motion of the base-slab will deviate from the FFM although the foundation has no mass.

Case studies of the KI phenomena are presented in Figure 2.2. It should be noted that foundations are considered to be massless in all circumstances, and short dash curves represent the FFM. Figure 2.2a depicts a pile that is embedded in the soil under influence of shear waves. Shear wave amplitude increases as it propagates vertically upward into the soil. However, the flexural rigidity of the pile averts it from obeying the FFM, which tends to alter the soil displacements near the pile shaft in comparison to the FFM. Further, the displacement of the soil around the pile causes to induce flexural moments, which could put at risk the stability of the pile.

The influence of the excitation motion frequency components on the response of an embedded massless foundation is compared in Figure 2.2b and c. When the embedded foundation (Figure 2.2b) is imposed to a high-frequency motion and that fluctuates horizontally, the foundation is not affected by the wave motion since the kinematic forces acting on it is neutralize. On the other hand, excited by a shear wave motion with lower-frequency, the foundation can translate and rock, giving rise to an FIM, although the FFM is purely translational (Figure 2.2c).

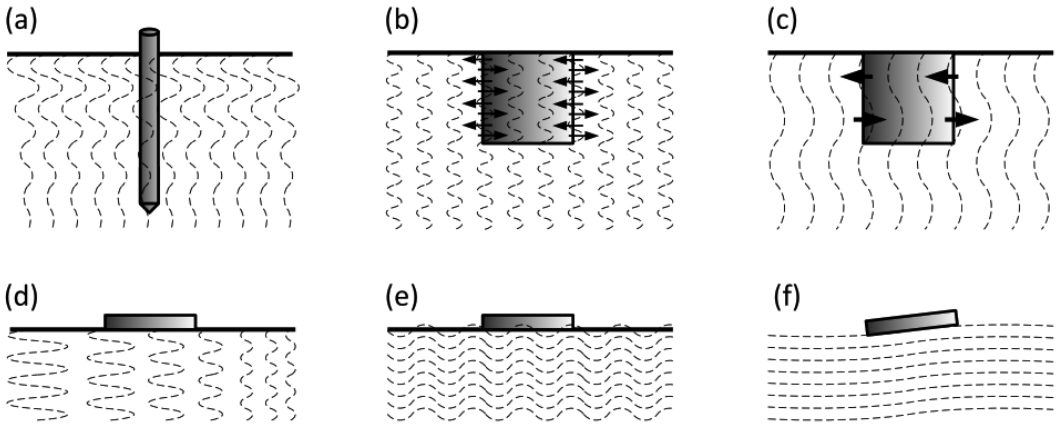

Figure 2.2 Influence of KI on shallow and deep foundations (Lu, 2016).

Even if KI occurs more commonly with embedded foundations, there are a few instances where this impact is as well considerable on surface foundations. Figure 2.2d illustrates a situation in which the surface foundation in-plane stiffness does not permit it to follow the underlying soil displacement shape. Furthermore, Figure 2.2e and f also show that excitation frequency

significantly affects the foundation response, which is again supporting the justifications provided in Figure 2.2b and c.

Generally, the influence of KI on the behaviour of foundation depends on the governing wavelength of the shear wave motion in relation to the characteristics dimension of the foundation. In the context of Figures 2.2a, b and e, as the wavelengths of high-frequency motions are negligible in comparison to the foundation dimension, their contribution to the response of foundation is virtually insignificant. In this regard, the foundation can be considered as a high-period-pass filter applied to the FFM of high-frequency components (FEMA 440, 2005). This impact is particularly prominent for short-period buildings and cause a large attenuation of seismic response demands.

When the foundation characteristic dimensions are equal to the wavelength of the motion, KI will modify the foundation modes of vibration (Figure 2.2c and f). However, the KI effect can be reasonably disregarded if the foundation dimension becomes sufficiently small in comparison to the wavelength of motion. Figure 2.2d depicts a phenomena known as the base-slab averaging effect, which occurs prevalent at high frequencies as well. It should be noted that KI is not involved in all cases (with reference to Figure 2.2d, e and f).

2.4.1.2 Inertial interaction

Inertial interaction (II) is the foundation-level displacements and rotations of a structure that are caused by inertia-driven forces developed within the structure such as base shear and moment. The two most essential aspects of inertial interaction are discussed further below.

Initially, in addition to the deformation caused by the FFM, the soil is also deformed by inertia-driven forces that developed at the foundation base. The stiffness of the soil and the amplitude vibration motion determine the magnitude of the deformation. The incorporation of compliant foundation soil causes the entire system of SSI problem to become more flexible and susceptible to longer-period ground motion components.

Then, the oscillated foundation acts as a vibration source and releases wave motions that propagate into the soil to infinity. The swaying response (u_h) of an embedded shallow foundation, as shown in Figure 2.3a, generates dilatational waves (P-waves) and shear waves (S-waves)

through compression/extension and friction among the foundation and the nearby soil, respectively. P-waves are generated predominantly by compressive pressures transferred from the foundation base to the underneath soil in the form of rocking mode of vibration, as depicted in Figure 2.3b.

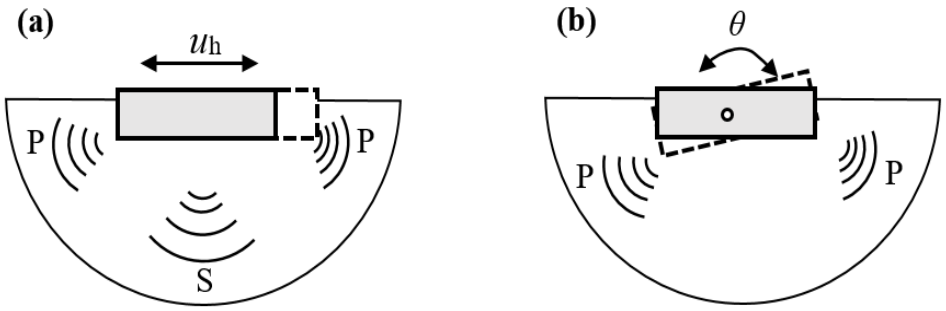

Figure 2.3 (a) swaying, and (b) rocking mode of vibration of foundation (Lu, 2016).

In inertial interaction, there are two primary types of wave energy dissipation mechanisms. The first type is often termed as radiation damping since the excited foundation radiates vibration waves into the soil deposit. This is due to the geometric reduction effect that occurs during wave propagation. The second type is called hysteretic damping, which relates to nonlinear behaviour of soil. If uplift motion of the foundation is permitted, the influence of the foundation on the soil and the resulting vertical vibrational motion dissipates a portion of the kinetic energy imposed on the foundation (Adamidis et al., 2014). In summary, the introduction of soil hysteretic damping and radiation damping into the vibrating system, as well as the lengthening of the vibration period are the major characteristics of inertial interaction.

2.5 Approaches to Seismic SSI Analysis

2.5.1 Direct Approach

The direct approach is one in which the whole SSI system is modelled and analyzed in a single step accounting for both KI and 'II'. It is the most complex method of solving a seismic SSI issue, which comprises simulating the whole SSS in the time domain, taking into account for material and geometric nonlinearities, variation of soil properties in space, complexities of wave propagation, and cautious treatment of boundary and soil-structure interfaces. As illustrated in

Figure 2.4, this approach is often performed by using the FEM. The governing EOM for an SSI FEM is given as in equation 2.1.

$$[\mathrm{M}]\{\ddot{\mathrm{u}}\} + [C]\{\dot{u}\} + [\mathrm{K}]\{\mathrm{u}\} = -[\mathrm{M}]\{m\}\ddot{\mathrm{u}}_{\mathrm{g}} + \{F_v\} \tag{2.1}$$

where, [K], [C], and [M] are respectively the stiffness, damping and mass matrices. {u}, {u̇}, and {ü} are respectively the displacements, velocities, and accelerations of nodes. $\ddot{u}_g$ is the earthquake-induced acceleration at the level of the bedrock. {m} is the mass participation factor. $\{F_v\}$ is the boundary-related force vector.

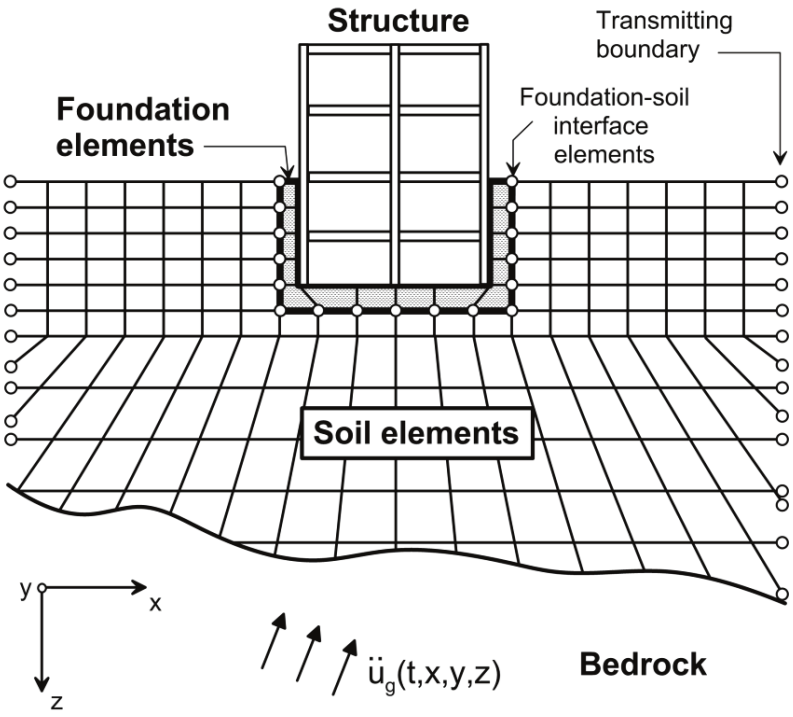

Figure 2.4 Schematic depiction of a direct approach for building with subterranean levels of SSI analysis using continuum modelling by FEM (adapted from (NIST, 2012))

Even if this approach is capable of treating the structure and the soil with the same rigor, it typically needs a significant computational effort and is challenging to implement. Because of this, practical engineers are more adapted the simplified techniques like a substructure approach during the preliminary design stage, which will be covered in the next part.

2.5.2 **Substructure Approach**

The substructure approach is also termed as a three-step approach. In this approach, the complicated soil-foundation-structure system is separated into KI and 'II' problems as shown in Figure 2.5, each of which is analysed individually and the results superimposed to yield the response of a structure.

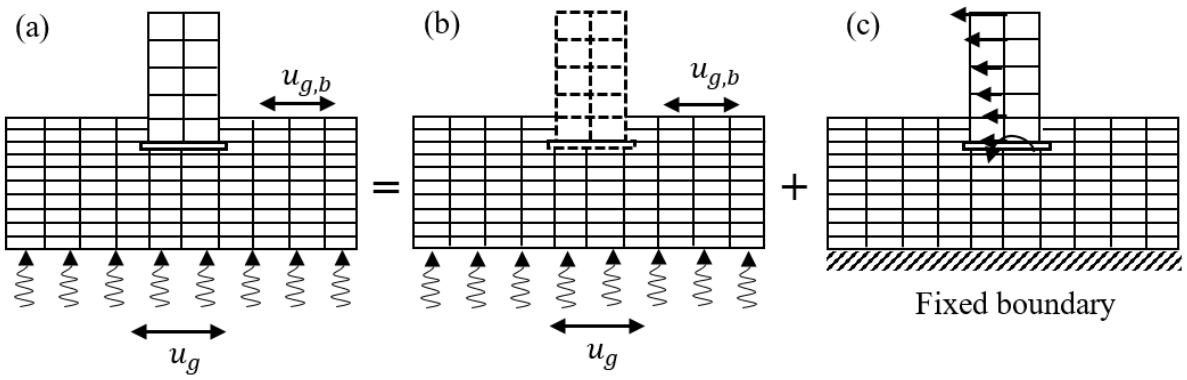

Figure 2.5 The seismic SSI response analysis: (a) a complete soil-foundation-structure system under seismic excitation, (b) a KI response, and (c) an inertial interaction response.

In the KI response analysis, ground excitation motions are incorporated at the lowest level of the SSI model where the entire structural system is assumed to have stiffness but massless (Figure 2.5b). The equation of motion for KI can be expressed as:

$$[\mathrm{M_{soil}}]\{\ddot{\mathrm{u}}_{\mathrm{KI}}\} + [\mathrm{k}]\{\mathrm{u_{KI}}\} = -[\mathrm{M_{soil}}]\{\ddot{\mathrm{u}}_{\mathrm{g}}\} \tag{2.2}$$

where $[\mathrm{M_{soil}}]$ is the soil mass matrix where the structural system mass is zero.

The equation of motion for inertial interaction can be calculated mathematically by subtracting those for the KI (equation 2.2) from the overall equation of motion (equation 2.1) and written as given in equation 2.3.

$$[\mathrm{M}]\{\ddot{\mathrm{u}}_{\mathrm{II}}\} + [\mathrm{k}]\{\mathrm{u_{II}}\} = -[\mathrm{M_{structure}}]\{\ddot{\mathrm{u}}_{\mathrm{g}} + \ddot{\mathrm{u}}_{\mathrm{KI}}\} \tag{2.3}$$

Where $[\mathrm{M_{structure}}]$ is the structural system mass matrix in which the soil entries are all 0 (i.e., $[\mathrm{M}] - [\mathrm{M_{soil}}]$), and $\{\mathrm{u_{II}}\}$ is the displacement vector of the 'II' component (i.e., $\{\mathrm{u}\} - \{\mathrm{u_{KI}}\}$).

It should be noted that for the DoF associated with the structure-foundation system, $\{u_{KI}\} + \{\ddot{u}_g\}$ is equal to the FIM. Specifically, for a foundation resting at ground surface subjected to shear waves propagating vertically, $\{u_{KI}\} + \{\ddot{u}_g\}$ at the level of foundation is equal to $\{u_{g,b}\}$, which is the FFM at the ground surface.

From the perspective of practical engineers, the soil domain is typically replaced by impedance function (springs and dashpots), which take into account the damping and stiffness features of the foundation-soil interaction, in order to simplify an SSI analysis. Figure 2.5 presents the procedures of this approach, which is also applicable for simple SSI problem.

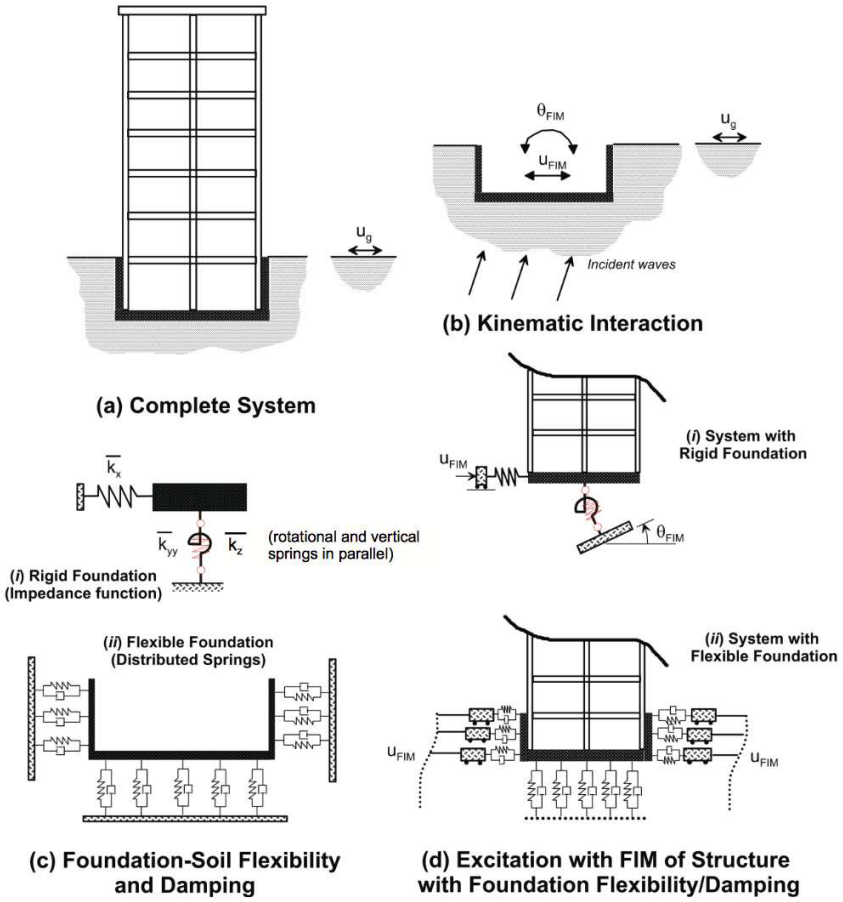

Figure 2.6 Schematic depiction of substructure approach for building with subterranean levels (adapted from (NIST, 2012)).

As displayed in Figure 2.6, the three basic steps often utilized in the substructure approach (Kramer and Stewart, 2004) are as follows:

(1) Evaluation of an FIM, which is the motion that would occur at the level of the foundation slab assuming the overall structural system is stiff or rigid but had no mass (Figure 2.6b). It is determined by the geometry and stiffness of the foundation as well as the soil.

The kinematic interaction component of SSI is also characterized by transfer functions. As given by equations 2.4 and 2.5, these functions are usually described using the ratio of foundation translational or rocking input motion to FFM as proposed by Elsabee and Morray (1977).

$$I_u = \frac{u_{FIM}}{u_g} = \begin{cases} \cos\left(\frac{\omega H}{V_s}\right) & \omega \leq 0.7\frac{\pi}{2}\frac{V_s}{H} \\ 0.453 & \omega > 0.7\frac{\pi}{2}\frac{V_s}{H} \end{cases} \tag{2.4}$$

$$I_\theta = \frac{\theta_{FIM} \cdot H}{u_g} = \begin{cases} \frac{2H}{B}0.257\left[1 - \cos\left(\frac{\omega H}{V_s}\right)\right] & \omega \leq \frac{\pi}{2}\frac{V_s}{H} \\ \frac{2H}{B}0.257 & \omega > \frac{\pi}{2}\frac{V_s}{H} \end{cases} \tag{2.5}$$

where I_u and I_θ are the translational and rotational transfer functions, respectively; u_{FIM} and u_g are the FIM and FFM, respectively; θ_{FIM} is foundation rocking; B is the width of foundation, ω is the excitation motion angular frequency and Vs is the supporting soil shear wave velocity (FEMA 440, 2005; Mylonakis et al., 2006).

Several synthesized transfer function models have been developed for circular or rectangular shapes a rigid massless foundation embedded in a homogeneous elastic or viscoelastic half-space (Brandenberg et al., 2015; Day, 1978; Dominguez and Roesset, 1978; Karabalis and Beskos, 1986; Luco and Wong, 1987; Mikami et al., 2008; Mita and Luco, 1989; Mylonakis et al., 2006; NIST, 2012). More recently, Conti et al. (2017 and 2018) have proposed an improved version of the above equations with the presence of massless stiff superstructure and foundation mass.

(2) Determination of the impedance function, which is the stiffness and damping characteristics of the foundation-soil interaction system to represent the inertial interaction effects. For a simple case of a very stiff foundation, which depends on foundation geometry, elastic soil

parameters (e.g., stiffness and Poisson's ratio), soil stratigraphy, and frequency of vibration. Its values also can be determined based on the degree of flexibility of the foundations: (a) for rigid foundations (Figure 2.6c-i) - using relatively simple impedance function models (e.g., Gazetas (1991)), or (b) for non-rigid but stiff foundations (Figure 2.6c-ii) - using a series of distributed springs and dashpots acting around the substructure. Few researchers (Gazetas, 1991; Mylonakis et al., 2006; Pais and Kausel, 1988) have developed impedance functions for different types of foundations and embedment depths. A general form of impedance function is presented in equation 2.6.

$$K_j(a_o) = K_j\left[k_j(a_o) + ia_o c_j(a_o)\right] \quad (2.6)$$

where K_j (a_o) is impedance functions as a function of dimensionless frequency. j is an index representing translational or rocking modes. a_o is a dimensionless circular frequency $a_o = \omega B/V_s$ (ω is the circular frequency of the motion, Vs is the shear wave velocity in the soil, B is the foundation half-width or ''equivalent'' radius). K_j is static stiffness coefficients. i is equal $\sqrt{-1}$. k_j and c_j are stiffness and damping characteristics as a function of a_o, respectively.

(3) Seismic response analysis of structure placing at top of the flexible base characterized by the impedance function and exciting the system base using the translational and rocking components of FIM (Figure 2.6d). It is also important to know that, in the case of the distributed spring and dashpot model, differential ground displacements over the embedment depth should rigorously be applied given the ground motion vertical variability (NIST, 2012).

It is also worth mentioning that the superposition inherent to the substructure method necessitates an assumption of linear behaviour of soil and structure (Kramer, 1996). To account for the frequency dependence of the substructure impedance functions, the method is most commonly used in the frequency domain. Adopting this method, several numerous numerical studies (Kutanis and Elmas, 2001; Leoni et al., 2012; Yang et al., 2008) have been carried out to evaluate the seismic response of structural systems considering the effect of SSI.

2.6 Commonly used Models for Seismic SSI Problems

The modeling of structural systems such as elements of the superstructure and subterranean components including foundation and subterranean levels is relatively easier than that of subsoil.

One of the most difficult elements of seismic SSI studies is the appropriate idealization of the soil domain near subterranean levels and beneath the foundation, their interaction, and boundary conditions in SSS. The soil behavior is complex, due to its anisotropic, heterogeneous, and nonlinear force-displacement characteristics. This complexity increases with the fluctuation of the water table. If the soil domain, soil-structure interfaces, and boundary conditions are simulated appropriately utilizing a suitable modelling approach, the seismic SSI response of the structural system can be evaluated more accurately (Raychowdhury, 2011; Yeganeh and Fatahi, 2019). Soil can be modelled in different ways with various levels of rigor. Although designers use spring-type models as a simple tool for evaluating seismic resistance of structures under 'II', domain-type models are more extensively utilized in research as a direct method. The geotechnical components are the main focus of this section.

2.6.1 **Modeling of Building Structures**

The building frame structural elements like beam and column of the structure can be modeled using two noded beam elements in a plane and space for 2D and 3D numerical analyses, respectively. The behaviour of the floor slabs and walls can be simulated by using the shell elements of suitable dimensions. The foundation element may be idealized with 3D solid (continuum) elements for 3D analysis. The structural system subjected to seismic loading can be analysed by taking into account the nonlinear behaviour of the structure by using the above idealization. An appropriate model has to be adopted based on the computational facility available and the accuracy required.

2.6.2 **Modeling of Soil using Domain-type models**

When a body of an arbitrary shape has nonlinear material property and is subjected to intricate dynamic loading conditions, domain-type models are often utilized to solve the problem. The domain is usually idealized as a continuum with an infinite number of DoF. To address such an issue, the entire domain must be discretized into several subdomains with a finite number of DoF. The discretization can be attained by utilizing either a FEM or an FDM. Figure 2.7 shows a direct approach of SSI analysis carried out using a FEM ABAQUS software.

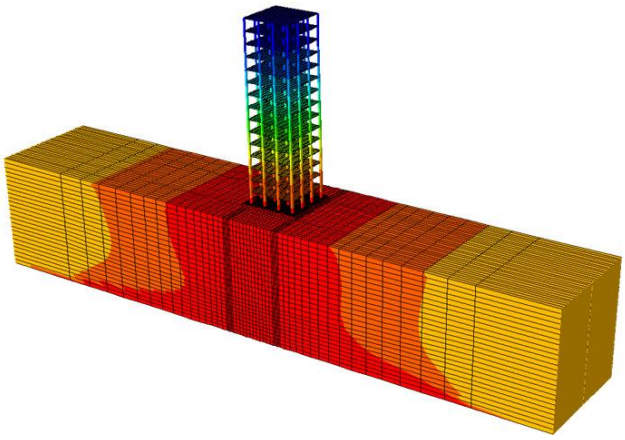

Figure 2.7 Application of FEM to direct approach of SSI analysis by using the numerical code ABAQUS (Nguyen et al., 2017).

In addition to numerical computational methods, two key aspects need to be carefully considered. The first concern is the simulation of soil behaviour, which is often accomplished using a suitable constitutive models. The second issue relates to a seismic SRA that takes into account boundary conditions and seismic loading, variation of material properties within a soil profile, and propagation of wave motion through the soil deposit. The following subsections discussed in detail about these two issues.

2.6.2.1 Dynamic behaviour of soil

In the event of an earthquake, a soil deposit in a site is imposed to stress variation during seismic wave propagation. Therefore, the primary focus of a geotechnical earthquake engineering problem is shear stress caused by the passage of shear waves.

As shown in Figure 2.8a, simple cyclic undrained shear test can be performed in the laboratory to assess the saturated soil seismic response under 1D shear waves. A hysteresis loop, as shown in Figure 2.8b, characterizes the steady-state cyclic soil response. A soil shear resistance in response to a shear deformation $\gamma_{textupcyc}$ is also frequently measured using a secant shear modulus $G_{sec} = G_{cyc}$, which is defined as the slope of the line joining the tips of the hysteresis loop. The energy lost during a cycle is represented by the area encircled by the loop and can be calculated quantitatively using the damping ratio as given in equation 2.7.

$$\xi_g = \frac{\Delta E}{4\pi E} \tag{2.7}$$

where ΔE and E are the amount of energy that is dissipated within a cycle and the maximum elastic energy stored during the cycle, respectively.

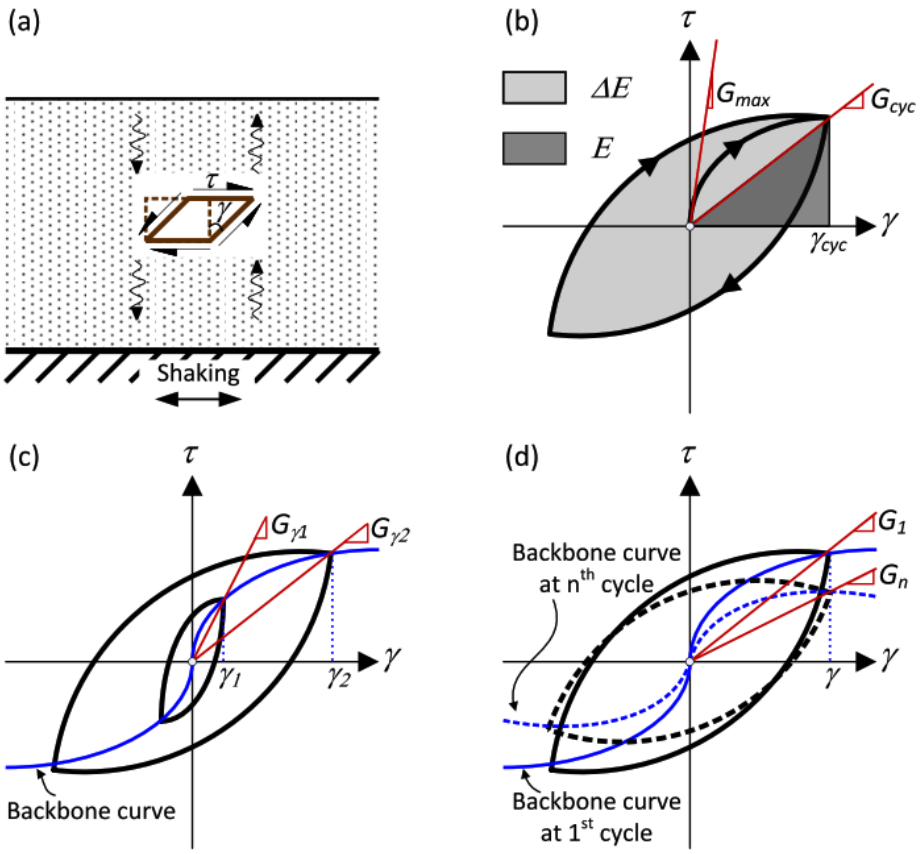

Figure 2.8 Dynamic behaviour of soil: (a) a soil profile under shear waves, (b) a hysteresis loop, (c) amplitude of cyclic strain, and (d) number of cycles (Lu, 2016).

Figure 2.8c illustrates how the secant shear modulus decreases as the amplitude of the cyclic shear strain increases. A backbone curve connecting the tips of hysteresis loops obtained at various strain amplitudes can be used to depict this relationship. As shown in Figure 2.8d, even with a constant shear strain amplitude, particularly at high strain levels, the hysteresis loop becomes flatter as the number of cycles increases. For saturated soils, an increase in the number of cycles is frequently associated with a decrease in stiffness and strength, resulting in a deteriorated

backbone curve. The effective confining stress and void ratio influence shear modulus degradation in sands, while the overconsolidation ratio (OCR) and plastic index (PI) influence it in clays.

As shown in Figure 2.9, a pair of dimensionless curves can also be used alternatively to describe the dependency of damping and shear modulus on cyclic shear amplitude, which was first reported by Seed and Idriss (1970).

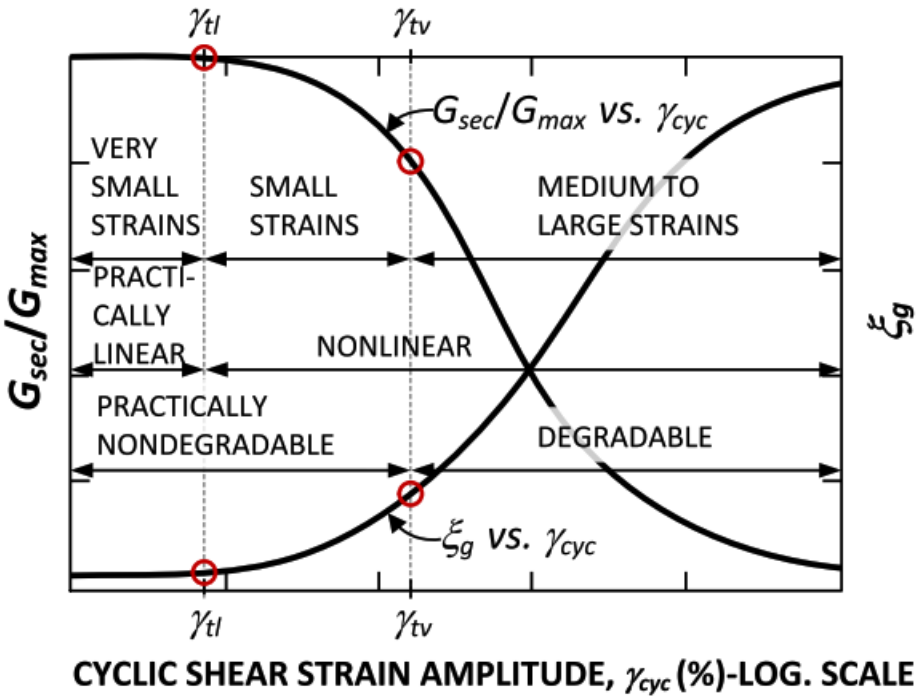

Figure 2.9 Backbone and damping curves for saturated soils with varying strain amplitudes (adopted after (Vucetic, 1994)).

These curves are widely utilized in practice and research (Vucetic, 1994) because (1) both the normalized G_{sec}/G_{max} and ξ_g are not considerably influenced by the OCR and effective consolidation stress; and (2) as presented in equation 2.8, the strain-dependent G_{sec} can be easily calculated from G_{max} which is often estimated using shear wave velocity V_s and density of soil ρ which are obtained from field-tests.

$$G_{max} = \rho V_s^2 \tag{2.8}$$

Numerous investigations have been conducted to ascertain normalized shear modulus and damping ratio verses cyclic shear strain (Hardin and Drnevich, 1972; Ishibashi and Zhang, 1993; Lee, 1978; Oztoprak and Bolton, 2013; Seed et al., 1986; Seed and Idriss, 1970; Sun et al., 1988; Zhang et al., 2005). These dimensionless curves led to the development of an EL technique, which is now frequently employed in geotechnical earthquake engineering to model real nonlinear behaviour of soil, particularly in seismic site response analyses. The EL approach is limited in its capability to account for plastic deformation caused by enormous strains; to this scenario, the nonlinear model is recommended. Using the cyclic threshold shear strains γ_{tl} noted on the curves in Figure 2.9, a simple criterion for choosing between a linear, EL, or nonlinear model can be established. The elastic γ_{tl} can be thought of as the boundary between the linear and nonlinear behaviour of soil, whilst the volumetric threshold strain γ_{tv} is the critical strain for the commencement of plastic deformations. As presented in Figure 2.10, the two threshold strains increase with plasticity index.

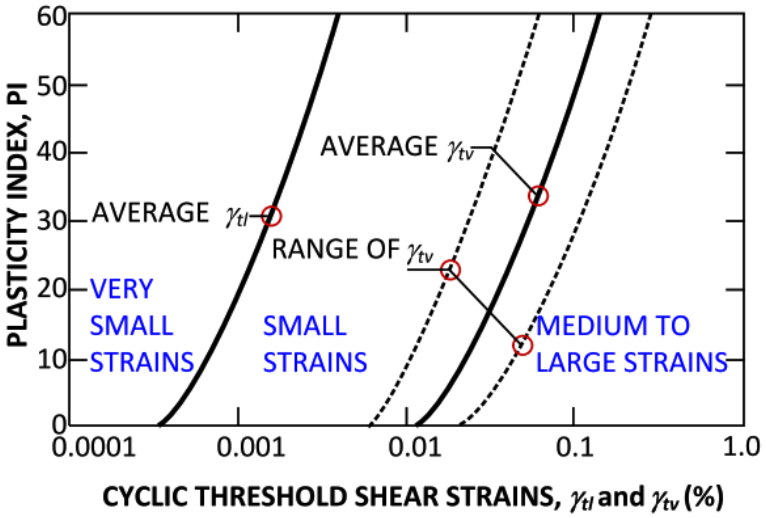

Figure 2.10 The cyclic threshold shear strains γ_{tl} and γ_{tv} variation with plasticity index (adopted after Vucetic (1994)).

2.6.2.2 Seismic site response analysis

While utilizing the domain-type model during seismic response analysis, it is crucial to verify that the wave propagation characteristics, input motions, and boundary conditions are properly represented.

a) Boundary conditions

In seismic SSI problems, in order to eliminate the effects of reflected waves from the base/lateral boundaries of the soil domain on structural response, the standard boundaries (i.e., fixed/roller) must be located at an adequate distance from the structure. However, increasing the soil domain size may cause more elements to be required for simulation, and as a result of which the computational cost is increased. Otherwise, the wave reflection effect can be prevented or reduced by utilizing special artificial boundaries. These boundaries are also known as quiet boundaries because they either allow incident waves to transmit through across them (Lindman, 1975; Smith, 1974; Zienkiewicz et al., 1983) or absorb wave energy (Lysmer and Kuhlemeyer, 1969). Studies on various boundary types often utilized in seismic response analyses (Roesset and Ettouney, 1977; Wolf, 1986) revealed that the viscous boundary using simple physical dashpots achieved a reasonable mix between efficiency and effectiveness.

As a method of absorbing incident waves, Lysmer and Kuhlemeyer (1969) presented dashpots attached separately to the boundary in the normal and shear directions. As given by equation 2.9, these dashpots provide viscous shear (τ) and normal forces (σ).

$$\tau = -\rho V_s v_s \qquad \sigma = -\rho V_p v_n \tag{2.9}$$

Where V_s and V_p are respectively the shear wave and dilatational velocities. v_s and v_n are components of tangential and normal velocity at the boundary, respectively.

This approach works almost perfectly when the incidence angle of the body wave is higher than 30 degrees relative to the viscous boundary, whereas some reflection will occurs at smaller incidence angles. Furthermore, it is simple to utilize for solving seismic SSI issues in engineering practice. Nevertheless, the geostatic strain and stress states must be attained prior to performing a seismic response analysis in order to apply these boundaries to nonlinear soil models.

b) Seismic input motion

If a raw acceleration time history data is utilized as an input motion for seismic response analyses, many issues could arise. The first major problem is that an integration of the acceleration

time history record across the entire period of motion may not be zero, resulting in an impractical residual displacement or continuing velocity after shaking. Therefore, a process of baseline correction (Boore, 2001; Boore and Bommer, 2005) can be carried out to adjust the input acceleration time history until both final displacement and velocity are reduced to zero.

The earthquake motions are usually recorded at the ground surface, also termed as FFM. In the case of domain-type models, however, the input motion is applied at the bottom of the model. In such instances, a process is needed to determine the input motion. In this case, an inverse wave propagation (deconvolution) analysis can be used to estimate an input ground motion at base level of models from the target FFM.

A 1D wave propagation problems, a linear or EL deconvolution analysis based on transfer functions is frequently used. These functions are frequency-domain ratios of the response at two different levels of a soil profile, which is mostly at foundation level and at ground surface.

To compute an input acceleration time history, initialy the ground motion changed into its Fourier series. The Fourier series of the input motion is then obtained by multiplying each term in the Fourier series using the relevant transfer function. Finally, an inverse Fourier transform is used to compute the input acceleration time history motion (Kramer, 1996). A commonly used computer program called DEEPSOIL (Hashash et al., 2020) for seismic SRA can be utilized to implement an EL approach to deconvolution.

For wave propagation numerical analysis, in order to prevent numerical distortion of transmitting waves, the chosen element size setting should satisfy the following condition (Kuhlemeyer and Lysmer, 1973).

$$\Delta l \leq \frac{\lambda}{10} \sim \frac{\lambda}{8} \tag{2.10}$$

where Δl is the element size and $\lambda = V_s / f_{max}$ is the minimum wavelength of the applied signals accompanying with the highest frequency component that containing significant energy, in which V_s and f_{max} are respectively the smallest soil shear wave velocity and the maximum frequency of interest. Equation 2.10 makes it clear that the maximum size that can be allowed for an element of

a domain-type model is determined by the frequency content of a ground motion. Therefore, higher frequency signals need a finer mesh size and a more expensive computation.

2.6.3 Modeling of Soil using a Spring-type model

In order to give reliable information for structure design, it is desirable for practicing engineers to have a model that is less complex in comparison to the domain-type model while yet accounting for the key characteristics of a dynamic foundation-soil system. To create such models, simplifying assumptions are made. The compliance soil domain can be replaced with coupled or uncoupled springs and its stiffness is either constant or deformation/frequency-dependent. In this section, the most popular basic foundation-soil interaction models in engineering practice are reviewed along with a summary of their strengths and limitations.

2.6.3.1 Beam on Winkler Foundation model

The Winkler model approach or the subgrade reaction theory is the simplest model representing the linear elastic behaviour of the soil for interaction among foundations and soils to predict a vertical deformation of the foundation because of the load acting on it. This approach uses a single bed of closely spaced series of independent, and linear elastic vertical springs attached to the foundation to represent the soil medium idealization (Bowles, 1997). It works on the assumption that a point experiences vertical deformation independently of its adjacent points. On the other hand, this implies that the particles that make up the soil medium do not interact with neighbouring ones. This assumption is incorrect because the continuity of the soil medium causes displacements at one point to be impacted by forces at adjacent points. These are the result of non-integrated vertical shear stresses, which would have connected the vertical deformations of adjacent locations to ensure displacement continuity. This flaw can be resolved by properly integrating the subgrade's shear stress components. As observed by some researchers numerous efforts have been endeavoured previously to integrate the shear stresses utilizing several methods (Gorbunov-Pasadov, 1949; Hetényi and Hetbenyi, 1946; Horvath, 1993; Kerr, 1965). The physical illustration of the Winkler foundation-soil model is illustrated in Figure 2.11. The differential equation of a beam or plate resting on an elastic foundation is a combination of the classical beam theory and the Winkler foundation-soil model, which has given by equation 2.11.

$$EI\frac{d^4w}{dx^4} + k_s w(x,z) = -q(x,z) \tag{2.11}$$

where q is, the contact pressure among the soil-foundation interface at an arbitrary point (x, z), w is the corresponding vertical deformation/settlement, and k_s is the modulus of subgrade reaction.

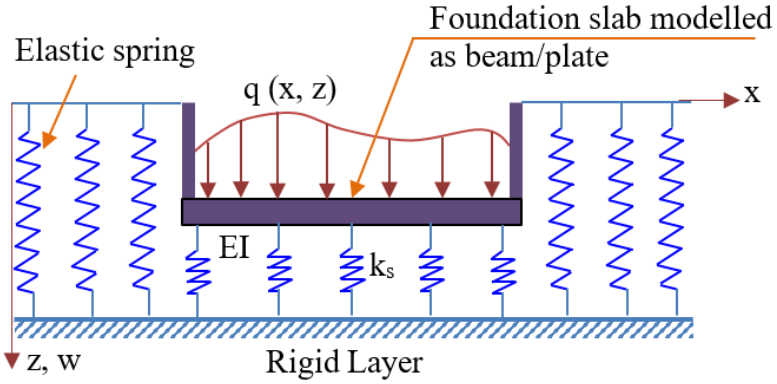

Figure 2.11 Winkler foundation-soil model.

The primary limitation of the Winkler theory, however, is that it only considers the vertical deformation of a series of springs located directly beneath the loaded area considering the soil's linear stress-strain behaviour alone. Accordingly, the impact of the externally exerted load gets confined to the point of its application only. It is also demanding to estimate accurately the elastic spring constant value. Several mathematical and empirical relationships have developed in the past to estimate the stiffness of elastic springs. The value of the subgrade reaction modules is dependent on the type of the subgrade as well as the size of the loaded region. As the subgrade stiffness is the sole parameter used to idealize the physical behaviour of the subgrade in the Winkler model, considerable caution should be given in determining it numerically and applying it to an SSI problem (Baker, 1957).

Despite these limitations, the Winkler model has remained in use due to its simplicity of the modelling procedure in practical applications, ease of implementation, low computing cost and time, and long-time familiarity with practicing engineers. The fact that, in more complex problems, due to soil parametric uncertainty might cause accuracy to be lost in analyses. As a result, numerous commercial software packages continued to include the model as a primary element of

their programs for the analysis and design of plates and beams on completely elastic foundations. More recently, Colasanti and Horvath (2010) presented the application of a new hybrid practical subgrade modelling software for improved SSI analysis that the model was developed in a companion paper (Horvath and Colasanti, 2011). Several studies (Bowles, 1997; Brown et al., 1977; Crouse et al., 1987; Gerolymos and Gazetas, 2006; Kramrisch and Rogers, 1961; Raychowdhury, 2011; Tahghighi and Mohammadi, 2020a; Varun et al., 2009; Vesic, 1961) have been undertaken based on the potential application of the Winkler model in the investigation of dynamic SSI problems. As a result, instead of carrying out an analysis utilizing the fixed base representation of structures, at the very least the Winkler model idealization must be used for practical purposes.

2.6.3.2 Foundation impedance function

A foundation impedance function is one of among a simplified spring-type models and often utilized by practical engineers. It characterizes the dynamic force-displacement relationship of a foundation having no mass embedded in or resting on an elastic soil medium, and varies depending on the soil profile, foundation geometry, and stiffness.

For a simple SDOF structure model with a surface foundation resting on an half-space elastic soil profile under a vertically propagating shear wave (Figure 2.12a), the motion of foundation can be appraised by utilizing a simplified model (Figure 2.12b) which represents the soil by a translational and rotation impedance functions and responds to the FFM. Each impedance function has imaginary and real components that are modelled parallelly by a spring and a dashpot, as given in equation 2.12.

$$\bar{k}_j(\omega) = k_j(\omega) + i\omega c_j(\omega) \tag{2.12}$$

where $\bar{k}$ is an impedance function that depends on the circular frequency of excitation motion ω and relates the generalized foundation forces F to the associated displacements u; i is the imaginary unity; j is an index represent the translation h and rotation θ modes of vibration; k is the spring stiffness; c is the dashpot viscous damping coefficient.

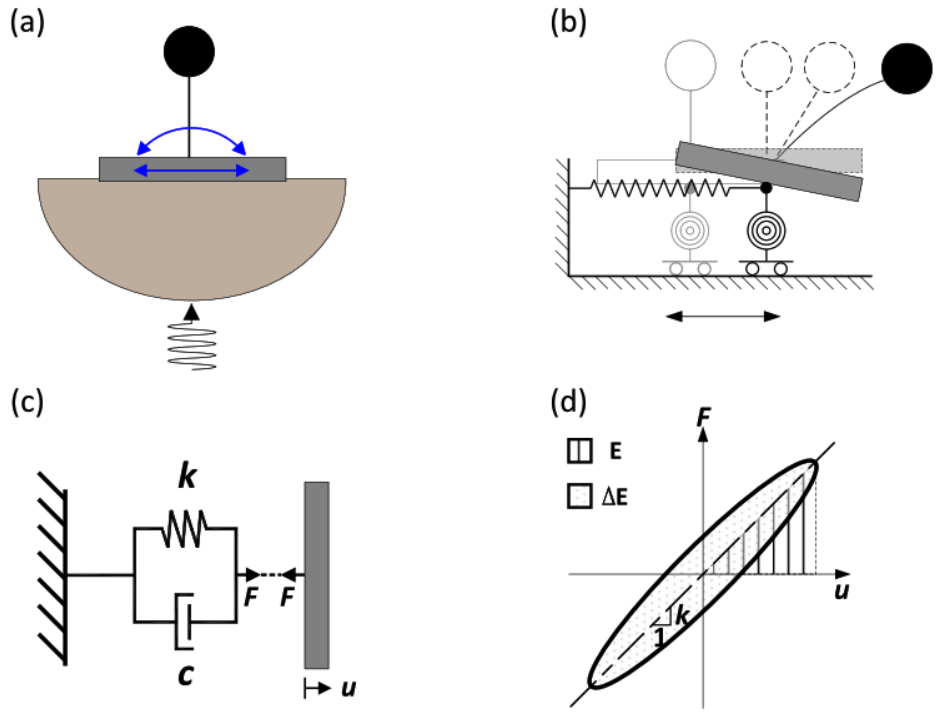

Figure 2.12 (a) A simple structure with surface foundation resting on an half-space elastic soil under vibration of a horizontal excitation; (b) a translational and a rotational impedance function represents the soil half-space; (c) physically representation of impedance functions; (d) the foundation impedance steady-state response (Lu, 2016).

The harmonic steady-state response of force-displacement configuration revealed in Figure 2.12c is illustrated in Figure 2.12d, it is quite comparable to the stress-strain loop depicted in Figure 2.8b. The area encompassed by the loop is equal to the dissipated energy over a force-displacement cycle ΔE (equation 2.13).

$$\Delta E = \pi c(\omega)\omega u^2(\omega) \tag{2.13}$$

where $u(\omega)$ is the displacement accompanying with the angular frequency of motion ω. The stored maximum elastic energy in a cycle E is obtained as:

$$E = \frac{1}{2}k(\omega)u^2(\omega) \tag{2.14}$$

Substituting equations 2.13 and 2.14 into equation 2.7, the damping ratio ξ is obtained as given by equation 2.15.

$$\xi = \frac{\omega c(\omega)}{2k(\omega)} \tag{2.15}$$

This foundation damping ratio incorporates effects from both soil nonlinearity and wave radiation, which is also valid when $k(\omega) > 0$.

Since a static foundation stiffness is related to a frequency independent stiffness, a frequency-dependent term can be obtained using $k_j(\omega)$ and explicitly expressed as a function of the static stiffness K_j and stiffness coefficient α_j:

$$k_j(\omega) = \alpha_j(\bar{\omega}, \upsilon, \xi_g)K_j \tag{2.16}$$

where υ is the Poisson's ratio of soil deposit; ξ_g is the hysteretic damping ratio of soil (equation 2.15); the dimensionless frequency $\bar{\omega}$ and static foundation stiffness K_j for a circular surface foundation are expressed as given in equation 2.17 and equations 2.18 – 2.19 (Poulos and Davis, 1974).

$$\bar{\omega} = \frac{\omega r}{V_s} \tag{2.17}$$

$$K_h = \frac{8Gr}{2 - \nu} \tag{2.18}$$

$$K_\theta = \frac{8Gr^3}{3(1 - \upsilon)} \tag{2.19}$$

where G is the shear modulus of the homogeneous soil deposit, and r is the radius of the foundation.

Luco and Westmann (1971) and Veletsos and Wei (1971) developed impedance functions for stiff circular foundations lying on an half-space perfectly elastic medium. The influences of foundation flexibility, shape, non-homogeneity variation of soil with depth, and embedment have been taken into account for through experimental or numerical methods (Apsel and Luco, 1987;

Bielak, 1974; Dobry and Gazetas, 1986; Elsabee and Morray, 1977; Iguchi and Luco, 1982; Kausel, 1974; Liou and Huang, 1994).

Although impedance functions can characterize the frequency-dependent response of the foundation force-displacement relationships, the performance of Fourier transforms are required in order to apply them in seismic SSI analyses. The structure nonlinear behaviour is not permitted in these analyses.

2.6.3.3 Discrete-element model based on cone theory

Simple models established by assembling springs, dashpots, and lumped masses to represent the influences of stiffness, damping, and inertia are more commonly utilized by practical engineers. A significant benefit of these models over the impedance functions is the frequency independence of each model element, which allows the model to be analyzed in the time domain taking into account the structural nonlinearity. Based on the cone theory, Ehlers (1942) proposed the first simplified lumped-element model, which was further expanded by Meek and Veletsos (1974), and Meek and Wolf (1992a, 1992b, 1994a, and 1994b). As illustrated in Figure 2.13, the essential principle of this theory is to replace the soil domain with a truncated cone.

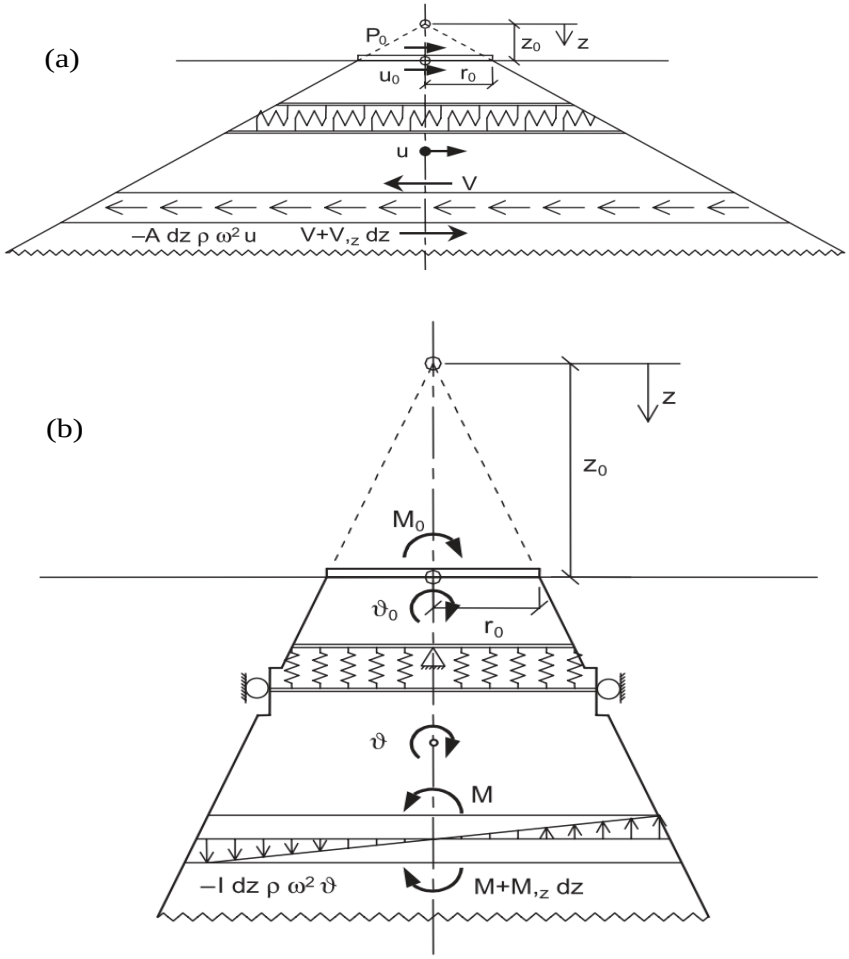

Figure 2.13 Equilibrium of infinitesimal element and truncated semi-infinite cones for (a) horizontal, and (b) rocking motion (adopted after (Wolf, 1994a)).

The simplified truncated semi-infinite cone model given by (Wolf, 1994b) has been widely utilized in practical applications to account for the SSI effects in structural response analysis (Mohasseb and Abdollahi, 2009). The proposed cone model's foundation dynamic-stiffness coefficient is close to the stiffness value reported by Gazetas (1991). The influence of frequency-dependent soil flexibility on the overall structural system behaviour is greater in the truncated semi-infinite cone model than in the Winkler model, which is based on frequency-independent behaviour (Bowles, 1997). In this method of analysis, the accompanying damping effect supplied by the soil to the entire system may also be appropriately accounted for it. Although, Izzuddin et al. (2007) suggested that this method is unable to account accurately for the nonlinearity behaviour caused by material and geometric factors while making assessing the nonlinear response of soil

and structural systems more difficult. However, there are several works in the literature dealing with the problem of including soil nonlinearity at least using an equivalent-linear approach (Brandenberg et al., 2015).

2.7 SSI in seismic design codes and standards

As already discussed in the previous sections, several studies have attempted to understand the significance of SSI on the response of building structures under seismic excitation. It is critical to comprehend which of these characteristics are crucial, as well as in what circumstances the SSI impacts should not be overlooked for proper structure analysis and design. Although numerous solutions have been proposed in the literature, a handful of international design codes and standards suggest some guidelines for incorporating SSI and making a compulsory consideration of SSI in their design. The following discussion lists various codes of practice and standard provisions related to the consideration of SSI.

2.7.1 Indian Standards

The Indian standard, IS 1893-3 (2014) mentions the detailed studies and fusion of SSI in the design of bridges for earthquake resistance, which are founded on deep foundations embedded in soft soil deposits. As the code suggested that the soil flexibilities included in modelling sub-structure and foundation of the bridge for SSI analysis it has ascertained that a longer natural period and reduced seismic demand forces while enhancing larger lateral displacements. In the analysis of industrial structures for seismic resistance and supported on a soil different from rock or rock-like material SSI effects are also need to be included (IS 1893 (Part 4), 2015). However, seismic codes for general buildings (IS 1893 (Part 1), 2016) and liquid retaining structures (IS 1893 (Part 2), 2014) are quiet about the phenomenon and also they do not recommend following other international codes and standard practices for consideration of SSI in the analysis and design of structures with embedded foundations.

2.7.2 Eurocode

Eurocode 8, EN 1998-5 (2004) recommends incorporation of dynamic SSI effect for tall structures which are either slender such as towers and chimneys or have second-order (P-δ) effects

that play a noteworthy role. Structures that rested on deeply embedded or massive foundations such as piles, bridge piers, silos, and offshore caissons also permit the inclusion of SSI in their design practice. In the design of structures to be supported on soils that typically have a very low value of shear wave velocity, $V_{s,30}$ (i.e., with $V_{s,30} < 100\, m/s$), small internal damping, an unusually extended range of linear behaviour, and can consequently produce abnormal seismic site amplification effects of SSI must be mandatorily taken in to account. Although the code suggests the conditions when SSI should be incorporated in design practice under seismic actions, it does not provide any explicit guidelines for computing SSI effects.

2.7.3 **Japan Standards**

The Japan standard, JSCE 15 (2007) suggests consideration of the dynamic interaction effects as compulsory among the structure and soil to assess the influence of earthquakes on the dynamic response characteristics difference among them. For seismic resistance design of structures like retaining walls, bridge abutments, basement walls, and deep-seated foundations such as piles and caissons require the consideration of the dynamic SSI among the SSS. Since the response of a structural system when subjected to seismic excitation is highly affected by the near-field soil within the vicinity of the subterranean levels, the analysis region is the entire structural system including the substructure system and the surrounding soil. Conversely, depending on the characteristics of the structural system and underlying soil type, however, the dynamic SSI can be ignored or modeled appropriately. In such instances, it is reasonable to model separately the structural system and the soil domain and perform the seismic response analysis of the structural system separately, i.e., a simplified (substructure) approach. If the effect of soil within the vicinity of the subterranean levels idealizes simply with springs and dashpots, only the structural system consider in the analysis region, and springs and dashpots are treated as boundary elements. Furthermore, the response of the structural system that expect to be affected by the separation of surrounding soil and subterranean levels, the code advises using interface components to characterize the influence of separation and sliding among the SSS. In addition, it recommends considering a large enough soil domain and usage of well-suited boundary conditions to ensure that input ground motion propagates properly. The code, on the other hand, makes no mention of identifying the scenarios in which the SSI effects must be disregarded.

2.7.4 **Mexicon Standards**

Due to the existence of soft soil conditions and earthquake incidences in important parts of Mexico City, SSI effects are a particularly sensitive issue. In the design of building structures, Mexico City Building Code (MCBC, 2004) provides specific and detailed regulations to account for the impacts of soft soil conditions and SSI. In addition, the code allows for the incorporation of SSI approximately by evaluating the structure's modified period (i.e., the ratio of the root-mean-square of the structure's period with fixed base conditions to the structure's period allowing just lateral and rocking movement). Therefore, an increased vibrational period has been observed from the result of the structure with a flexible base system.

2.7.5 **American Standards**

In addition to the foregoing international codes and guidelines, the most well-known codes of United States (ASCE/SEI 7-10, 2010; ASCE/SEI 7-16, 2018; FEMA 356, 2000; FEMA 440, 2005; FEMA 450, 2003; NIST, 2012; PEER, 2017) for seismic design practices prescribe the inclusion of SSI effects in various ways for the design of structures. Alternatives are (1) modifying the results of the non-flexible base analysis, (2) adjusting the FFM to FIM at the structure's base, and (3) incorporating the soil flexibility by a simplified (substructure) approach. ASCE/SEI 7-10 (2010) and FEMA 450 (2003) advised a base shear force reduction to be lower than seventy percent of the original value, by considering a longer modified natural period and higher damping revealed by structure systems compared to their non-flexible base complements. Alternatively, the code recommends that the flexibility of foundation is considered as an option and that the flexibility of soil is represented by an equivalent linear behaviour. This technique necessitates modifying the seismic input motion at the structure's base, and in that aspect, the former technique is more acceptable for design reasons. Because it provides guidelines for the modification of the FIM, FEMA 440 (2005) also can be utilized in combination with FEMA 356 (2000) and ATC 40 (1996). In contrast to non-flexible base models, the total foregoing set of guidelines focuses on reducing seismic demand on the structural system generated by kinematic interaction or foundation dampening effects.

Based on the survey of various codes of practice and standards on SSI, the majority of the international seismic resistance design codes provide some conditions for taking into account SSI throughout the design process. However, there are still no adequate guidelines for assessing the SSI effect and incorporating it into design practices. Concerning SSI provisions and procedures for its inclusion, the American standards and Japanese code are much more progressive. The latter recommends that SSI be modelled as exactly as possible using several constitutive models and interface non-linearity, whereas the former is primarily concerned with SSI design procedures and other linear models.

2.8 Seismic SSI Studies on Building with Subterranean Levels

The most widely built low-rise to the high-rise building structures in the urban area is planned with one or more subterranean levels for parking and other amenities. For all intents and practical purposes, it is necessary to study the effect of subterranean levels, foundations, and SSI on building structures to gain a comprehensive understanding of their response. This section discusses the application of SSI studies to building with subterranean levels based on existing literature. The majority of contemporary research in the field has been carried out for various reasons using different SSI analysis methods, namely: to assess the effects of SSI, to comprehend the influence of incorporating subterranean components, and to evaluate foundation soil modelling method effect on the seismic response of a certain type of building structure. In addition, to address the effect of filtering action induced by embedded subterranean modules on the kinematic translational and rotational interaction factors for seismic SSI analysis using the simplified three-step approach.

Naeim et al. (2008) investigated the impact of SSI modelling on the seismic performance of a moment resisting steel frame high-rise building with subterranean levels supported by a mat foundation in layered soil. Various simplified modelling methods, with or without the SSI effect, were utilized in this study. It has been observed that accounting correctly for soil/foundation deformations does not considerably alter the high-rise building vibration periods, but does have a significant influence on storey lateral displacement over the height of the building. Additionally, the two frequently used approximations in engineering practice such as fixing the base of the structure at ground level under input FFM, and modelling soil layers along subterranean levels

utilizing a series of horizontal springs, fixed at their far ends, and subjected to input FFM were failed to produce satisfactory results.

Stewart and Tileylioglu (2007) reviewed simple models that describe the effect of kinematic SSI based on a numerical method for embedded rigid foundations and successfully validated against recordings from nuclear structures characterized by very stiff embedded foundations. The foundation flexibility effect on foundation motion was evaluated using appropriately full-scale observation (instrumented building). Furthermore, they presented how the earthquake ground motions can apply as input motion for high-rise building structures seismic resistance analysis and subsequent design by using a substructure approach including subterranean levels. A comparison between a relatively well-suited proposed modelling method that anticipates being simulated realistically the SSI issues and modelling methods widely utilized in the seismic resistance design process was carried out in this study. It has been observed that the most prevalent fixed base modelling method utilized in engineering practice, in which the FIM is assumed to equal the FFM, was failed to capture many of the main characteristics of SSI. The impacts of kinematic interaction on the movements of subterranean levels, which may result in reduced ground motion lateral movement and the introduction of rotational movement, is one of the most important features that has not yet been discovered.

Ganainy and Naggar (2009) studied the seismic resistance performance of low- to mid-rise moment-resisting steel space frame buildings with from one to multi-level underground stories founded on a shallow foundation in a firm and soft soil deposit under synthetic earthquake records as input motion. In order to simulate the nonlinear behaviour of the foundation and the subterranean levels of the surrounding soil, the Beam-on-a-Nonlinear Winkler Foundation approach was adopted by the authors. In this investigation, emphasis was given to the effect of subterranean levels, base soil, and side soil on the seismic performance of the model buildings. The simulations were carried out using Perform-3D the nonlinear structural analysis program. The seismic performance of the structure was evaluated in the study in terms of structural system deformations and seismic force demand. It has been revealed that the incorporation of SSI in the analysis caused augmented shear and moment demands for buildings founded in soft soil. It has also been observed that the effect of SSI is considerable in the case of buildings supported on

compliant ground surfaces without subterranean levels but gradually reduced with the number of subterranean levels increased.

Saad et al. (2012) investigated the seismic response performance of low- to high-rise reinforced concrete buildings having multi-level underground floors resting on shallow foundations in stiff soil. The major goal of the study was twofold: (i) to assess the seismic performance of building structures in different subsurface soil conditions while altering the number of aboveground and subterranean levels; and to seek an appropriate recommendation concerning the inclusion of the number or percentage of subterranean levels in the modelling and analysis of reinforced concrete frame buildings. The multi-linear kinematic plastic link attribute in SAP2000 software was used to describe the behaviour of horizontal earth pressure acting on the basement walls, which was represented using force versus displacement functions (p-y curves). The seismic performance study was first carried out on a 2D frame model, with the results subsequently confirmed on a 3D model. Buildings modelled with a fixed base at the ground surface were adopted as a baseline, and then changes in the performance of buildings were investigated increasing the number of basements incrementally. The preliminary results have revealed that the inclusion of SSI plays a considerable effect in relatively low-rise buildings by increasing the seismic force demands such as story shear and moment. This effect has been visible, especially in buildings simulated on softer soils.

Anwar et al. (2019) assessed the importance of incorporating the influence of SSI on the seismic performance of a reinforced concrete core wall high-rise building with subterranean levels resting on mat foundation embedded in stratified soil. A 3D linear and nonlinear numerical analysis was carried out utilizing both direct and substructure approachs. This study intended to address some important practices and issues in the field of seismic SSI and to reveal the worth of incorporating SSI impacts in structural modelling and analysis while providing a comprehensive understanding of practical applications in real projects. It has been observed that using different modelling approaches and the incorporation of SSI could alter the seismic performance of the structure at different levels. Additionally, the direct modelling approach described in this investigation gives enhanced results in contrast with various approximate approaches. As a result, it has been proposed that the structural system dynamic behaviour could be studied more accurately by taking into account SSI effects and 3D modelling of near-field soil (direct modelling

approach) rather than idealizing the base of the structure with simplified (substructure) approaches and rigidly fixed support conditions.

Turan et al. (2013) utilized an experimental (i.e., shaking table test) and analytical method to perform the seismic SSI response analysis on buildings with subterranean levels resting in a stiff clay soil deposit. To enable for the examination of buildings with subterranean levels in this investigation, they modelled the structural system with an assembly of a simple SDOF system and a rigid segmental box foundation. The period of vibration was evaluated using shaking table test results and it was observed that the modified period ($\tilde{T}/T$) of the structure was reduced for the long-period structure whereas raised for the short-period structure, with increasing depth of embedment. The analytical method results have also been compared with experimental tests and they found that the analytical technique was also capable to account for the SSI effects within an acceptable range of accuracy and predict SSI effects.

It is important to mention that the SSI effects also depend on the type of subterranean level system and structural flexibility that exists beneath the superstructure. Vega et al. (2013) performed a 3D linear SSI analysis on a large non-slender partially embedded in a soil structure hosting a reservoir pumping unit. The analysis was conducted utilizing both the method of sub-structuring procedure under the assumption of a perfectly rigid structure and direct approach, in which the SSS was modelled as an interdependent system with its actual geometry and flexibility. This study aims to characterize the demand at the ground surface and specific points of the structure, as well as to assess the effect of the degree of flexibility of the structure on the response value. Results of SSI analyses indicated that considerable variation was shown among predictions using the two approaches. Furthermore, taking not into account for the flexibility of the structure results in a significant underestimation of spectral accelerations at specific locations.

Tehranizadeh and Barkhordari (2018) investigated the effect of wall openings along the periphery of the partially embedded subterranean level, as well as the number of subterranean levels on the base level of the metal-braced framed tube system in high-rise buildings. The evaluation was carried out on a 2D nonlinear soil-structure model utilizing a direct approach subjected to near-field earthquake ground motion with SSI. The findings revealed that where the opening was larger than fifty percent of the basement wall, the base level has to be one storey

lower than the ground level, implying that ignoring the influence of opening in high-rise building analysis could result in non-conservative outcomes. On the other hand, raising the number of basement floors from three to six has an insignificant effect on the structure-soil systems base level.

Piro et al. (2020) investigated the effects of SSI on the seismic performance of out-of-plane loaded unreinforced masonry buildings, which was representing the masonry building transverse sections, using a two-dimensional elastic soil-foundation-structure numerical model under earthquake excitation. In this investigation, different superstructures (two, three, and four-storeys), substructures (either a shallow foundation or underground floors), and homogeneous or layered soil configurations were considered. The effectiveness of simplified (analytical) approaches in capturing the dynamic out-of-plane response was also investigated under the effects of SSI in comparison to the numerical model. According to the numerical model results, the dynamic response of the structure was influenced by SSI, and in turn, such interactions were also dependent on the deformability of soil. Whereas, the effects of SSI were reduced due to the presence of subterranean floors and increasing superstructure height. Analyses of structures rested on stratified soil deposits reveal that the upper soil layer, rather than the stiffer foundation soil, has the most impact on the fundamental period. In this regard, an equivalent soil-structure stiffness parameter was presented to incorporate the contribution of embedded subterranean levels and/or a stratified sub-soil deposit, greatly improving analytical fundamental frequency predictions.

Scarfone et al. (2020) assessed the dynamic SSI effect and the foundation system role on a high-rise building having a wall-frame structural system in two different soil profiles. In this assessment, three foundation systems: – a shallow mat foundation, a deep mat foundation, and a pile foundation with basement floors were considered. A 3D numerical analysis was performed using the FLAC3D finite difference program by applying the standard boundary conditions during static and dynamic loading stages. The soil domain was modelled using an elastic-perfectly plastic material with Mohr-Coulomb failure criteria as well as a standard non-associated flow rule in this study. A hysteretic model was used to incorporate nonlinear and hysteretic behaviour for stress paths inside the yield surface during the dynamic stage. It has been demonstrated that increasing foundation flexibility reduces the maximum seismic force demand, leading to a larger rigid rotation of the foundation, but not considerably higher structural displacements.

Hoseny et al. (2022 and 2023) carried out both laboratory tests using shaking table tests as well as numerical simulations in order to verify the suitability of the small scaling factor method in the dynamic response analysis and investigate the seismic behaviour of tall buildings with subterranean levels taking into account the effect of different embedment depths and SSI. Since the concrete structure models are not favorable for small-scaled tests, equivalent steel structure models have been created using the similitude rule. Because of the dimensions and maximum load capacity of the shaking table and similitude laws, a geometrical scaling factor (λ) of 1:50 has been adopted for both structural and soil models. PLAXIS 3D software was used to implement the numerical scaled coupled models, which were then verified using the experimental results. The building frame response results show that, in comparison to a fixed base, the SSI plays a crucial role in amplifying the lateral deflection of structures, and that the embedded depths have a substantial impact on the lateral seismic response of the buildings under consideration.

In addation to the influence of subterranean levels on the seismic response performance of building structures, it can be significantly influences the characteristics and magnitude of the input ground motion at the foundation level due to the kinematic SSI and nonlinearity effects (Stewart, 2000). Based on the characteristics of ground motion, the properties of the soil deposit, the stiffness of the foundation and subterranean components, and embedment depth, the seismic signal frequency may be attenuated and this impacts the seismic response of the structure.

Elsabee and Morray (1977) derived simplified rules and formulas for the first time to account for the foundation embedment effect in the analysis of SSI problems from the results of parametric studies of a three-dimensional cylindrical axisymmetric finite element formulation. The well-known substructure approach was adopted for parametric studies under shear waves propagating vertically. They suggested that these simplified procedures could be employed at least for preliminary analyses in order to assess the significance of the SSI effect and other parameters.

More recently, Conti et al. (2017 and 2018) studied the filtering effect caused by embedded rigid rectangular massless and massive foundations using both theoretical and numerical approaches in a homogeneous half-space under vertically propagating shear wave velocity. The authors presented new analytical expressions for KI influence factors based on the results of the parametric investigation, which was an improved version of Elsabee and Morray (1977).

Furthermore, a significant favourable effect on filtering action has been reported for high values of foundation width (B)-to-embedment depth (D) ratio (B/D > 4) and foundation-to-soil mass density.

Sotiriadis et al. (2019 and 2020) assessed the influence of SSI on foundation-level motions directly utilizing real earthquake signals of the instrumented building structures with subterranean levels. Instrumentation is present at both the foundation level of the buildings and the ground surface. For investigation, the substructure approach was applied in the frequency domain. From results of the study observed that due to the presence of the building's subterranean components, the high frequencies of the ground motion at the level of the foundation have been filtered significantly compared to the FFM.

2.9 Summary/Concluding Remarks

A comprehensive review of the literature was carried out as explained in the above sections, covering seismic response of building structure obtained from experimentation, theoretical and numerical methods, as well as different aspects of SSI studies by considering the superstructure, substructure, and soil as a single unit. After a detailed literature survey, the following observations can be made:

- Numerous research works are available on the interaction analysis of the building structure without subterranean levels resting on the shallow and deep foundations subjected to seismic loads.
- In the case of the SSI analysis, most of the researchers have focused on the seismic response behaviour of the superstructure by varying the foundation types and soil parameters.
- Structures resting on compliant soil exhibit different seismic responses compared to their fixed-base conditions. This alteration results from KI and inertial interaction.
- A fixed-base model cannot account for SSI effects whilst failing to capture the effects of subterranean system and foundation flexibility, as well as kinematic interaction on the motions of shallow to deeply seated foundations.

Very few researchers have highlighted the consideration of the subterranean levels flexibility effect on the seismic response behaviour of building frames resting on different foundations subjected to seismic loads by incorporating the SSI effect.

CHAPTER - 3

METHODOLOGY

3.1 Introduction

This chapter presents the methodology adopted to comprehend the influence of subterranean levels on the seismic response behaviour of building frames in various subsoil conditions under the influence of selected seismic excitation. The adopted system under investigation, the materials used, and earthquake input motions are presented in detail. Different elements of the structural system, as well as bounded and unbounded soil domains for SSS finite element models in the ABAQUS software, are also explained. Validation of the finite element models with a simulation of seismic wave propagation and previous experimental studies have been provided in this chapter.

3.2 Methodology

Building structures featuring subterranean levels could alter the characteristic and magnitude of the foundation level motion, as well as the seismic response behaviour of the superstructure. The research methodology adopted for achieving the objectives in the present work is given in Figure 3.1.

In order to comprehend various influences due to the presence of subterranean levels in the seismic resistance design of building structure, the total work has been divided into four phases.

Phase I: Numerical analysis to study the influence of subterranean levels on the foundation input motions subjected to earthquake ground motion.

Phase II: Evaluation of the applicability range of theoretical models for quantifying the foundation input motion in comparison to nonlinear numerical models.

Phase III: Assessment of different alternative modelling approaches for seismic response history analysis of building frame structure with subterranean levels under excitation of earthquake ground motions using numerical analysis.

Phase IV: Investigation of the influence of subterranean levels and embedment depths on the seismic response of the building frame considering SSI subjected to seismic loads by conducting numerical analysis.

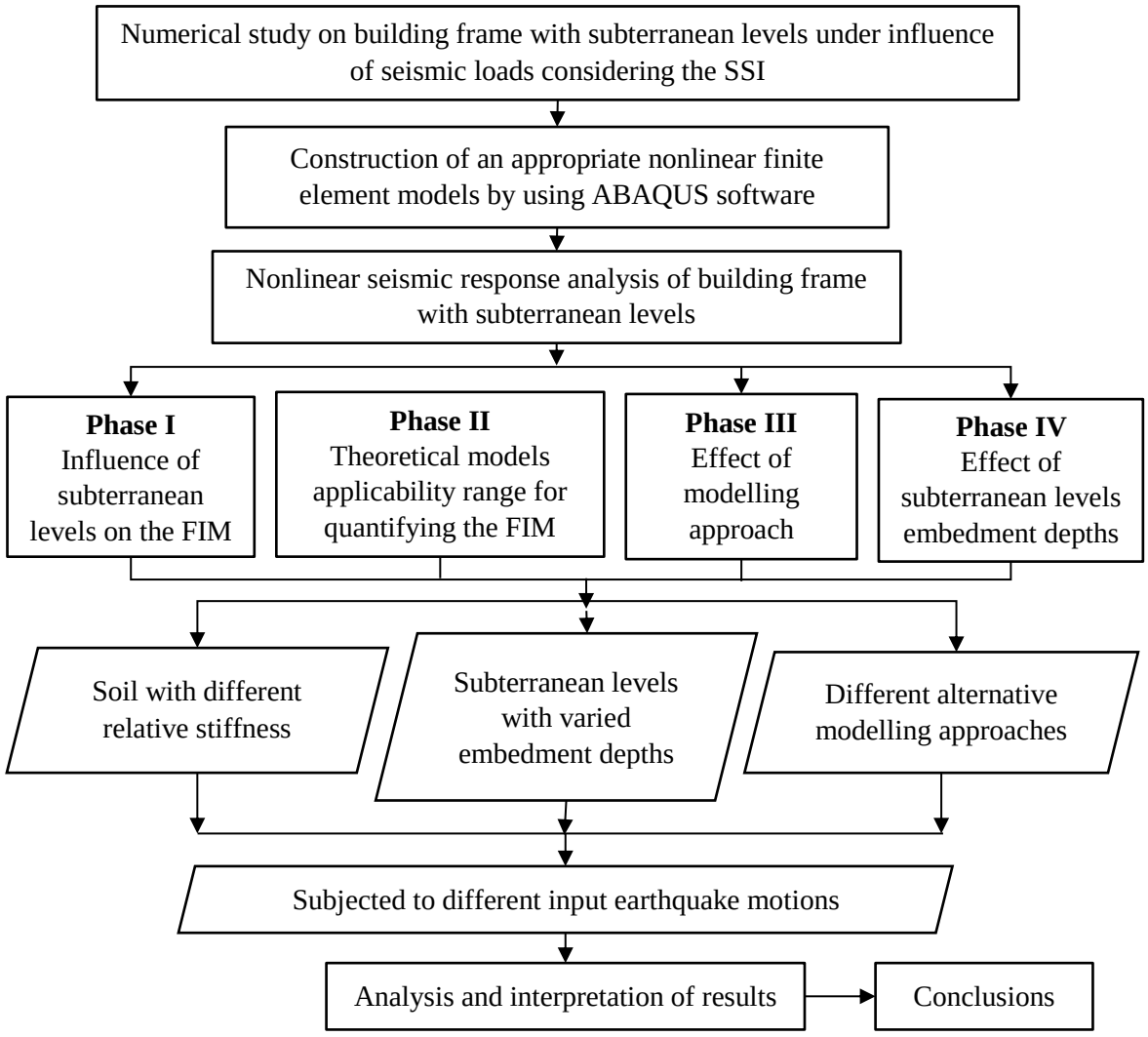

Figure 3.1 Schematic diagram of the methodology adopted for the research work.

The details of work done in each phase is explained below.

Phase I: Numerical analysis to study the influence of subterranean levels on the foundation input motions subjected to earthquake ground motion.

A substructure approach is often utilizes in seismic response analysis of building structures built on compliant foundations (see section 2.5.2 Figure 2.6), in which the subterranean

components, mostly soil, are not directly integrated, but are instead replaced by foundation impedance (springs and dashpots), and the analyses are performed subjected to the excitation of ground motion at the structure foundation level. The ground motion is suitable for input to the foundation-level or free end of the springs, also referred to as the foundation input motion (FIM). Two-dimensional numerical nonlinear kinematic SSI analyses were performed to evaluate the influence of subterranean levels on the foundation input motions. The details of soils and the criteria used for this study are given in Tables 3.1 and 3.2, respectively.

Table 3.1 Engineering properties of the soil considered in this study (Massumi and Tabatabaiefar, 2007; Tabatabaiefar and Fatahi, 2014b).

Soil property	Notation	Unit	Value		
			Soil type (ASCE/SEI 7-10, 2010)		
			C (dense GM)	D (medium CL)	E (soft CL)
Shear wave velocity	$V_{s,30}$	m/s	600	320	150
Shear modulus	G_{max}	MPa	623.4	177.3	33.1
Mass density	ρ	kg/m^3	1765	1716	1470
Elastic modulus	E	MPa	1608.3	484.9	91.7
Poisson's ratio	υ	-	0.28	0.39	0.40
Plasticity index	PI	%	-	20	15
Cohesion stress	C'	kPa	5	20	20
Angle of internal friction	ϕ'	Deg.	40	19	12
Damping	ξ	%	5	5	5

Table 3.2 The details of Phase I.

Subsurface soil condition	Soil type D and E as per ASCE/SEI 7-10 (2010)
Material and structural system	RC-MRF building
Number of storey above ground	15-storey (15S)
Number of underground storey	0BS, 1BS, 3BS, and 5BS, where BS = basement storey
Selected model for kinematic SSI study	Detailed 2D Finite Element Method - direct approach (see section 3.5.2.1)
Seismic input motion	7 (seven) earthquake input motion as per ASCE/SEI 7-16 (2018)

Phase II: Evaluation of the applicability range of theoretical models for quantifying the foundation input motion in comparison to nonlinear numerical models.

The theoretical transfer function models often used in the literature to estimate the FIM was assessed in this study. The simplified analytical expressions documented in NIST (2012) and presented by Conti et al. (2018) were employed in this investigation. The details of phase II are given in Table 3.3.

Table 3.3 The details of Phase II.

Subsurface soil condition	Soil type D and E as per ASCE/SEI 7-10 (2010)
Number of underground storey	0BS, 1BS, 3BS, and 5BS
Selected theoretical models	NIST (2012) and Conti et al. (2018) (see section 3.4.1)

Phase III: Assessment of different alternative modelling approaches for seismic response history analysis of building frame structure with subterranean levels under excitation of earthquake ground motions using numerical analysis.

Three-dimensional numerical nonlinear seismic response analyses were performed to assess the effect of alternative modeling approaches of building frame structures with subterranean levels for response history analysis. The parameters used for the study under seismic loads are given in Table 3.4.

Table 3.4 The details of Phase III.

Subsurface soil condition	Soil type C, D and E as per ASCE/SEI 7-10 (2010)
Material and structural system	RC-MRF building
Number of storey above ground	15-storey (15S)
Number of underground storey	0BS and 3BS
Selected model type for seismic SSI study	Model 1A, 1B, 2A, 2B, and 3A (see section 3.5.2.2)
Modelling approaches	• Conventional method, i.e., Fixed-base model (Model 1A and 1B) • Spring-Dashpot model (Model 2A and 2B) • Detailed 3D Finite Element Method (Model 3A)
Seismic Input motion	7 (seven) earthquake input motion as per ASCE/SEI 7-16 (2018)

Phase IV: Investigation of the influence of subterranean levels and embedment depths on the seismic response of the building frame considering SSI subjected to seismic loads by conducting numerical analysis.

Direct approach 3D nonlinear SSI seismic response analysis was executed to investigate the effect of subterranean levels and embedment depth on the seismic response of the building frame. The criteria used for the study are given in Table 3.5.

Table 3.5 The details of Phase IV.

Subsurface soil condition	Soil type C, D and E as per ASCE/SEI 7-10 (2010)
Material and structural system	RC-MRF building
Number of storey above ground	15-storey (15S)
Number of underground storey	0BS 1BS, 3BS, and 5BS
Selected model for seismic SSI study	Model 1A and 3A
Modelling approaches	• Conventional method, i.e., Fixed –Base model (Model 1A) • Detailed 3D Finite Element Method (Model 3A)
Seismic Input motion	7 (seven) earthquake input motion as per ASCE/SEI 7-16 (2018)

A detailed description of the system under investigation, materials used, and the numerical analysis has been given in the subsequent sections.

3.3 System under investigation

3.3.1 Studied building

A 15-storey RC-MRF building regular in elevation (Figure 3.2a) and plan (Figure 3.2b), representing the conventional medium-rise buildings in zone – V as per IS 1893-1 (2016) was considered for this study. The preliminary sections of the building frames of the superstructure were specified after performing a regular design procedures that was governed by Indian standards IS 456 (2000) after undertaking dynamic response spectrum analysis with a fixed-base condition at the ground surface.

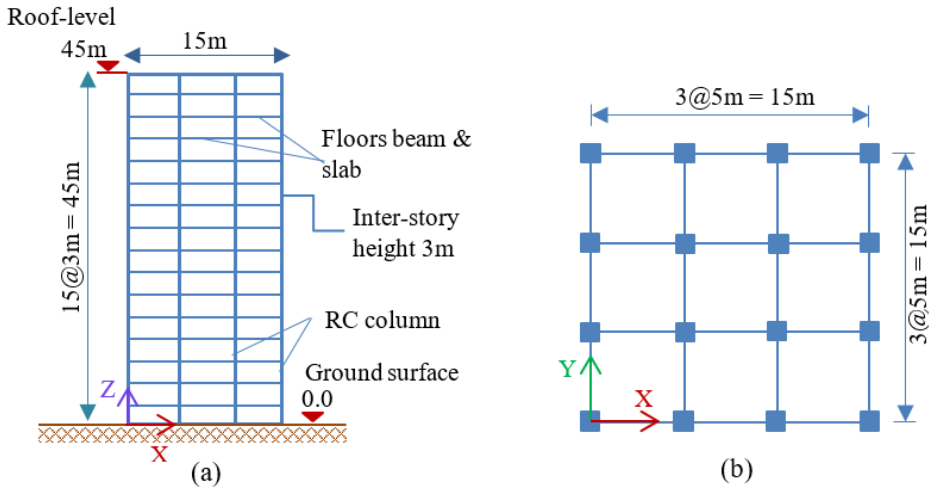

Figure 3.2 The layout of the fifteen-storey RC-MRF building adopted in the study: (a) elevation view of the superstructure; and (b) the building typical floor plan.

SAP2000 (CSI, 2020) software was utilized for the analysis and design of the building frames. The specified preliminary building frame sections would be augmented by the subterranean levels, foundation and the compliant underlying soil for further seismic performance analysis. Instead of evaluating the seismic design of building frames, this study aimed to assess the influence of foundation soil modelling and subsurface levels on the seismic performance of the superstructure. Thus, the column sections were increased below ground to account for the

additional gravity loads from the subterranean levels. According to IS 875-1 (1997) and IS 875-2 (1987), the material strength of the structure and the gravity loads, which comprising both permanent and superimposed actions, were estimated and incorporated to the structural model. The characteristic compressive strength of concrete (f_{ck}) and the yielding strength of reinforcement steel (f_y) are assumed to be M30 and Fe415, respectively. The value of the elastic modulus of concrete (Ec, MPa) was estimated as given in equation 3.1 according to IS 456 (2000) clause 6.2.3.1.

$$E_C = 5000\sqrt{f_{ck}} \tag{3.1}$$

Table 3.6 provides the characteristics of the concrete and steel reinforcement used in structural designs.

Table 3.6 Characteristics of concrete and steel reinforcement used in structural designs.

Concrete grade	Steel reinforcement grade	Elastic modulus, E (MPa)	Poisson's ratio, ν
M30 (f'_c = 30MPa)	Fe415 (f_y = 415MPa)	27386.13	0.2

The super dead loads (1.5 kN/m^2) and super-imposed loads (3 kN/m^2 floor live load and 1.5 kN/m^2 roof live load) were adopted. The loads were calculated as uniformly distributed loads over the floors. In accordance with IS 1893-1 (2016), the seismic design parameters such as zone factor, Z = 0.36, response reduction factor, R = 5, importance factor, I = 1.5, soil condition (Type-III), and damping, ξ = 5% were considered.

In dynamic analysis, the P-Delta effects were considered according to IS 456 (2000). Furthermore, cracking of the structural elements should be controlled during the design stage for a concrete structure to be serviceable. In order to reflect this, the stiffness values of the structural members (EI) corresponding to the uncracked sections were multiplied by stiffness modification coefficients in accordance with IS 16700 (2017). Table 3.7 presents the section of building structure members which represent the structural standards and construction practices of building structures, and which were specifically utilized to assess the influence of foundation soil modeling and subterranean levels on the seismic performance of the building in this study.

Table 3.7 Details of designed structural sections of RC-MR building frame.

Level	Elevation (m)	Column sections			Beam sections		
		A_s (m^2)	I_x (m^4)	I_y (m^4)	A_s (m^2)	I_x (m^4)	I_y (m^4)
Basement	-9.0 – 0.0	0.4225	1.49E-02	1.49E-02	0.2275	8.01E-03	2.32E-03
1	0.0 - 9.0	0.36	1.08E-02	1.08E-02	0.2275	8.01E-03	2.32E-03
2	9.0 - 18.0	0.3025	7.63E-03	7.63E-03	0.21	6.30E-03	2.14E-03
3	18.0 - 27.0	0.25	5.21E-03	5.21E-03	0.1925	4.85E-03	1.97E-03
4	27.0 - 36.0	0.2025	3.42E-03	3.42E-03	0.175	3.65E-03	1.79E-03
5	36.0 - 45.0	0.16	2.13E-03	2.13E-03	0.1575	2.66E-03	1.61E-03

Floor slab, t_s (m)	Basement wall, t_w (m)	Foundation, t_f (m)
0.15	0.25	1

In the present study, a reinforced concrete mat foundation is selected without and with subterranean levels (Figure 3.3). Following the routine engineering design procedures (Bowles, 1997; IS 456, 2000), the mat foundation was designed to support the structure against static and dynamic loads, as well as to meet the requirements for bearing capacity and maximum settlement, while basement retaining walls to support the lateral earth pressure, the bending moment and shear. The detailed characteristics of the floor slabs, basement walls, and foundation are presented in Table 3.7.

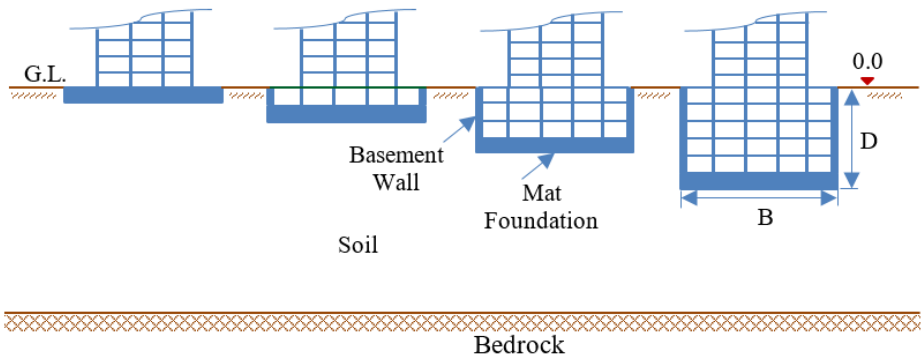

Figure 3.3 The subterranean levels layout with 0, 1, 3, and 5 subterranean levels.

3.3.2 Soil profiles

The structural systems selected in this study seated on deep homogenous dense, medium, and soft soil that is categorized as soil type C (i.e., Vs = 360 - 760 m/s), D (i.e., Vs = 150 - 360 m/s), and E (i.e., Vs less than 150 m/s), respectively, according to ASCE/SEI 7-10 (2010). It is described as a site having a soil profile depth of more than 10m and an average shear wave velocity, $V_{s,30}$ of 600 m/s or less. Table 3.1 presents the geotechnical parameters of the soils utilized in this study. These subsoils were obtained from field and laboratory tests (Massumi and Tabatabaiefar, 2007; Tabatabaiefar and Fatahi, 2014b), so they are preferable to the presumptive ones. In this study, the water table is considered to be below the bedrock, the soil profile is uniform, and the shear-wave velocity is consistent with depth.

3.3.3 Earthquake Records

The nonlinear time history analysis is usually acknowledged to be a more accurate analysis, however, selecting the appropriate earthquake motions is not an easy operation. As earthquake motions are not always readily available, it involves a variety of criteria for a given building site. In the lack of such data for the evaluated building models, there are many resources available on the web which provide an earthquake record. In this study, a suite of seven acceleration data from major earthquake events was acquired on the selected types of soil classes for the analyses consistently according to ASCE/SEI 7-16 (2018) from the PEER strong motion database (PEER). Magnitude, source mechanism, distance, and fault type were used as selection criteria to confirm the consistency of the records. These earthquake ground motions were imposed onto the FEM numerical simulation while carrying out a nonlinear time history analysis. As presented in Figure 3.4 and Table 3.8, unscaled seven earthquake ground motions from different locations of the world were chosen. To be consistent for designed RC-MRF building model bases and subsurface soil types, the selected motions have a shear velocity of less than 600 m/s at the recording station. The chosen earthquake ground motions are FFM. To determine the signal at the top of the bedrock, it is necessary to solve an inverse wave propagation problem (deconvolution) and rebuild the acceleration time history from the FFM.

Table 3.8 Earthquake ground motion data considered for the present study.

ID	Earthquake Event	Year	Station	Mw (R)	Mechanism	Distance (km)	PGA (g)
EQ1	Christchurch, New Zealand	2011	Christchurch Resthaven	6.2	Reverse Oblique	5.13	0.371
EQ2	Kobe, Japan	1995	Takatori	6.9	Strike Slip	1.47	0.671
EQ3	Imperial Valley-06	1979	Holtville Post Office	6.53	Strike Slip	7.5	0.258
EQ4	Erzican, Turkey	1992	Erzincan	6.69	Strike Slip	4.38	0.496
EQ5	Friuli, Italy-01	1976	Tolmezzo	6.5	Reverse	15.82	0.357
EQ6	Umbria Marche, Italy	1997	Assisi-Stallone	6.0	Normal	16.55	0.188
EQ7	Loma Prieta	1989	Anderson Dam (Downstream)	6.93	Reverse Oblique	20.26	0.246

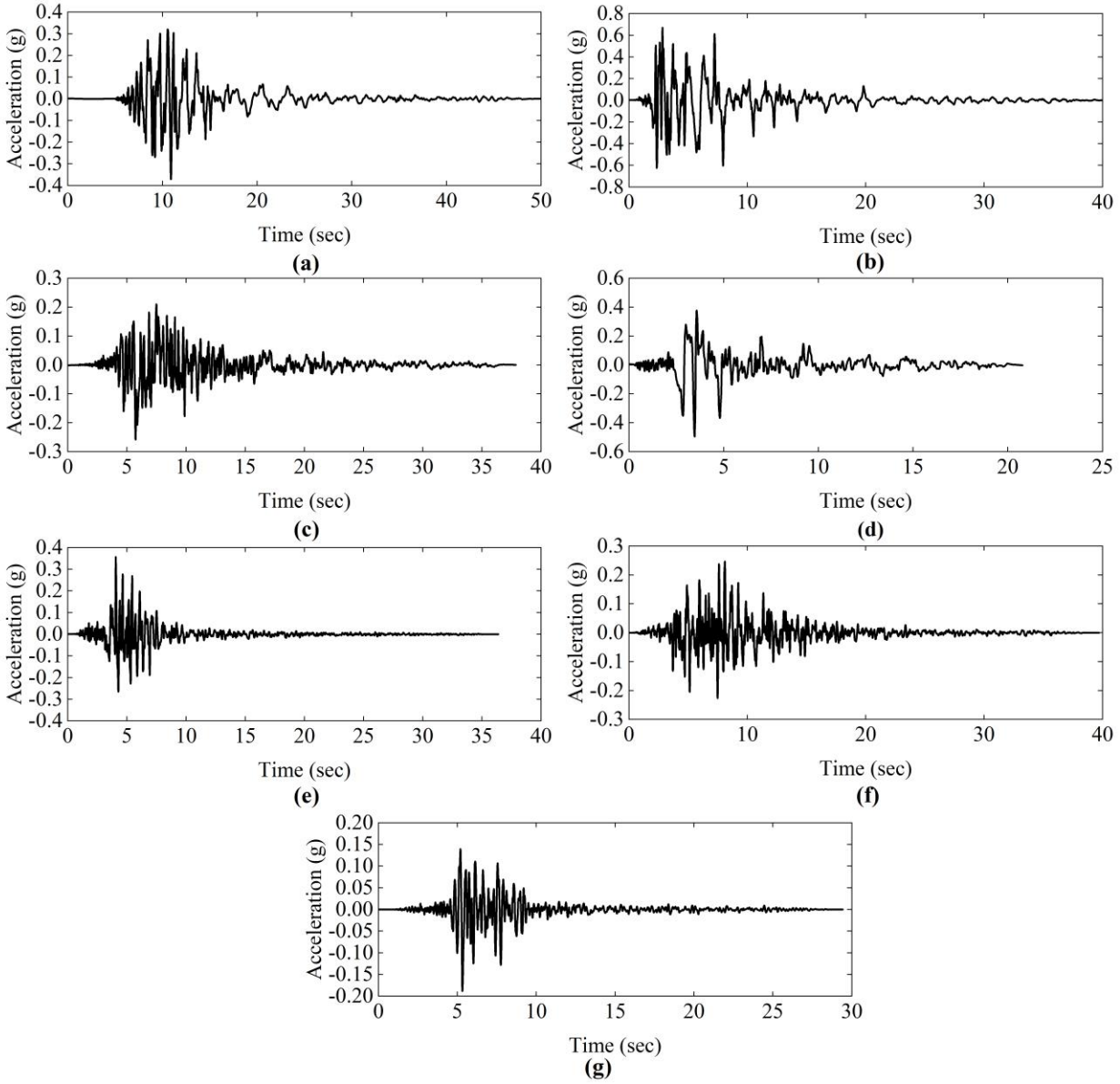

Figure 3.4 Utilized earthquake ground motions in this study: (a) Christchurch earthquake (2011), (b) Kobe earthquake (1995), (c) Imperial Valley-06 earthquake (1979), (d) Erzican earthquake (1992), (e) Friuli earthquake (1976), (f) Umbria Marche earthquake (1997), and (g) Loma Prieta earthquake (1989).

3.4 Transfer function

Transfer functions (KI factor) represent the ratio in the frequency domain of two ground motions, at foundation level to free-field ones. As a result, these functions make it simple to

determine the KI impacts in terms of changes in a ground motion at the structure foundation level relative to the FFM. In this process, besides standard baseline and filtering correction, signal processing may be required for the evaluation of transfer functions, such as windowing (to obtain the S-wave portion of the record) and smoothing (to attenuate scatter that can hide physically significant trends) (Mikami et al., 2008) as illustrated in Figure 3.5.

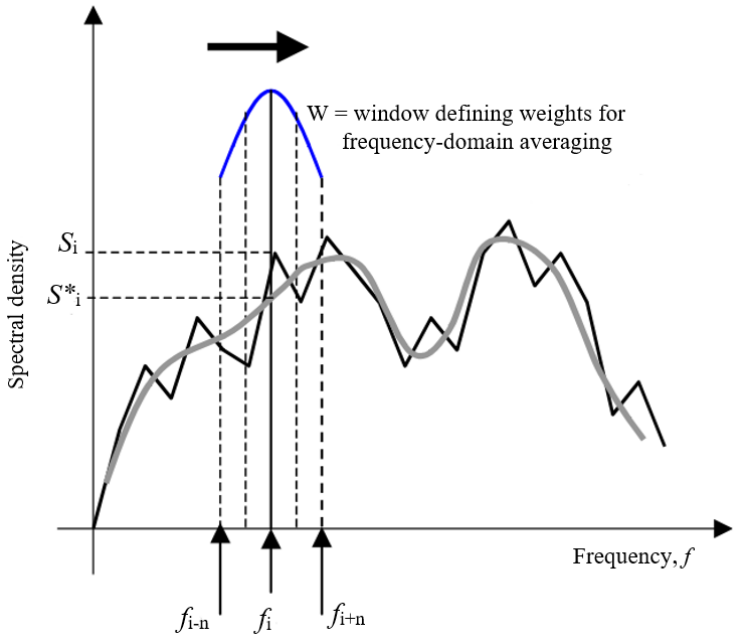

Figure 3.5 Schematic depiction of unsmoothed (original) and smoothed spectral density function including window characteristics employed in frequency domain smoothing (Mikami et al., 2008).

However, while the window length and degree of smoothing can have a local effect on the transfer function ordinates, the general shape and magnitude of the transfer functions remain essentially unchanged (Mikami et al., 2008). Because of this, in the present investigation, a simple moving average was used to analyse the transfer functions that were derived numerically, which was adequate to enable easy comparisons between the numerical and the analytical transfer functions that were reported in the previous studies. Transfer function models are often expressed by the translational and rotational components of the FFM. However, when the slenderness of the embedment (D/B) is small, as it is for the building adopted in this study, the rotational component of the transfer function is not considered to be significant. Hence, only the translational components of the transfer functions of numerical solutions were considered in this study.

3.4.1 Analytical-based solution of transfer function

In this study, two translational transfer function models were adopted from the literature to evaluate the applicability range of such closed-form solutions for SSI response analysis. The first model is the one reported by NIST (2012). It is an analytical solution proposed by Day (1978) and Kausel et al. (1978), applicable to rigid cylinders embedded in a homogeneous soil of finite or infinite thickness (half-space). This transfer functions model can be adapted to rectangular shapes embedded foundation and the horizontal foundation translation transfer function component is expressed in NIST as given in equation 3.2.

$$I_u\left(\frac{\omega D}{V_s}\right) = \frac{u_{FIM}}{u_g} = \begin{cases} cos\left(\frac{\omega D}{V_s}\right), & \frac{\omega D}{V_s} < 1.1 \\ 0.45, & \frac{\omega D}{V_s} > 1.1 \end{cases} \tag{3.2}$$

The other transfer function model assessed in this assessment is the simple analytical expression proposed by Conti et al. (2018) for rigid massless and massive embedded foundations (equation 3.3). This is an improved version of Elsabee and Morray (1977) taking into account the normalized parameters such as B/D, $\omega D/V_s$, and ρ_F/ρ_s.

$$\left|I_u\left(\frac{B}{D},\frac{\rho_F}{\rho_s},\frac{\omega D}{V_s}\right)\right| = \frac{a_1}{\sqrt{1+\left(\frac{\rho_F}{\rho_s}.\frac{\omega D}{V_s}\right)^2}} + \frac{(1-a_1)}{\left[1+\left(\frac{\omega D}{V_s}\right)^2\right]^{a_1 a_3}}.\left|cos\left(a_2\frac{\omega D}{V_s}\right)\right| \tag{3.3}$$

where a_1, a_2 and a_3 are the coefficients depending on the ratio B/D and ρ_F/ρ_s whose expressions are given in equation 3.4. ρ_F and ρ_s are foundation and soil mass densities.

$$a_1\left(\frac{B}{D},\frac{\rho_F}{\rho_S}\right) = \frac{(B/D)^\alpha}{\beta+(B/D)^\alpha} \qquad \alpha = 1.0 + 0.6\left(\frac{\rho_F}{\rho_S}\right) \quad \beta = 3.3 - 1.4\left(\frac{\rho_F}{\rho_S}\right)$$

$$a_2\left(\frac{B}{D}\right) = \frac{1+0.7(B/D)}{1+(B/D)} \tag{3.4}$$

$$a_3\left(\frac{\rho_F}{\rho_S}\right) = 2.2 - 1.6\left(\frac{\rho_F}{\rho_S}\right)$$

3.5 Numerical modeling development and analysis

In the present study, the seismic response analyses were carried out using FEM based ABAQUS (Duval et al., 2014) software to study the SSS interaction. The structural members were modeled to behave linearly and nonlinearly in the case of KI analysis and for dynamic response analyses, respectively, whereas the soil was simulated to behave nonlinearly for both analyses. The details of the adopted numerical models are presented in the following sections.

3.5.1 Elements of the structural system and soil modeling

The reinforcement concrete frame structural elements (beams and columns) were modeled using standard 2-node linear beam elements in a plane (B21) and a space (B31) for 2D and 3D numerical analyses, respectively. The floor slabs, basement walls, and foundation (in the case of a plane (2D) model) were modeled using a 4-node, quadrilateral, stress/displacement shell element with reduced integration (S4R). In the case of 2D KI analysis, the soil was simulated using 2D plane strain shell element CPE4R (4-noded bilinear plane strain quadrilateral, reduced integration, hourglass control). The foundation element and soil were simulated with 3D solid (continuum) elements, 8-node linear brick, reduced integration, hourglass control (C3D8R) for 3D dynamic response analyses. The element types utilized in the finite element models are shown in Figure 3.6.

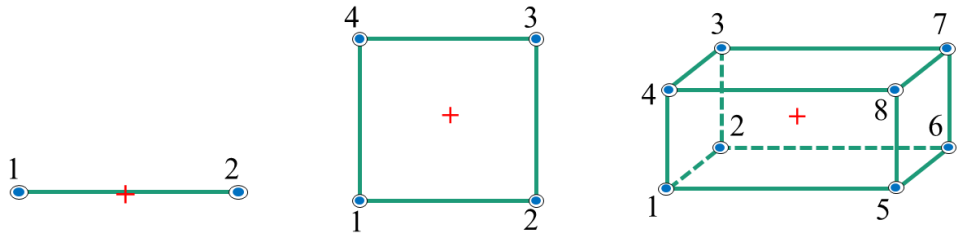

Figure 3.6 Different types of elements used in the finite-element model for elements of the structure and soil (a) beam element (B21/B31: Beam, 2-D/3-D, 1st-order interpolation (2-node linear)), (b) Shell element (S4R: Shell, 4-node, Reduced integration or CPE4R: Continuum, Plane Strain, 4-node, Reduced integration), basement walls, and foundation in plane/space models, and (c) Solid element (C3D8R: Continuum, 3-D, 8-node, Reduced integration).

For nonlinear analysis, the structural elements were modeled by applying an elastoplastic constitutive model that considered Rayleigh damping. According to Ryan and Polanco (2008), the Rayleigh damping matrix [C] has a linear combination of mass-proportional and stiffness-proportional components as given in equation 3.5.

$$[C] = \alpha[M] + \beta[K] \tag{3.5}$$

where [K] and [M] are, respectively, the stiffness and mass matrix of the structural system. α and β are the model coefficients, chosen to determine the model damping ratio in two modes. By assuming the same damping ratio (ξ), 5% considered in this study, for two selected modes with frequencies ω_i and ω_j, the model coefficients α and β are calculated as given in equations 3.6 and 3.7.

$$\alpha = \xi \frac{2\omega_i \omega_j}{\omega_i + \omega_j} \tag{3.6}$$

$$\beta = \xi \frac{2}{\omega_i + \omega_j} \tag{3.7}$$

The damping ratio, on the other hand, in any vibration mode with frequency ω_n for given model coefficients can be estimated by using equation 3.8 (Chopra, 2007).

$$\xi_n = \frac{\alpha}{2\omega_n} + \frac{\beta\omega_n}{2} \tag{3.8}$$

The two frequencies, ω_i and ω_j in equations 3.6 and 3.7 respectively, are usually assigned to be the frequency of the first and other higher modes, such that damping is confined over the frequency range that encompasses the majority of the modal involvement. Accordingly, the first and higher mode frequency of the system was selected to take into account the important modes of the soil-structure system in this study.

The elements of each structural system were specified by their material and geometric properties; however, they are linear-elastic materials by default with no failure limit, though the plastic moment capacity can be applied to consider the structural system's inelastic behavior. In the present study, the inelastic behavior of structural systems was simulated utilizing elastic-

perfectly plastic material behavior by specifying the yield stress. It is assumed that structural elements behave elastically until they reach the defined yield stress, after which the element that reaches its yield stress can continue to deform without inducing additional stresses.

3.5.2 Soil-structure system modeling

The need for consideration of subterranean levels and incorporating SSI in the analysis of the seismic response of the building frame is emphasized by the numerical investigation by comparing the behaviour of the building frame with different modelling strategies and varying the subterranean levels and foundation embedment depths in various subsoil profiles under the seismic load.

3.5.2.1 2D soil-structural system modeling

In the present assessment, 2D kinematic SSI analysis is performed with the numerical method. The adopted building with subterranean levels is simulated in ABAQUS software using the direct approach, in which the superstructure, subterranean levels with mat foundation, and subsoil deposit are directly incorporated utilizing a complete 2D finite element model (Figure 3.7).

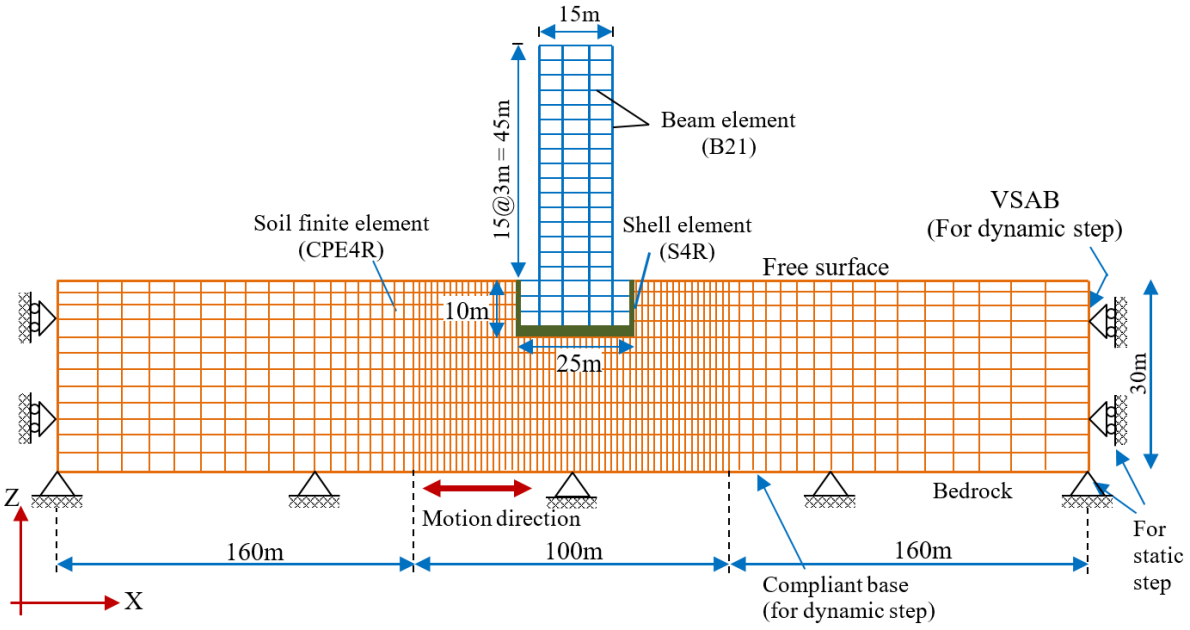

Figure 3.7 The direct method configuration employed for simulating the integrated soil-structure system of a fifteen-storey building with subterranean levels.

Since the structural system seismic response analysis is not the aim of the investigation, the structural members were modeled to behave elastically. The soil model, however, was the only one given the ability to capture nonlinear seismic responses.

To simulate the kinematic SSI correctly, as well as to integrate the various mechanical properties of the substructure system and the surrounding soil, the contact surfaces are used during dynamic analysis to capture any possible slide and uplifting of the subterranean level system over the subsoil. In ABAQUS, surfaces or contact elements can be utilized to model the interfaces. In this investigation, hard surface-to-surface-based interaction contact surfaces were defined by employing the Mohr-Coulomb failure model. Since the normal and tangential behavior of the contact surfaces could affect the numerical response analyses results, the mechanical properties of the contact surfaces should be carefully chosen. Figure 3.7 depicts the 2D numerical model of a building with subterranean levels of 10 m embedment depth found in a 420 x 30 m^2 soil deposit. In addition, the weight of the structural system was overlooked in the structural model, since capturing the filtering effects of kinematic SSI is the only target of this assessment. The subterranean level system is considered a rigid foundation, taking into account the large flexural stiffness of the basement floor beam-column frame system, floor slabs, as well as the presence of basement walls along the periphery, which are expected to contribute significantly to the overall stiffness of the subterranean level system. As observed in the literature, some of the past dynamic response analysis is carried out by introducing rigid systems within the embedment depth of the subterranean system, disregarding the superstructure. In this study differently, the massless superstructure system also is modeled properly taking into account the system stiffness.

In order to prevent multiple reflections of seismic waves, to reduce the soil medium dimension in space, and to optimize the computational effort during the dynamic response analysis, the infinite soil medium is simulated with a viscous-spring artificial boundary (VSAB) that incorporates elastic springs and dashpots (Lysmer and Kuhlemeyer, 1969). Kinematic constraints are applied along the lateral boundaries in order to replicate appropriate dynamic boundary conditions and eliminate the soil mass flexure mode of vibration (Sextos et al., 2017). These constraints prevent lateral spread of the soil mass because of gravitational load effects and enable the shear behavior between adjacent soil layers. As suggested by Fatahi and Tabatabaiefar (2014), the lower level of the soil domain (i.e., top of bedrock) was modeled by a rigid boundary condition

during the dynamic response analysis, whereas the earthquake input ground motion is exerted at the bottom of the soil medium and propagates upwards through the entire model. In this investigation, a soil domain with a longitudinal extent of 420 m was considered after performing several seismic wave propagation analysis. According to some experimental and numerical studies (Rayhani and Naggar, 2008), as well as seismic resistance design codes (ATC-40, 1996; FEMA 450, 2003) the local site intensification often arises within the top 30m of the soil profile. In this study, therefore, the vertical extent of the finite element soil domain was restricted to 30m.

The 2D finite element model of the soil profiles was simulated as both linear elastic and nonlinear elastic-plastic material using the Mohr-Coulomb failure criterion. These profiles were first employed having linear soil attributes to evaluate theoretical models under the underlying assumption that they were built, which is a homogenous linear soil profile. The same profiles were subsequently examined in the nonlinear elastoplastic constitutive model that considered viscous damping (Rayleigh damping).

The size of elements in most finite element dynamic SSI analyses is determined mainly by the geometry of the embedded part of the structural system and loading conditions. They refined near to the targeted area to account for the high stress gradients and plasticity experienced in the soil medium, whilst a gradual transition to a coarser element considers the soil medium in lateral directions far from the targeted area. The size of elements in the vertical direction, on the other hand, is kept constant to allow for uniform dispersion of shear waves propagating vertically. Furthermore, to avoid the numerical distortion of frequency content in wave propagation issue simulation and to accurately characterize the minimum wavelength of the applied signals, the maximum size, $h_{\max}$, of the elements was evaluated in this study applying equation 3.9.

$$h_{max} \leq \frac{1}{\mathrm{a}} \times \lambda \tag{3.9}$$

where $\lambda = V_s/f_{max}$, in which V_s and f_{max} are the smallest shear wave velocity of soil and the excitation motion maximum frequency of interest, and a = 5, 8, and 10 as per ASCE/SEI 4-98 (1998), Kuhlemeyer and Lysmer (1973), and ASCE/SEI 4-16 (2017), respectively. The minimum Vs was 150 m/s, and the earthquake ground motion had a cut-off frequency equal to 10 Hz. Thus, a maximum element size of 1.0 m was utilized near the structure.

Along the vertical direction, the soil profiles were divided into 30 layers of one meter each. The proposed element size settings in finite element modeling were tested by model validation, comparing the 2D finite element model results obtained in the ABAQUS with a similar equivalent linear (EL) model built in DEEPSOIL.

3.5.2.2 3D soil-structural system modeling

To assess the effects of foundation soil modeling and subterranean levels incorporating the seismic SSI on the structural response, three base conditions and five different models were considered (Table 3.9 and Figure 3.8).

Table 3.9 Summary of different alternative models considered in this study.

Model	ID	Flexibility						Input motions
		Superstructure	Subterranean levels	Foundation	Soil			
					Spring	Dashpot	Continuum	
1	1A	●	–	–	–	–	–	FFM
2	1B	●	●	●	–	–	–	FFM
3	2A	●	●	●	●	–	–	FIM
4	2B	●	●	●	●	●	–	FFM & FIM
5	3A	●	●	●	–	–	●	BRM

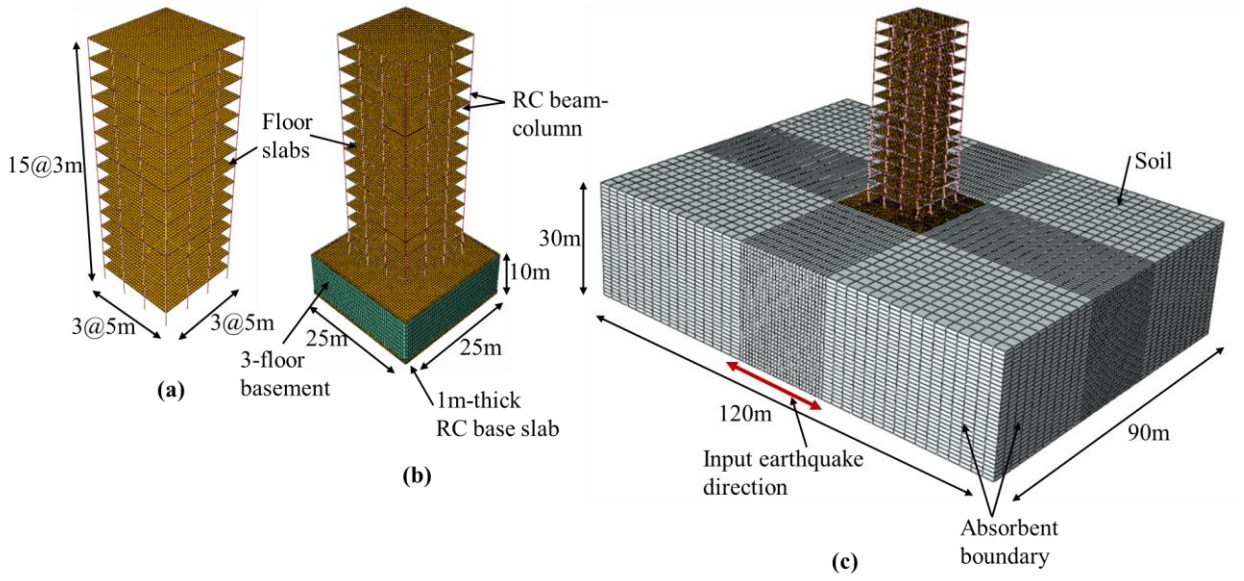

Figure 3.8 Geometry of the numerical models using ABAQUS, with different alternative modeling strategies: (a) 1A, (b) 1B, 2A and 2B, and (c) 3A.

The first case is a fixed-base model represented by Model 1A (Figure 3.8a), in which the building is modeled above the ground portion, and the base of the structure is assumed to be fixed at the ground surface (i.e., flexible superstructure, rigid subterranean levels, foundation, and soil). The second case is also a fixed base model represented by Model 1B (Figure 3.8b), but in this case, the building model is extended to the mat foundation level with subterranean levels. In this alternative model, the soil on the basement walls is overlooked (no SSI), but the subterranean level is directly comprised in the model. The lowest level of the entire structural system model is considered as the base, where it is fixed. The third case is the flexible-base model represented by Model 2A (Figure 3.8b), in this model horizontal and vertical springs, are employed to account for the influence of the surrounding and foundation soil, respectively (i.e., flexible superstructure, subterranean levels, foundation, and soil). The fourth case is also a flexible-base model represented by Model 2B (Figure 3.8b), in which dashpots are added parallelly with springs to capture the soil damping variation (i.e., flexible superstructure, subterranean levels, foundation, and soil), rocking mode of foundation motion is taken into account, as well as multi-support excitation is employed via the horizontal springs, causing the inputs to vary up the height of the basement walls.

The stiffness of springs and damping of dashpots were estimated and are presented in Table 3.10 according to equations proposed by Gazetas (1991) and also later reported by NIST (2012).

Table 3.10 Foundation level impedance functions for the overall foundation system.

Impedance functions	Soil type			Unit
	C	D	E	
K_z	9.95E+04	2.62E+04	1.42E+03	kN/m
$K_{x=y}$	1.74E+06	4.43E+05	4.64E+04	kN/m
$K_{xx=yy}$	3.26E+09	9.65E+08	1.44E+08	kN.m
C_z	4.20E+04	2.29E+04	9.22E+03	kN.s/m
$C_{x=y}$	4.38E+05	2.45E+05	9.83E+04	kN.s/m
$C_{xx=yy}$	1.95E+09	1.27E+09	6.5E+08	kN.s.m

As shown in this table, first the translational and rotational stiffness for square rigid foundations were calculated. The related dashpot coefficients are also estimated utilizing these equations. Using equations of surface foundation and the seismic shear wave velocities of the soil beneath the base slab (mat foundation), the stiffness portion that can be assigned to the base slab was determined for translation. Because of the embedment effect, the entire translational stiffness of the foundation level springs is increased, and the difference between the foundation level and the surface level was applied as horizontal springs dispersed throughout the height of the basement walls. The detailed expressions of related modification factors and distribution of impedance functions are described in NIST (2012).

The fifth case (Model 3A) is a thorough three-dimensional finite element model created using a direct approach (Figure 3.8c). The superstructure, subterranean levels with the foundation, and soil are all explicitly depicted in this model. Surface-to-surface-based interaction contact surfaces were defined by employing the Mohr-Coulomb failure model to simulate the dynamic SSI features and incorporate the variation in mechanical properties between the surrounding soil and the substructure system. During dynamic analysis, this model captures any possible uplifting and slide of the subterranean level system over the subsoil. In this model, an elastic-perfectly

plastic behavior was adopted for the soil medium using the Mohr-Coulomb yield criterion with an unassociated flow rule.

3.5.3 Analysis procedures of earthquake input motions

The earthquake input motions were applied to different numerical models while carrying out a nonlinear time history dynamic response analysis. The selected earthquake ground motions are FFM; so, it needs modification to apply for each model with the three base conditions. As a result, for the present investigation, three different earthquake input motions are required. These are FFM for the first two fixed-base models (Model 1A and 1B); FIM for the third flexible-base model (Model 2A); FFM and FIM for the fourth flexible-base model (Model 2B); and bedrock motion (BRM) for the fifth model (Model 3A). Due to the presence of subterranean levels, the FIM differs from that of the FFM (Tadesse et al., 2022). Hence, with the use of transfer functions (Conti et al., 2018), the modified FIM will be calculated. The FFM are then scaled to the modified transfer function to obtain the FIM. To predict the bedrock earthquake motion, free-filed ground motions will be converted to bedrock level using DEEPSOIL (Hashash et al., 2020) software by the inverse wave propagation analysis. Applying this procedure, the target FFM is given at the top of the soil, and because the bedrock is considered to be rigid, the 'within' bedrock motion is produced.

The selected free-field earthquake ground motions were matched to elastic response spectrums of IS 1893-1 (2016) for each soil type using SeismoMatch (2018) software. The lower and upper bound matching periods of $0.2T_1$ and $2T_1$, respectively, are considered as per ASCE/SEI 7-16 (2018) recommendation, where T_1 is the maximum fundamental period of the building. Figure 3.9 depicts the spectral acceleration of the free-field earthquake records after matching the target response spectrum.

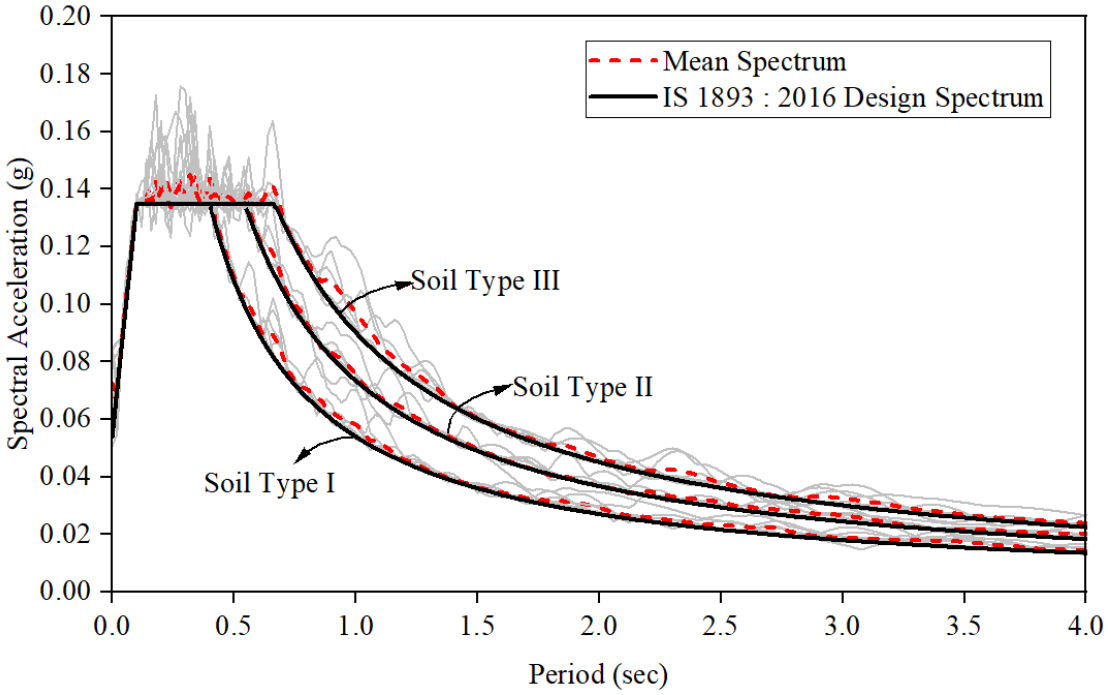

Figure 3.9 Earthquake records compatible with the elastic response spectrum at 5% damping, along with their mean value and the target spectrum of different soil types for a 15-storey building.

3.5.4 Validation of the model

In this phase, numerical analyses were carried out to calibrate finite element models for dynamic SSI response analysis that account accurately for the physical phenomena experienced, such as the wave propagation, the nonlinear behaviour of both structure and soil, as well as the soil-structure interface issue.

3.5.4.1 Seismic site response analysis

In order to validate the accuracy of the chosen element size settings in the 2D finite element model for simulation of wave propagation, a two-step approach (Feldgun et al., 2016; Robert, 2009) was carried out, and are schematically depicted in Figure 3.10. In which:

(i) An equivalent nonlinear 1D inverse wave propagation (deconvolution) problem was solved for a simple soil column of the foundation soil built in DEEPSOIL (Hashash

et al., 2020). In this process, the target FFM was deconvoluted to the top of the bedrock level through a 1D equivalent linear (EL) model built in DEEPSOIL (Figure 3.11). The shear modulus and damping reduction curves as presented in Figure 3.12 were obtained using Vucetic and Dobry (1991) classical formulas.

(ii) The obtained bedrock motion was imposed as a ground motion to a 2D nonlinear finite element model at the base of the soil profile in ABAQUS and the corresponding free-field ground motion was recorded at top of the model (convolution). In order to implement the defined physical model, 2D nonlinear shell elements for simulating the soil profile, and Lysmer (Lysmer and Kuhlemeyer, 1969) energy absorber elements along the side of the model were created in ABAQUS (Figure 3.13).

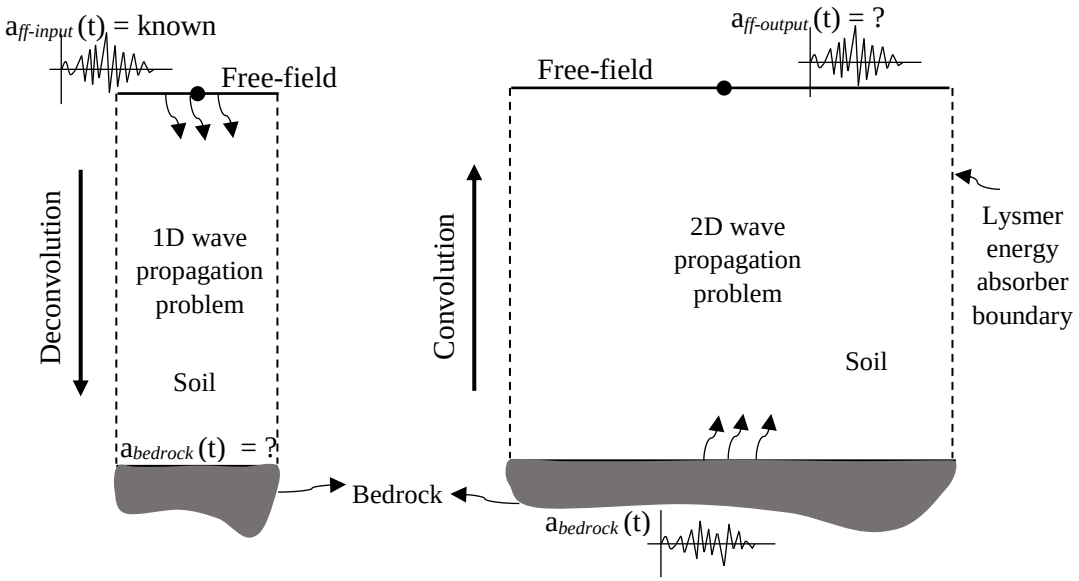

Figure 3.10 Schematic depiction of the 1D and 2D seismic site response analysis.

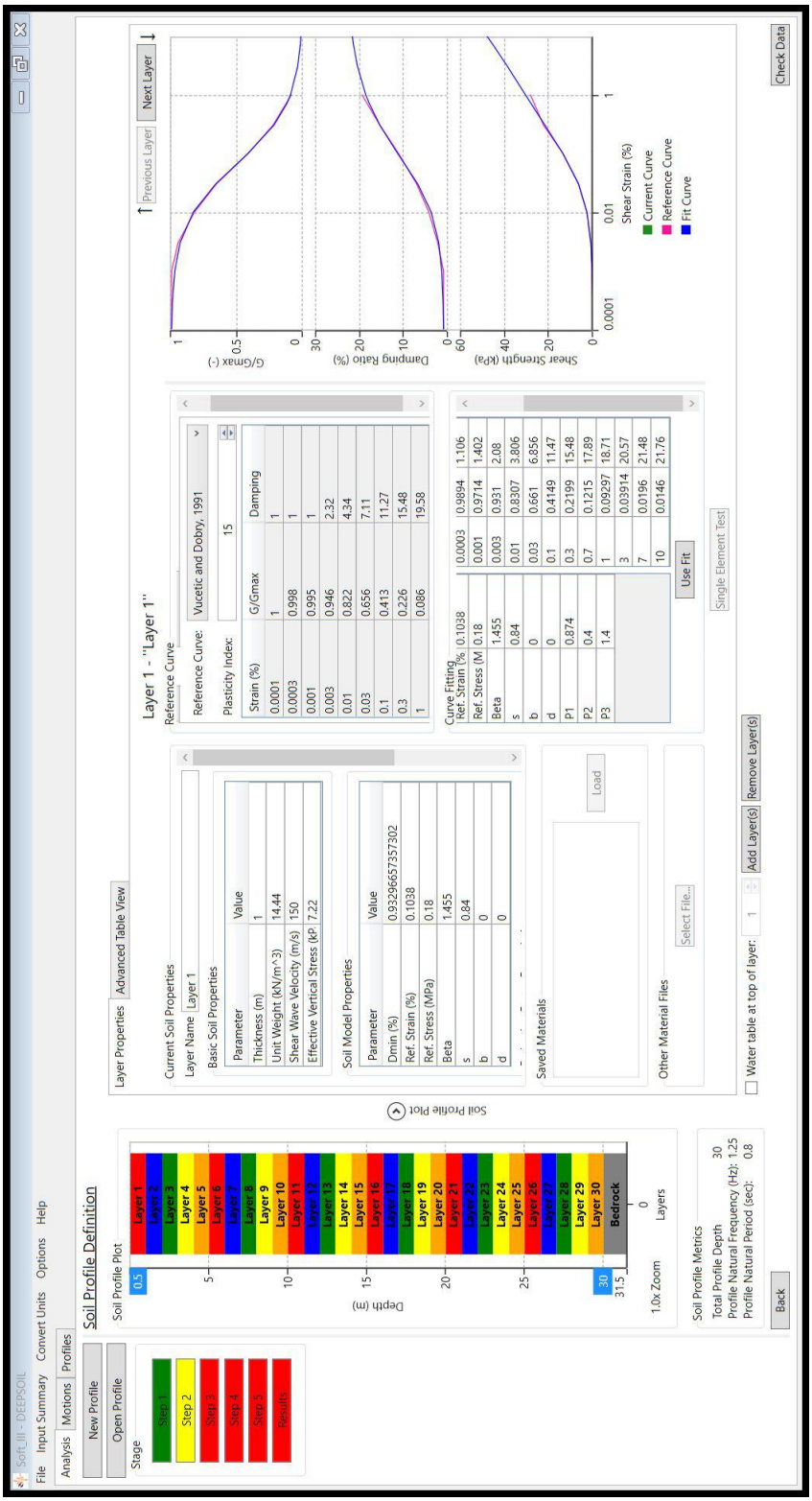

Figure 3.11 Application of a 1D seismic site response analysis in DEEPSOIL software.

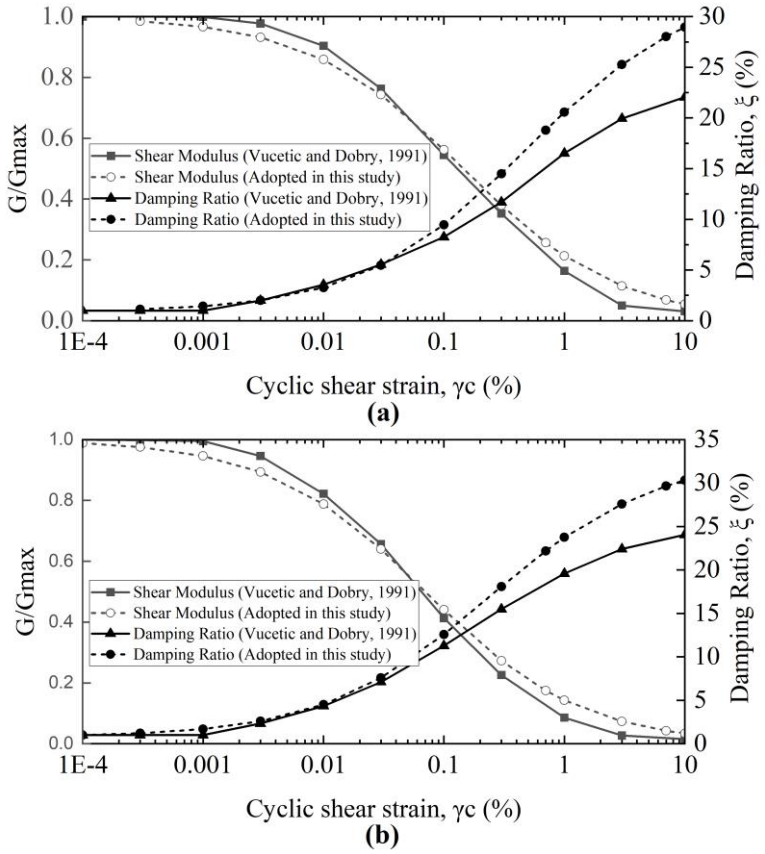

Figure 3.12 Adopted backbone curves for (a) soil type D and (b) soil type E.

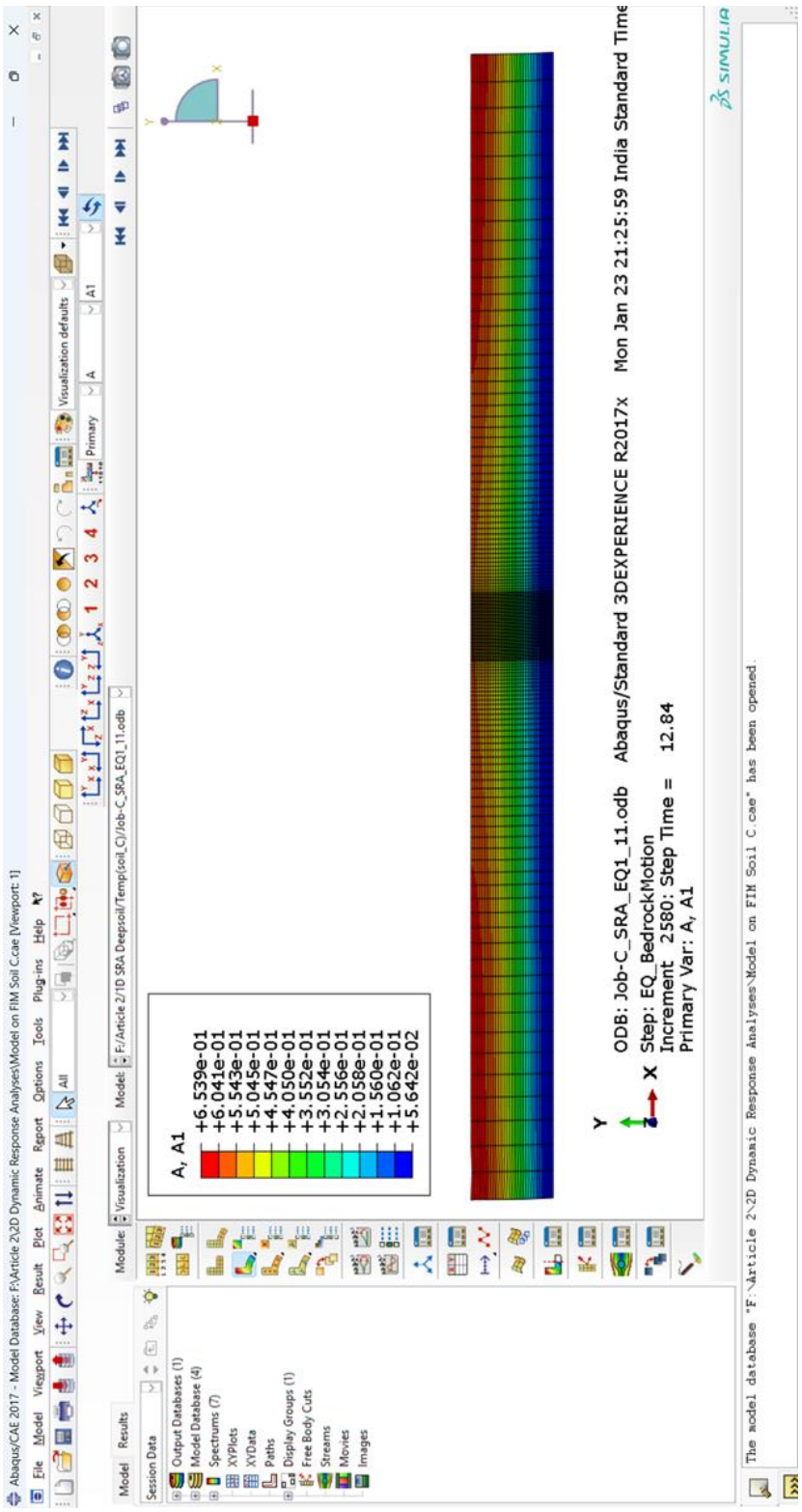

Figure 3.13 Application of a 2D seismic site response analysis in ABAQUS software.

Figure 3.14 presents, for one of the applied earthquakes (EQ1), the comparison of the free-field acceleration time history and the corresponding response spectra (5% damping ratio) obtained from DEEPSOIL and ABAQUS. Although 1D DEEPSOIL and 3D ABAQUS models use distinct solution equations, a reasonably good matching was observed throughout the entire period.

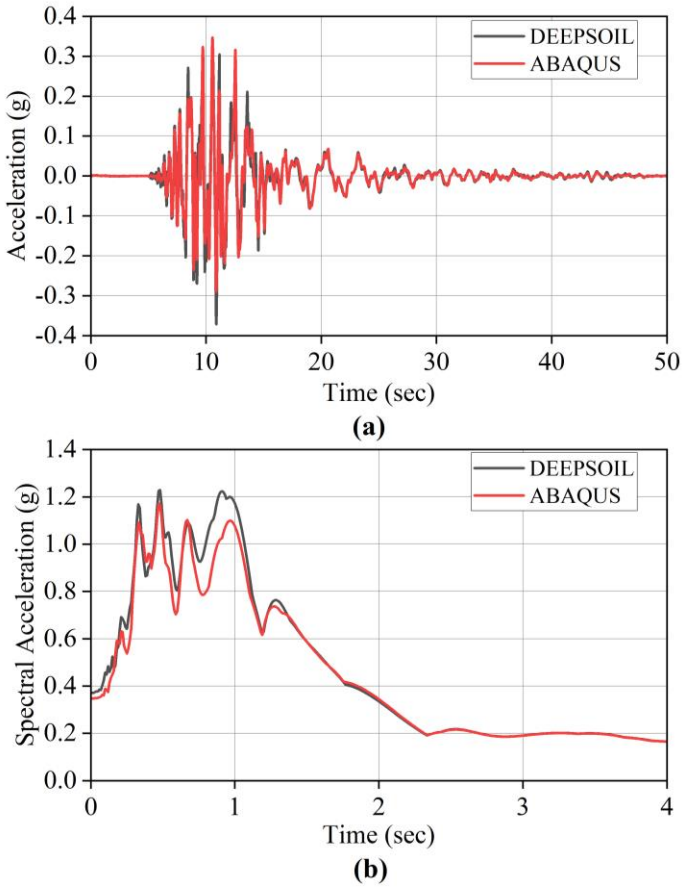

Figure 3.14 Comparison of (a) free-field acceleration time history, and (b) the corresponding 5% damped spectral acceleration of "Christchurch, New Zealand", in soil type E.

3.5.4.2 Nonlinear seismic response analysis

The numerical modeling techniques, along with suitable experimental validation are required to determine the important aspects of the seismic SSI mechanism. Shaking table test results were used to calibrate the numerical models and predict prototype dynamic responses. In the present study, 3D ABAQUS numerical models were validated using the results from the shaking table tests as reported by Hoseny et al. (2022 and 2023). In this report, shaking table tests

(physical modeling) and numerical modeling were employed to investigate the reliability of the small-scaled coefficient in representing the dynamic behavior of structures, and the influence of SSI and subterranean levels on the dynamic response of building structures under earthquake excitation. Due to the fact that the concrete frame models are unsuitable for small-scale testing environment, equivalent steel structure models have been created using the similitude rule. Based on the shaking table dimensions and maximum load capacity, as well as the similitude laws, a geometrical scaling factor (λ) of 1:50 was adopted for both structural and soil models. As a result, Table 3.11 shows the scaling relations between the scaled model and prototype in terms of the geometric scaling factor for the parameters contributing to the main modes of system response. The scaling relations have been employed by several researchers (Hoseny et al., 2022, 2023; Goktepe et al., 2019; Meymand, 1998; Moss et al., 2010; Tabatabaiefar et al., 2014; Turan et al., 2009).

Table 3.11 Scaling relations for physical modeling in terms of the geometric scaling factor.

Mass density	1	Acceleration	1	Length	λ
Force	λ^3	Shear wave velocity	$\lambda^{0.5}$	Stress	λ
Stiffness	λ^2	Time	$\lambda^{0.5}$	Strain	1
Modulus	λ	Frequency	$\lambda^{-0.5}$	EI	λ^5

In this study, to validate numerical models, real dimensions (prototypes) were obtained and utilized. The structural response for the 15-storey building model with two subterranean levels (S15+2b) was adopted as a reference. A view of the shaking table test fixed and flexible base models are shown in Figure 3.15a and b, respectively.

(a)

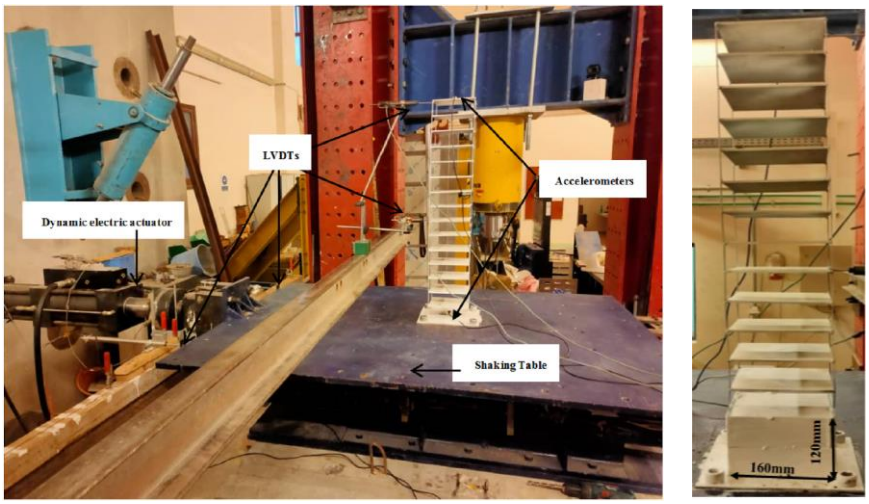

(b)

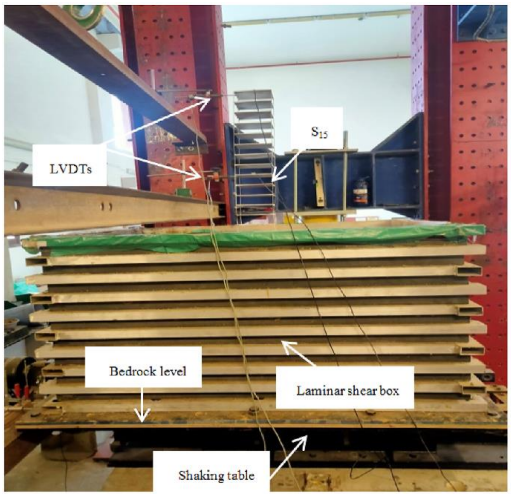

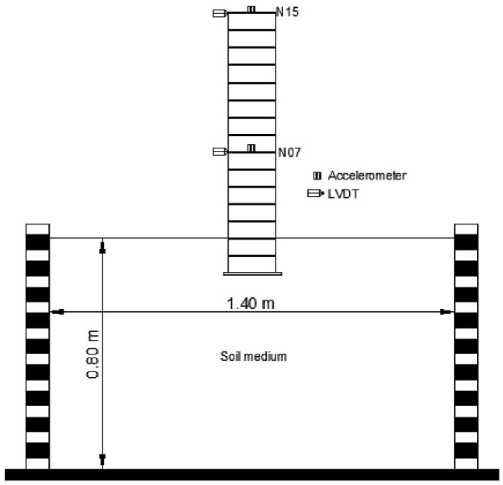

Figure 3.15 Installation steps implemented for a 15-storey building with two subterranean levels on the shaking table: (a) fixed base, and (b) flexible base (Hoseny et al., 2023).

The dimensions of the experimental and the corresponding real model, as well as the specifications of the materials, are presented respectively in Tables 3.12 and 3.13, and Table 3.14.

Table 3.12 The dimensions of steel columns, slabs, and walls (Hoseny et al., 2023).

Model	Steel column		Steel plate (floor slab)			Steel plate (basement wall)		
	Depth (m)	Width (m)	Length (m)	Width (m)	Thickness (m)	Width (m)	Height (m)	Thickness (m)
Experimental	0.0065	0.0015	0.16	0.16	0.0045	0.16	0.12	0.0015
Prototype	0.325	0.075	8	8	0.225	8	6	0.075

Table 3.13 The dimensions of the prototype and scaled system based on the adopted scaling factors (Hoseny et al., 2022, 2023).

Model	Building				Soil				
	width (m)	length (m)	storey height (m)	total height (m)	length (m)	width (m)	depth (m)	volume (m^3)	mass (kg)
Experimental	0.16	0.16	0.06	0.9	1.4	1.0	0.8	1.12	19993.6
Prototype	8.0	8.0	3.0	45	70	50	40	140,000	249,200,000

Table 3.14 Materials specifications of the physical model (Hoseny et al., 2022, 2023).

Materials	Parameters	Notation	Units	Values
Soil	Average unit weight	γ	kN/m^3	17.8
	Shear modulus	G	kN/m^2	1758
	Young's modulus	E	kN/m^2	4571
	Poisson's ratio	υ	-	0.3
	Shear wave velocity	Vs	m/s	31.13
	Compression wave velocity	Vp	m/s	58.23
	Cohesion	C	kN/m^2	60
	Friction angle	ϕ	deg.	31.8
	Dilatancy angle	ψ	deg.	1.8
Steel	Density	ρ	kN/m^3	78.50
	Yield stress	f_y	MPa	240/350

To simulate the described physical model in ABAQUS, 1D linear beam elements for the frame, 2D linear shell elements for plates, 3D solid elements for modeling the soil mass, and Lysmer (Lysmer and Kuhlemeyer, 1969) boundary elements on the side of the model were utilized. Also, to increase the accuracy of the finite element model in wave propagation, in the case of the flexible base model, the element size of 1.0 m was considered for near-field soil, which is smaller than the interest shear wavelength.

The geostatic stage of soil initial stress has been determined by applying the gravity load and horizontal pressure coefficients. During this stage, the standard boundary conditions were applied, that is fixed nodes at the base of the soil medium (bedrock level) and zero horizontal displacements along the lateral boundaries. During the dynamic (subsequent) step, the seismic input motions were applied to the base of the structural system and the base of the soil medium, in the case of fixed and flexible base models, respectively. Similar to the shaking table test of Hoseny et al. (2022 and 2023), the surface-to-surface-based structure-soil interaction was considered by employing the Mohr-Coulomb failure model in the case of the flexible base model. Moreover, the horizontal component of the Northridge 1994 and Kobe 1940 earthquakes (Figure 3.16) was applied as the input to the model. Figure 3.17 shows the configurations of the prototype fixed and flexible base models in ABAQUS.

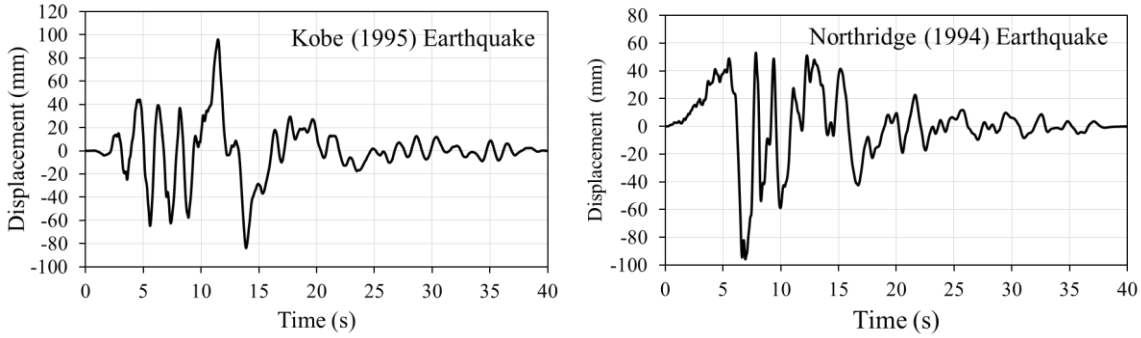

Figure 3.16 Input earthquake motions for validation of numerical models.

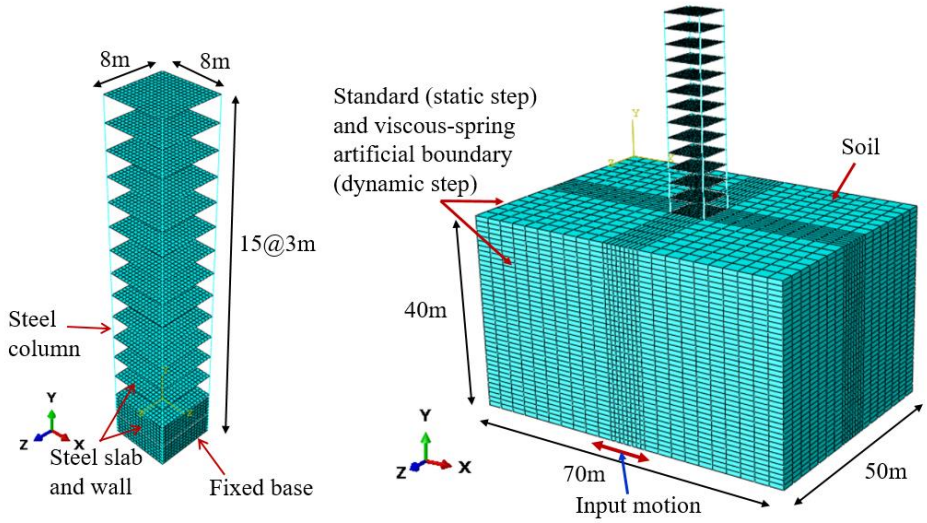

Figure 3.17 Configurations of the prototype fixed and flexible base models.

To verify, the maximum absolute lateral displacements obtained from the physical model carried out by Hoseny et al. (2023), and the executed model in ABAQUS were compared at two levels situated on the structure under two different earthquakes for fixed and flexible base conditions. To evaluate the differences between experimental and numerical results, the deviations have been calculated for each level and base condition and presented in Table 3.15.

Table 3.15 The maximum absolute lateral displacements at different levels in experimental and numerical modeling.

Model	Level	Base	Northridge (1994) earthquake			Kobe (1995) earthquake		
			Shaking table test (m)	Numerical model (m)	Deviation (%)	Shaking table test (m)	Numerical model (m)	Deviation (%)
S_{15+2b}	15	Fixed	0.00250	0.00268	6.7	0.00220	0.00228	3.5
	7		0.00210	0.00226	7.1	0.00170	0.00173	1.7
S_{15+2b}	15	Flexible	0.00340	0.00319	6.6	0.00290	0.00313	7.3
	7		0.00230	0.00242	5.0	0.00230	0.00251	8.4

It can be observed from the results that the measured response at the target point of the model is in good match with the experimental tests, with the maximum deviation percentage not

exceeding 9% (Hoseny et al., 2023). Furthermore, by extending the identical procedures of experimental outcomes for a 15-storey real reinforced concrete building, the lateral displacements along the height of the structure were reported to study the seismic behavior of the structure considering SSI and the effects of embedded depths. Figure 3.18 presents the maximum relative lateral displacement of a 15-storey reinforced concrete building with two subterranean levels on fixed-base and flexible-base conditions under two earthquakes.

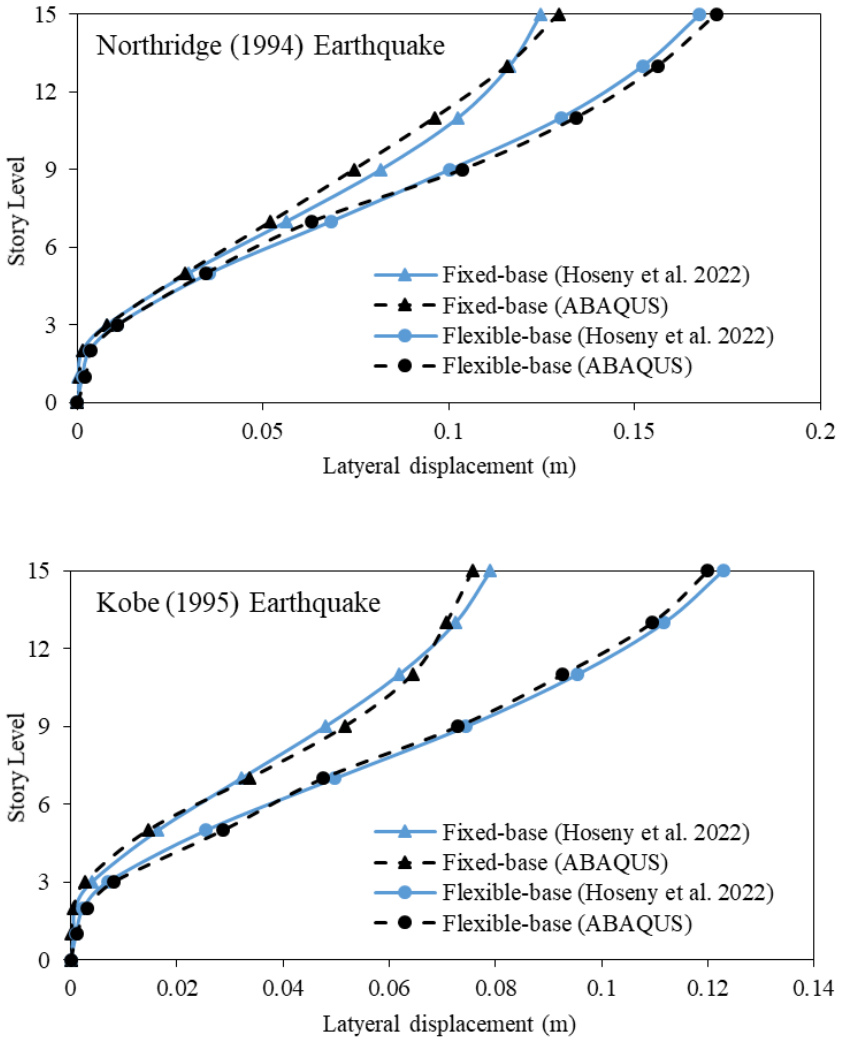

Figure 3.18 Comparison of the maximum relative lateral displacement along the height of 15-storey with two subterranean levels (S15+2b) of the real reinforced concrete building structure.

3.6 Summary

The numerical technique has been widely applied to simulate the seismic response of structures incorporating the influence of SSI. The seismic SSI problem assessed in this work was presented in detail by describing the adopted system under investigation, the materials used, and earthquake input motions. The constitutive models utilized for the numerical modelling of soil, the soil-structure interface, and structural components, as well as bounded and unbounded soil domains for finite element models, were presented. These nonlinear constitutive models take into consideration certain critical characteristics of the dynamic nonlinear behaviour of the various materials involved. In order to justify different finite element modeling choices adopted in this study, the validation process was presented in the form of one-, two-, and three-dimensional models with a simulation of seismic wave propagation and previous experimental.

The finite element numerical simulations presented in this chapter were carried out in nonlinear elasticity for both, structure and soil. The next chapters are devoted to presenting the results of several non-linear seismic SSI response analyses to comprehend the influence of subterranean levels on the seismic response of building structures in various subsoil conditions under the influence of selected seismic excitation.

CHAPTER - 4

RESULTS AND DISCUSSIONS

4.1 General

The preceding chapter discussed the materials utilized and the methodology employed in the present study. In this chapter, the results from studies carried out on the influence of subterranean levels on the foundation level motion and seismic response history of building frames in various soil profiles with different aspects under the influence of earthquake motions have been discussed.

In the present study, as summarized in section 3.2, the entire work has been carried out through four phases. Out of four phases, the first two phases deal with the numerical analysis (numerical-based solutions) and theoretical models respectively to comprehend the influence of subterranean levels on the foundation input motion (FIM) and to evaluate the applicability range of theoretical-based solutions to estimate the FIM in comparison to numerical-based solutions. The other two phases deal with finite element analysis to evaluate the effect of different foundation-soil modeling approaches on the seismic response history analysis of building frame with subterranean levels; and to investigate the variation of subterranean level depths on the seismic response characteristics of the building frames.

The variation of foundation level motions of the building frame with subterranean levels was observed from the results of nonlinear kinematic interaction (KI) response finite element analysis. The foundation level motions were studied in terms of spectral accelerations and translational transfer functions (KI factor, $|I_u|$). The influence of different foundation-soil modeling strategies and variation of subterranean level depth on the building frames was investigated in terms of seismic response demands such as storey level lateral displacements as well as inter-storey drift. A parametric study for respective conditions was performed by changing the relative density of subsoil conditions, embedment depths of subterranean levels, and applying different modeling approaches subjected to several earthquake loads. In the following sections, results from the above studies are discussed.

4.2 Phase I: Influence of subterranean levels on FIM

As mentioned above, Phase I deals with the influence of subterranean levels on FIM. To provide a more in-depth understanding of the KI response of the SSS under the applied earthquake motions, spectral acceleration, and time-dependent transfer functions will be used in particular. A comprehensive parametric study has been carried out to analyze the kinematic SSI effect on FIM for building with various subterranean levels in different subsurface conditions under the influence of earthquake motions. The objective of Phase I is to assess the influence of the main parameters governing the seismic response of the building structural systems: the embedment of subterranean levels, the properties of the subsurface soil condition, and the nonlinear behavior of soil. The analysis scenario covers a wide range of possible two soil profiles (i.e., soil type D and E) as shown in Table 3.1 and allows for investigating the effects of subsurface soil conditions on structural system seismic responses for different soil conditions and various subterranean level embedment depths. The seismic response of the soil-structure system was evaluated for vertically propagating shear waves. It was defined at the top of the bedrock level or bottom of the soil deposit. Foundation-level motions were evaluated at the top of the mat foundation for selected earthquake acceleration time history.

4.2.1 Foundation level motions in terms of spectra acceleration

The existence of the superstructure and the type of substructure system could have an effect on the seismic motion characteristics at the level of the structure base. KI alters foundation level motion relative to free-field motion (FFM) since the substructure system and surrounding soil stiffness are different (Veletsos and Parsad, 1988). As a result of SSI, the motion encountered at the foundation base may be stronger or weaker than FFM (Rayhani and Naggar, 2007). Response spectrums are often utilized to incorporate the characteristics of structural dynamics into structures design and the creation of lateral force requirements in building codes (Chopra, 2007). The response spectra present the peak of acceleration response of a SDOF system having 5% damping and various natural periods for the recorded earthquake motions.

Figure 4.1 presents foundation level motions in terms of 5% damping elastic response spectra at the base of the substructure for different subterranean levels and subsoils under the influence of all seven applied earthquake motions. For comparison, also the FFM elastic response

spectra values are illustrated. Due to its shallow embedment, the spectral ordinate values of a building with one subterranean level in both subsoils were slightly reduced (it was close to FFM) compared to the FFM in majority of the cases evaluated in this study. On the other hand, the effect of kinematic SSI on the base motion was apparent in cases of deeply embedded subterranean levels (i.e., 3BS and 5BS), with the increase in filtering effect for lower periods.

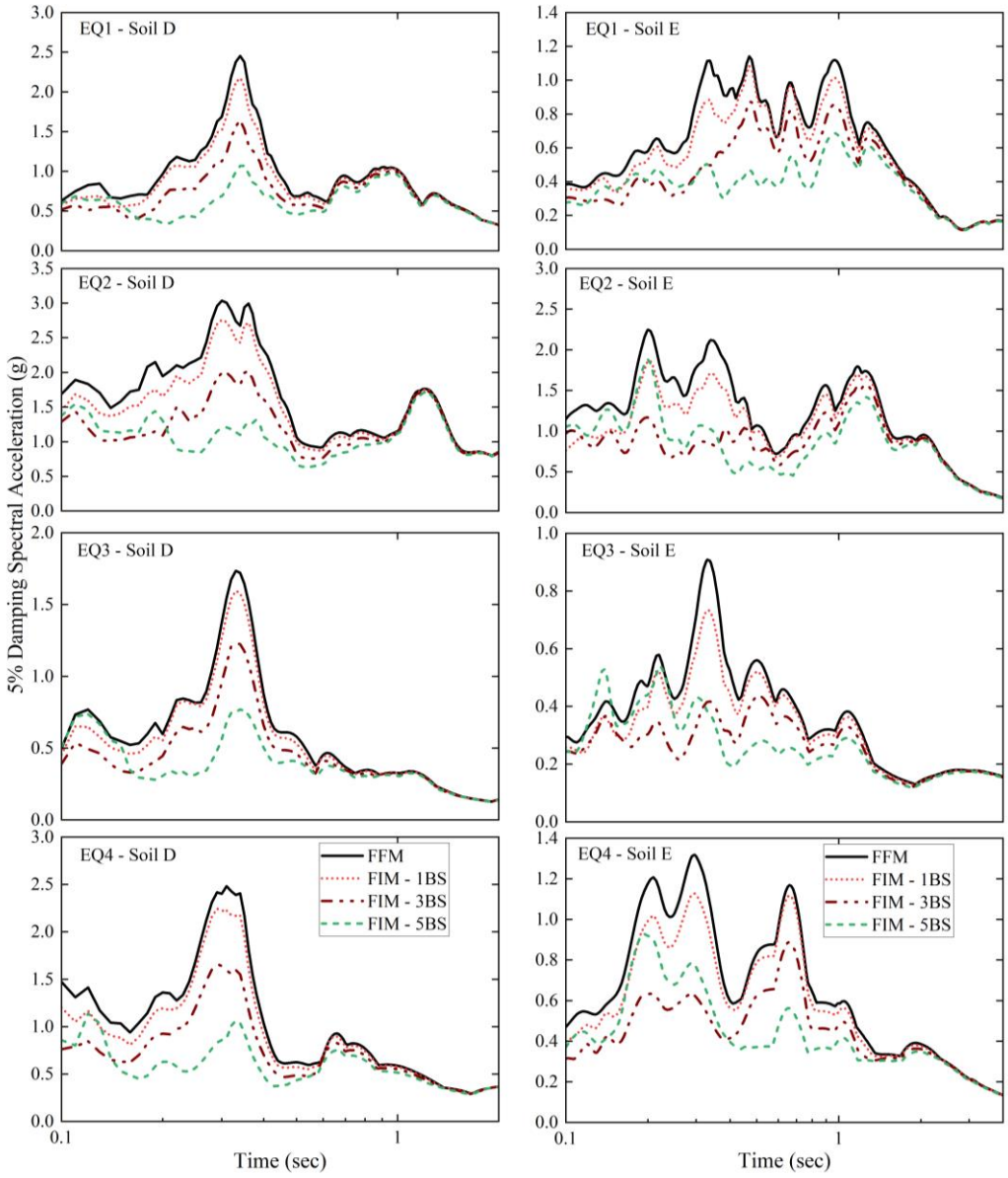

Figure 4.1 Comparison between the 5% damping elastic response spectra of the FFM and FIM for the structure with different subterranean levels and subsoil under the influence of earthquake.

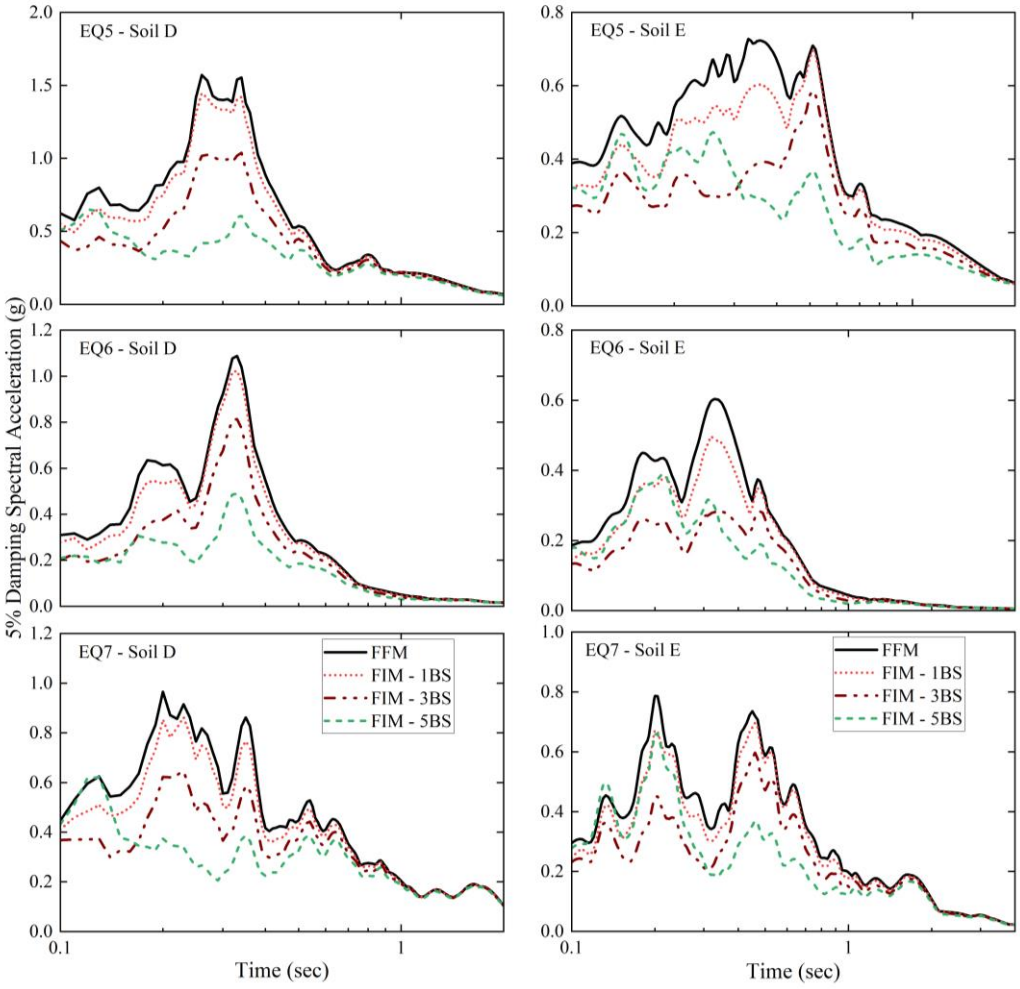

Figure 4.1 (Continued).

4.2.2 Foundation-level motions in terms of transfer functions

4.2.2.1 Numerical-based transfer functions

As a result of the KI between the components of the subterranean level and the near-field soil, the lateral displacement of the foundation is normally attenuated with respect to the FFM, and a rotation component can arise, which is also influenced by the substructure system. The two dimensionless factors, I_u and I_θ, which are frequency-dependent transfer functions that relate the motion of the foundation to the FFM, are able to quantify this KI effect, which is essentially related to the incapacity of subterranean components to accommodate soil displacements.

In this study, the effect of KI was assessed utilizing to the 2D finite element model of the sole SSS, by considering only the horizontal component of the foundation level motion, as the geometry of the subterranean level system (the slenderness of the embedment is low) makes the corresponding kinematic rotational component indeed insignificant. Figure 4.2 shows, for all seven applied earthquake motions in the two subsoils, the numerical values of the transfer function ($|I_u| = |u_{FIM}/u_{FFM}|$), computed as the ratio between the amplitudes of the signals' Fourier transforms at the top of the foundation (u_{FIM}) and the free-field surface (u_{FFM}).

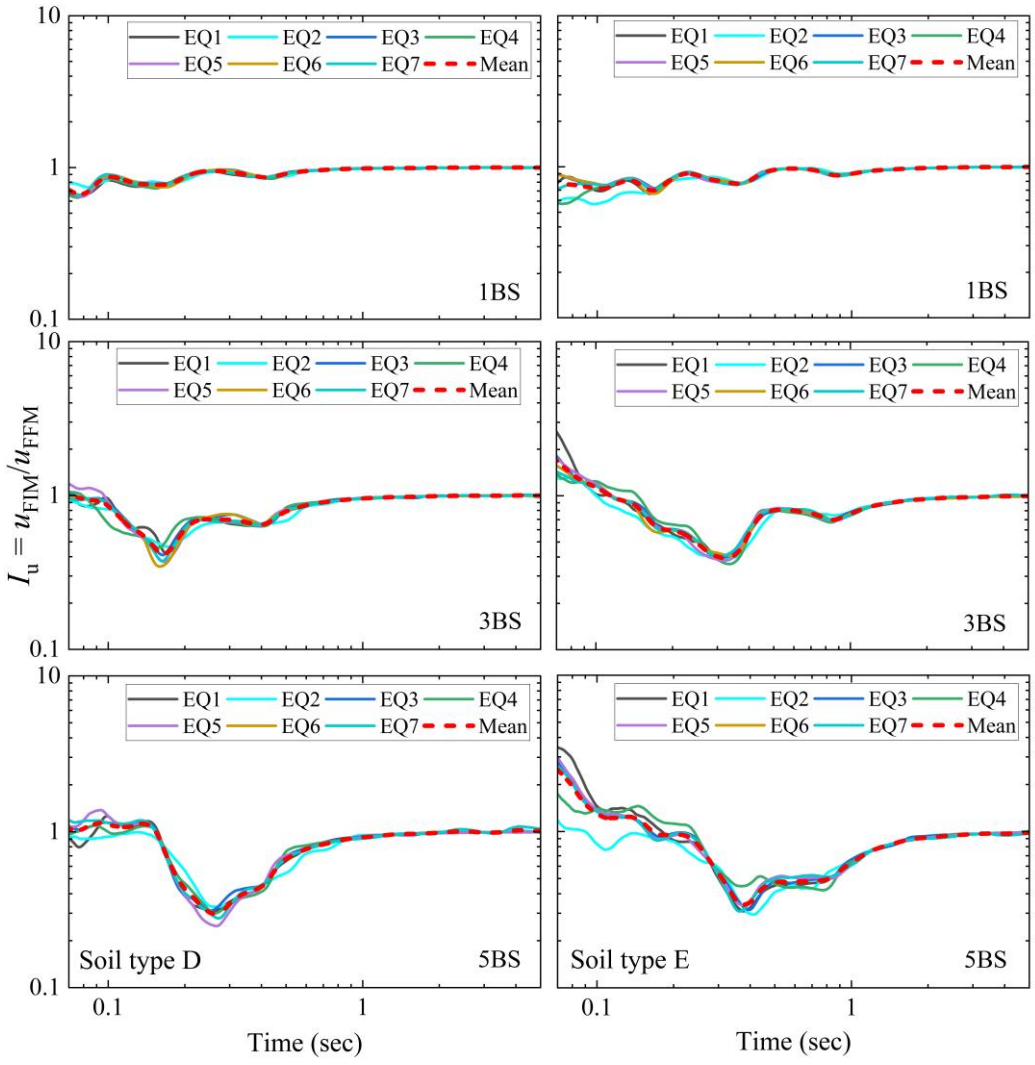

Figure 4.2 Transfer functions obtained from nonlinear soil model numerical solutions in different soil types and subterranean levels.

4.2.2.2 Effect of subterranean levels embedment depths and subsoil conditions on FIM

In this section, to highlight the influence of subterranean levels and subsoil on FIM, the mean values of the transfer functions obtained from numerical analyses for all seven applied earthquakes are presented in Figures 4.3 - 4.5, which summarize the KI effects in subsoil D (Figure 4.3) and E (Figure 4.4) with different subterranean levels.

In both subsoil types, a building with one subterranean level yields a limit attenuation of the transfer function with respect to the FFM. It is because of the shallow embedment depth of the subterranean components. On the other hand, the influence of subterranean levels on transfer functions was notable in cases of deeply embedded subterranean levels (i.e., 3BS and 5BS), with the KI impact increasing for lower periods. As far as subterranean levels are concerned, transfer functions are always lower than one in the case of medium-dense (subsoil D) and soft soil (subsoil E), with the filtering impact increasing for lower periods. This effect is less noticeable in the soil type D building with 5 subterranean levels, and for the subsoil type E, the building with 3 and 5 subterranean levels, where the subterranean level provides transfer functions even larger than one for periods less than 0.2 s. Furthermore, the transfer functions can be affected by the type of subsoil. As illustrated in Figure 4.5, the effect of subsoil type E (soft soil) provides a reduction in the transfer function than subsoil D (medium dense).

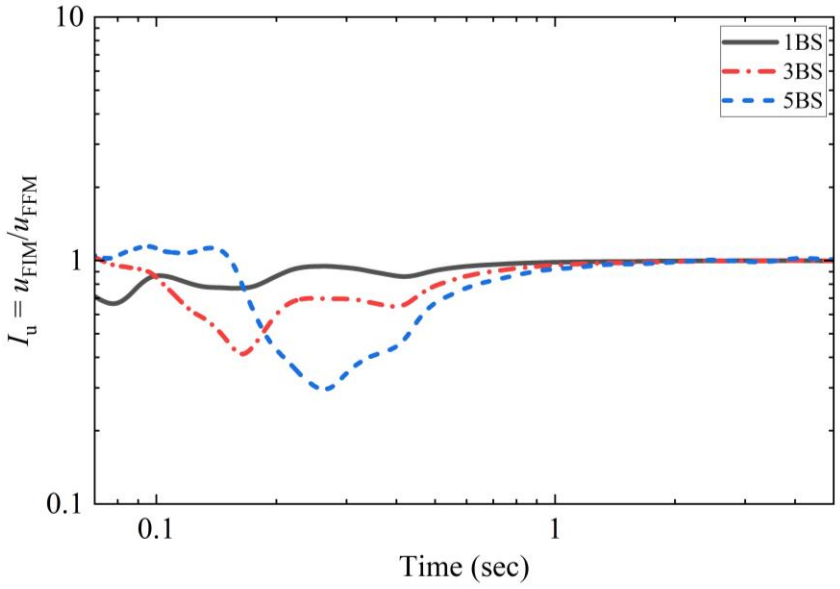

Figure 4.3 Effect of the embedment depth of subterranean levels on the FIM in soil type D.

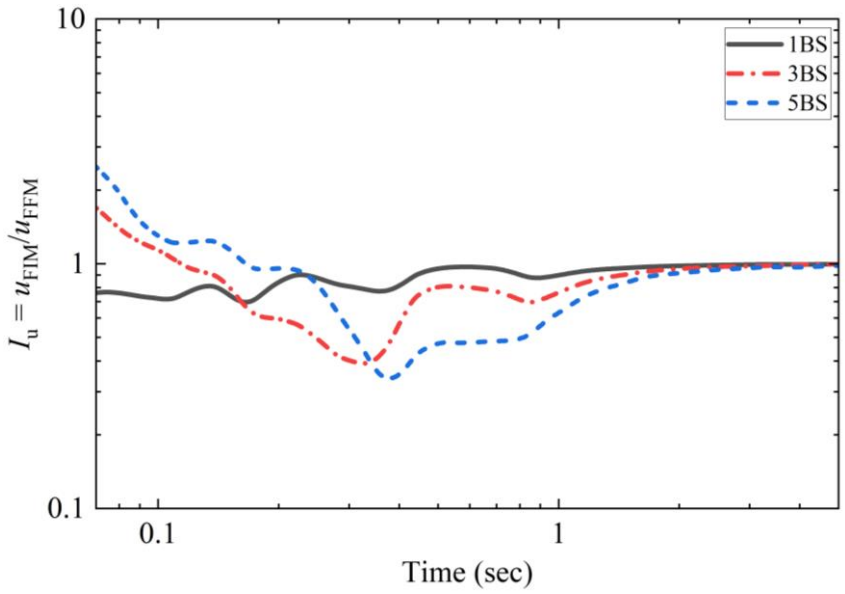

Figure 4.4 Effect of the embedment depth of subterranean levels on the FIM in soil type E.

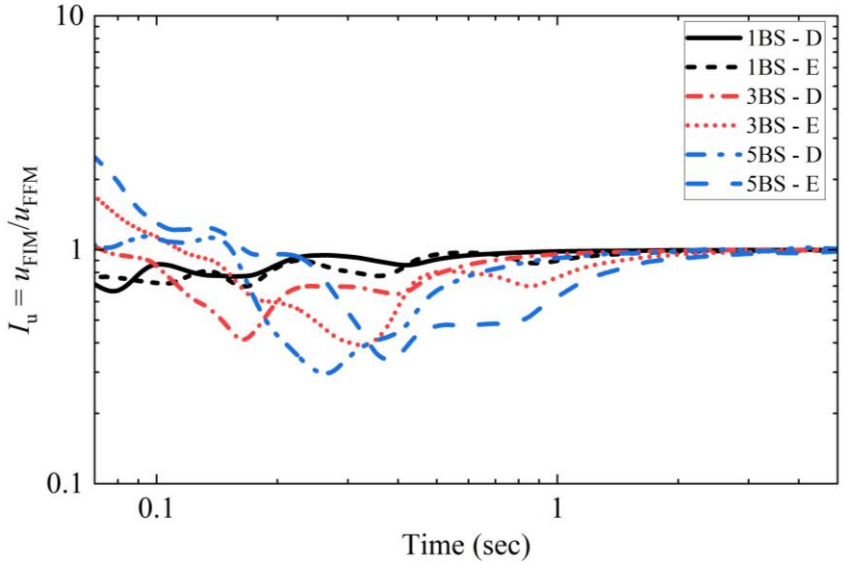

Figure 4.5 Effect of soil profiles into various subterranean levels on the FIM.

4.2.3 Inference from Phase I

In this section, the results obtained from the numerical studies on the influence of subterranean levels on foundation-level motion are presented. The conclusions obtained from these studies are as follows.

i) Due to its shallow embedment, the response spectral ordinate values of a building with one subterranean level (1BS) in different subsoils were slightly reduced (it was close to FFM) compared to the FFM in the majority of cases investigated in this study.

ii) On the other hand, the effect of subterranean levels on the base motion was significant in cases of deeply embedded subterranean levels (i.e., 3BS and 5BS), with the filtering effect increasing for lower periods.

iii) It can be observed that from the numerical analyses, the motion at the subterranean level of a building decreases within the period range between 0.3 to 1.0 sec as the basement level depth increases, whereas in contrast more intense than the FFM revealed especially at lower periods and for higher subterranean levels, predominantly in subsoil E (soft soil).

iv) Similarly, the effect of soil properties on FIM exhibits the same characteristics as the stiffness of the soil properties decreases from dense soil to soft soil.

v) Overall, the results demonstrate clearly how the embedded stiff subterranean level existence in different subsoil conditions causes the high frequencies to be filtered or the reduction of FIM with respect to FFM.

vi) However, depending on the dynamic characteristics of the building structure, the surrounding soil deposit as well as the input motion of the earthquake can contribute to the rising partially or full amplification or reduction of foundation level motion.

4.3 Phase II: Applicability of the analytical-based solutions

Phase II is aimed to evaluate the applicability range of theoretical models for the prediction of the FIM in comparison to the nonlinear numerical-based solution. The theoretical transfer function models often used in the literature to estimate the FIM was assessed in this section.

4.3.1 Analytical-based transfer functions

The simplified analytical expressions, obtained for homogeneous isotropic viscoelastic soil deposits, documented in NIST (2012) and presented by Conti et al. (2018) were employed in this investigation. The variation of foundation level motion of the building with subterranean level in terms of transfer function obtained from theoretical-based solution is shown in Figure 4.6. The results appeared to reveal that theoretical transfer function models can only accurately predict the effect of embedment. The theoretical-based solutions also give the transfer function as less than

one (i.e., $|I_u| < 1.0$), which implies the reduction of FIM compared with that of FFM. More variations with embedment were observed respectively within the range of 0.05 – 0.4 sec and 0.1 – 1 sec in soil type D (Figure 4.6a) and E (Figure 4.6b), which indicates the influence of soil type on FIM, whereas in the remaining lower and higher periods range the theoretical KI factor value remains constant.

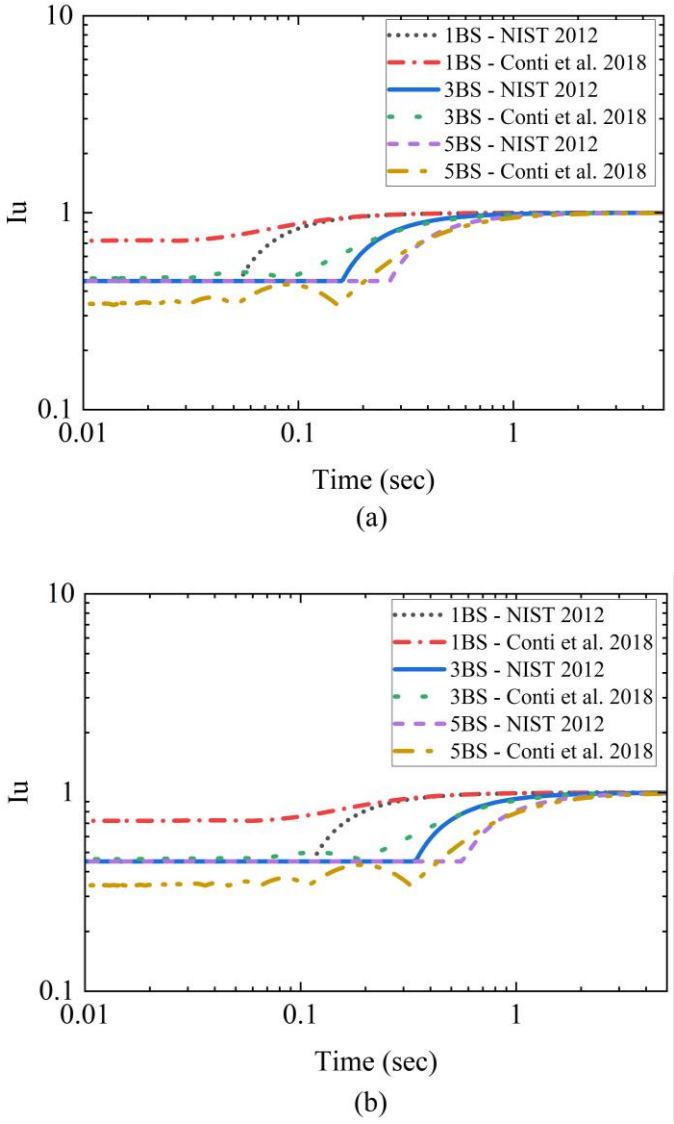

Figure 4.6 Theoretical transfer function models on (a) soil type D, and (b) soil type E.

4.3.2 Comparison of numerical solutions with analytical models

In this subsection, the horizontal transfer function $|I_u|$ obtained from the 2D nonlinear numerical analyses and those derived from analytical models are compared. In Figures 4.7 - 4.9, the transfer functions obtained from analytical and nonlinear numerical solutions in different subsoils and subterranean levels are presented for comparison. It can be observed that the two assessed analytical models yield identical transfer functions, diverging only at lower periods. The divergence is more noticeable for the deeper embedment depth of 3 (Figure 4.8) to 5 (Figure 4.9) subterranean level, predominantly within a small period range of 0.1 - 0.4 sec in soil type E (soft soil) and also the foundation level motion of a building can be more intense than the FFM. A constant transfer function value of 1.0, which is likewise obtained from the numerical analyses, is correctly predicted by the models at larger periods. Based on these findings, it can be observed that both analytical models are capable of accurately predicting the embedment effects.

On the other hand, completely different behavior is obtained for deeply embedded subterranean levels of 3BS (Figure 4.8) and 5BS (Figure 4.9), particularly in the case of subsoil E, where the transfer function values even greater than one are obtained for periods less than 0.2 sec, showing that the foundation motion is intensified in comparison to the FFM in this period range. Additionally, the analytical and numerical values of the transfer functions differ significantly from one another in this case. Overall, the comparisons depicted in Figures 4.7 - 4.9 and the plots of the spectra and numerical-based transfer function in Figure 4.1, and Figures 4.3 - 4.4, respectively, show that contrary to the general trends and what analytical models anticipate, motion at the subterranean level of a building can be appear stronger than FFM. This is more likely occur at lower periods and for higher subterranean levels. It should be mentioned that NIST (2012), as well as the study of Sotiriadis et al. (2019 and 2020) and Scarfone et al. (2020), reported comparable findings of frequency-dependent foundation motion that is amplified with respect to the FFM. This disparity may be caused by (i) the simplified fundamental hypotheses utilized to create analytical models (i.e., (a) rigid subterranean system comprising foundation, it could be stiff but not rigid; (b) embedded in an half-space homogeneous elastic soil deposit), and (ii) the complexity of nonlinear numerical models using the direct approach.

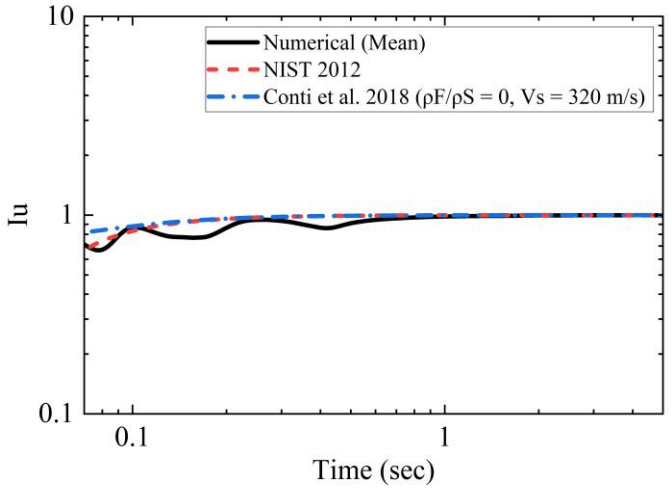

(a)

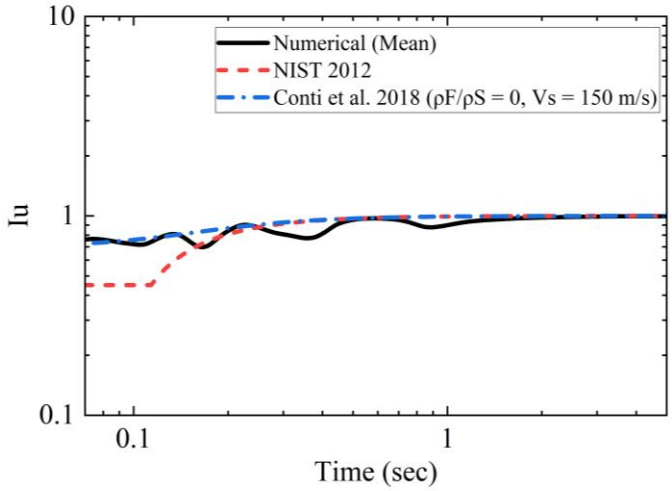

(b)

Figure 4.7 Transfer functions obtained from analytical solutions and nonlinear soil model numerical solutions on soil type with 1BS in (a) soil type D, and (b) soil type E.

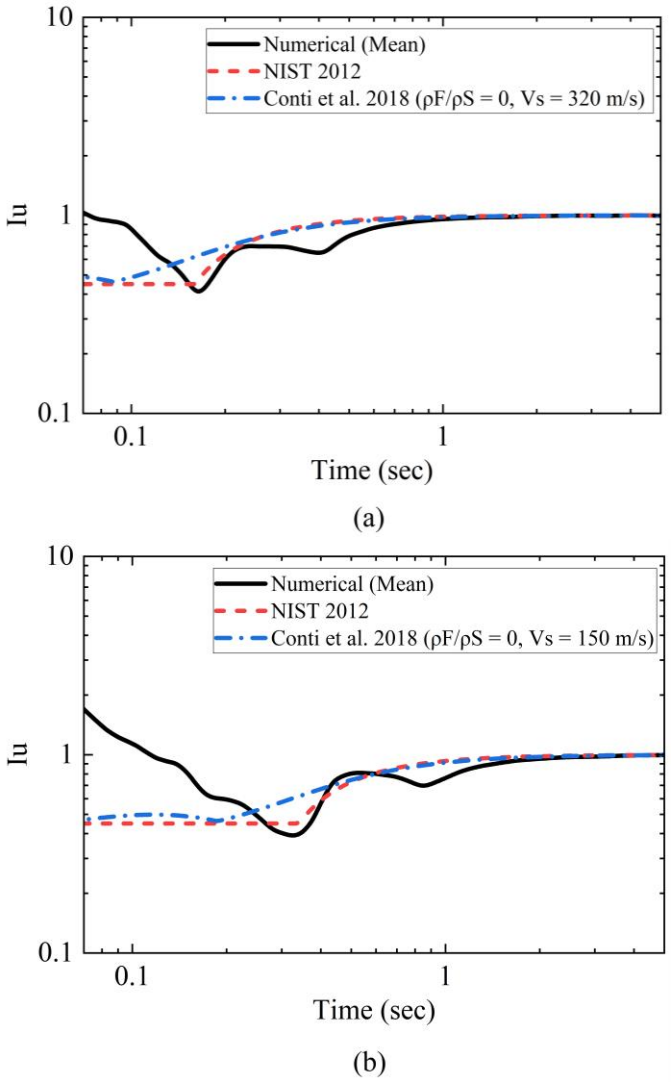

Figure 4.8 Transfer functions obtained from analytical solutions and nonlinear soil model numerical solutions on soil type with 3BS in (a) soil type D, and (b) soil type E.

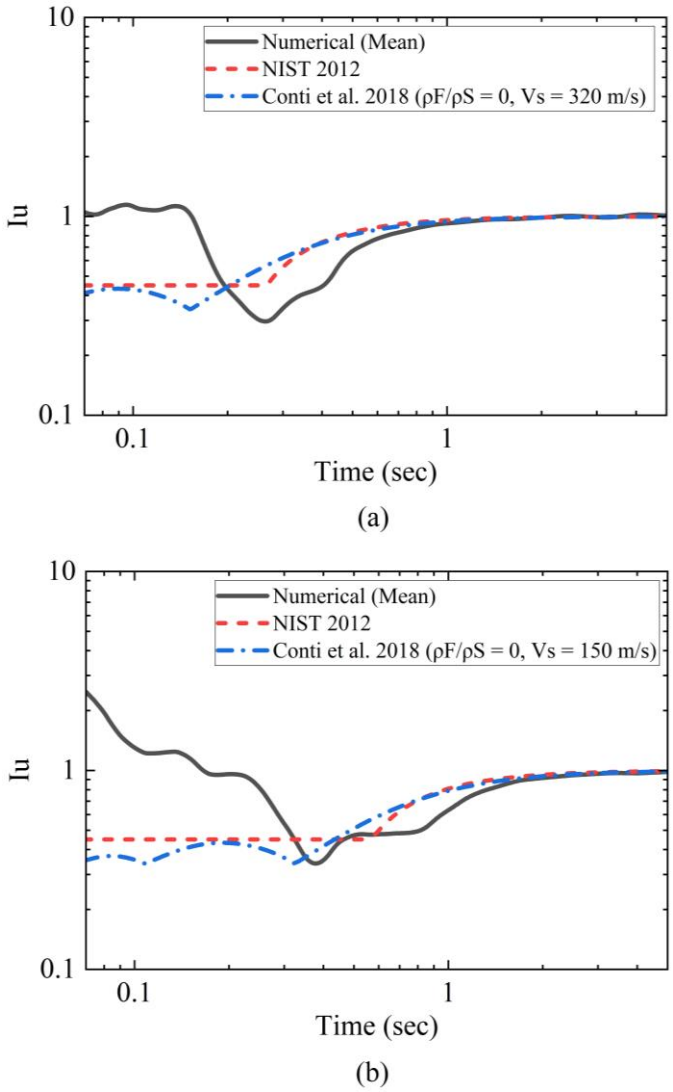

Figure 4.9 Transfer functions obtained from analytical solutions and nonlinear soil model numerical solutions with 5BS in (a) soil type D, and (b) soil type E.

4.3.3 Inference from Phase II

In this section, the horizontal transfer function $|I_u|$ obtained from the 2D nonlinear numerical analyses and those derived from analytical models are compared. The conclusions obtained from these studies are as follows.

i) The results appeared to reveal that theoretical transfer function models can only accurately predict the effects of embedment.

ii) The theoretical solutions also give the transfer function as less than one (i.e., $|I_u| < 1.0$), which implies the reduction of FIM compared with that of FFM.

iii) The applicability range of analytical transfer function models was also compared with numerical model results. The models properly anticipate a constant transfer function value for higher periods, which is consistent with the numerical analyses, whereas the divergence is more significant, especially within a small time range. This is because most analytical models always give a smooth reduction in the foundation level motion compared to FFM.

iv) Considerable variances, on the other hand, are noticed for the presence of deep subterranean levels. This disparity may be caused by (i) the simplified fundamental hypotheses utilized to create analytical models (i.e., (a) rigid subterranean system comprising foundation, it could be stiff but not rigid; (b) embedded in an half-space homogeneous elastic soil deposit), and (ii) the complexity of nonlinear numerical models using the direct approach.

v) It can be seen that the numerical models can estimate more consistently taking into account the effects of embedment depths and soil nonlinearity. Nevertheless, the analytical models fail to account for certain crucial features, such as subterranean levels flexibility, nonlinear behavior of soil deposit, and frequency-dependent amplification of foundation level motion relative to the FFM.

4.4 Phase III – Effect of different foundation-soil modeling approaches on the seismic response history of building frames

Phase III deals with the effect of different foundation-soil modeling approach on the seismic response history analysis of building frames with subterranean levels. The analysis scenario encompasses different modeling strategies and possible three soil deposits under the specified seven earthquake input motions and allows for investigating the seismic response demand of the medium-rise RC-MRF building with subterranean levels. This comprises dynamic characteristics and other responses of the building structure. The most common displacement measure for evaluating the structural dynamic behavior under a given seismic load is lateral displacement. In this study, the relative maximum horizontal displacement has been computed from the nonlinear seismic response analysis of all building models across the height of the structure. This consideration has been made to visualize the effect of different modeling strategies on the seismic

response of the structures. To have a thorough comparison between the outcomes as well as draw a clear conclusion about the effect of various modeling strategies and subsoil conditions, average maximum values of storey-level relative lateral displacements and inter-storey drift ratios are estimated. The following sections contain a detailed discussion of the results.

4.4.1 Modal analysis

The modal analyses were carried out to predict natural modes of frequencies for the structural and soil model with different alternative models in various soil deposits. The results of this analysis are applied to estimate the Rayleigh damping coefficients and damping ratio using equations 3.5 - 3.8 for nonlinear dynamic response analysis. The application of Rayleigh damping is a very popular and effective method of accounting damping effect in incremental nonlinear finite element analysis (Khazaei et al., 2017; Manolis and Markou, 2012). The results of the first mode analyses are presented as period values in Table 4.1. Since models 1A and 1B have fixed-base and are independent of the soil condition, their period values are the same for all three soil types, as indicated in the table. The fundamental period of vibration of models 1B, 2A, 2B, and 3A on soil type C increased by 14%, 46%, 31%, and 19%, respectively, in comparison to the fixed-base model (1A) without subterranean levels and SSI. Likewise, resting on soil type D increased by 14%, 78%, 60%, and 41%, and on soil type E increased by 14%, 98%, 75%, and 57%, respectively. The results of period lengthening show good agreement with provisions of ASCE/SEI 7-10 (2010), particularly for flexible-base models.

Table 4.1 Fundamental period of vibration (T_1) of the soil structure system with different alternative models in various soil deposits.

Soil type	Alternative models				
	1A	1B	2A	2B	3A
C			2.66	2.38	2.16
D	1.82	2.08	3.23	2.92	2.57
E			3.60	3.18	2.86

4.4.2 Storey lateral displacement

4.4.2.1 Effect of different modeling strategies

The average maximum lateral displacements along the storey level of the five alternative models subjected to the seven ground motions considered have been plotted in Figure 4.10. It is observed that the relative lateral storey displacement profile over the height of a building with different alternative models varies nonlinearly with superstructure height. Comparing the results for average lateral displacements of the fixed-base and flexible-base alternative models resting on subsoil types C (Figure 4.10a), D (Figure 4.10b), and E (Figure 4.10c), the horizontal storey level displacements of the flexible-base conditions for all soil types are higher than corresponding fixed-base conditions. It is evident from the result that as the flexibility of the base increases, the relative storey lateral displacements increase.

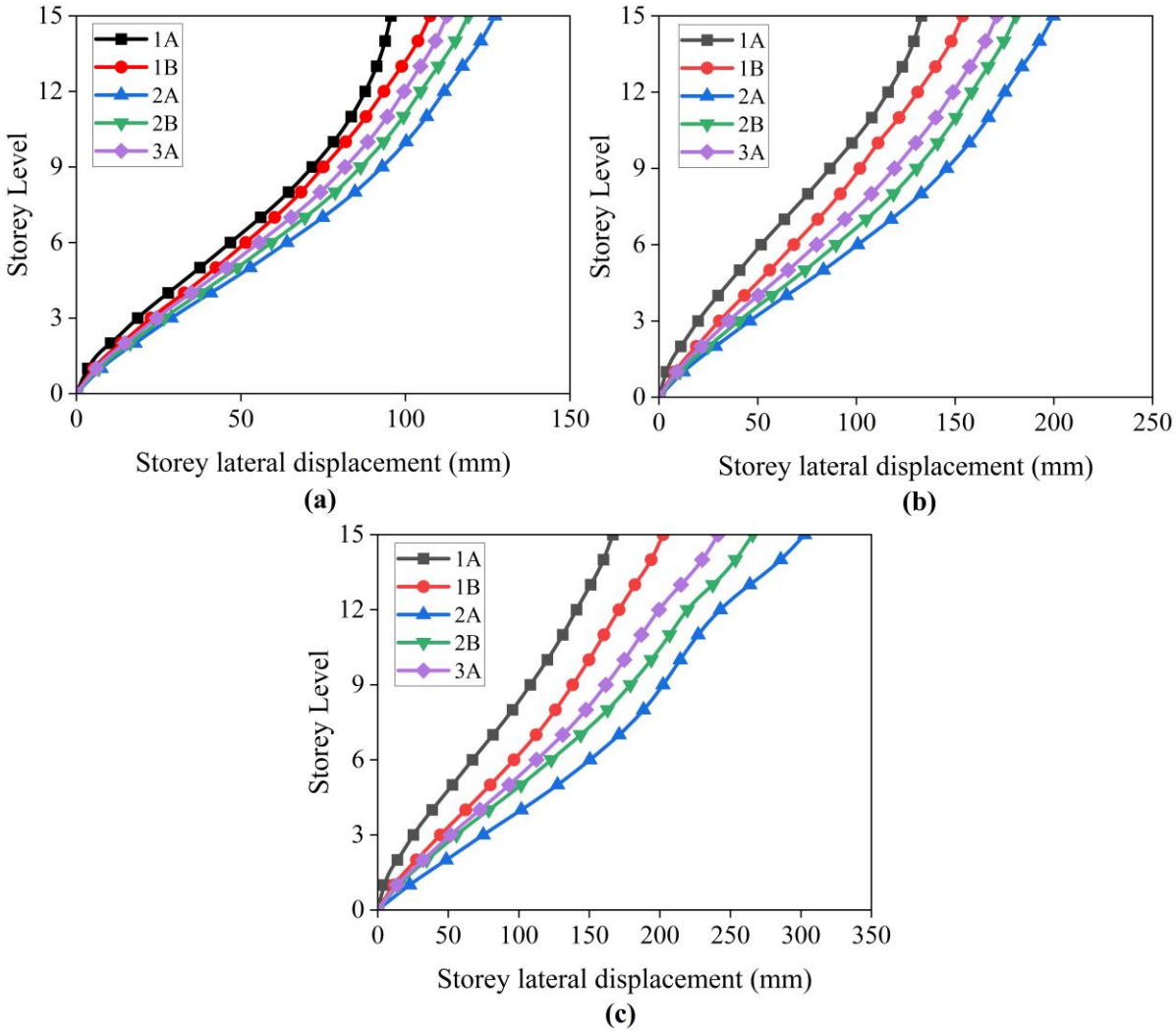

Figure 4.10 Average storey level lateral displacement results of nonlinear seismic response analyses of a 15-storey model for five different alternative models on soil type: (a) C, (b) D, and (c) E.

The maximum relative displacement response demands of the structure with 1A, 1B, 2A, 2B, and 3A alternative models in different soil profiles reach: for soil type C 96 mm, 107 mm, 127 mm, 119 mm, and 113 mm, respectively; for soil type D 133 mm, 154 mm, 200 mm, 181 mm, and 171 mm, respectively; and for soil type E 167 mm, 202 mm, 303 mm, 266 mm, 241 mm, respectively (Figure 4.11a).

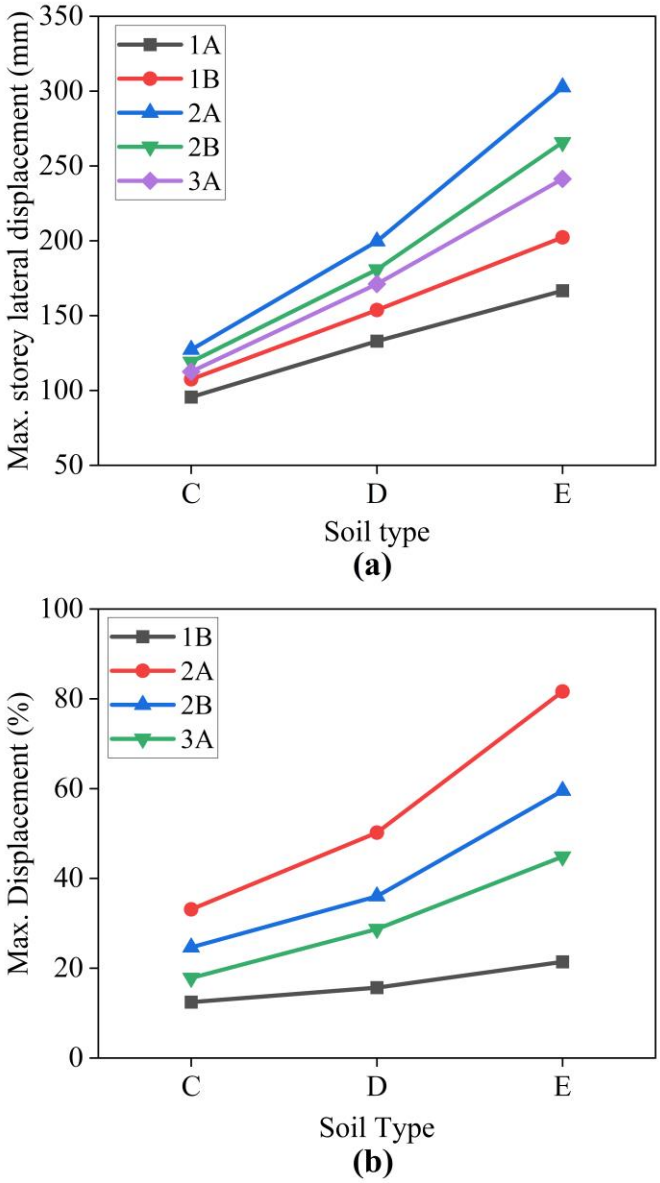

Figure 4.11 The maximum storey lateral displacement.

As presented in Figure 4.11b, the maximum lateral displacements of the building with different base models resting on soil type C increased by 12%, 33%, 25%, and 18% for 1B, 2A, 2B, and 3A models, respectively, in comparison to fixed-base model (1A). For the models on soil type D, it is increased by 16%, 50%, 36%, and 29% for 1B, 2A, 2B, and 3A models, respectively, in comparison to the fixed-base model (1A). Similarly, it increased by 21%, 82%, 60%, and 45% for the models on soil type E. It has been shown that a noticeable increase in displacement arises

in flexible-base models and the effects are more prevalent in soil type D (medium) and soil type E (soft).

The ratio of (U_{SBSI}/U_{FB}) relative lateral storey displacement of soil-basement-structure interaction (U_{SBSI}) to relative lateral storey displacement of fixed-base without subterranean levels (U_{FB}) was plotted. Figure 4.12 shows the normalized relative lateral displacement variation in comparison to fixed-base building structures without subterranean levels and SSI in three different soil types. From this figure, it has been observed that the lower storeys are more influenced by the interaction between soil, subterranean levels, and superstructure, particularly in a soft soil medium with flexible-base models. Furthermore, the flexible-base model represented by model 2A exhibits the highest relative lateral storey displacement in comparison to all other models.

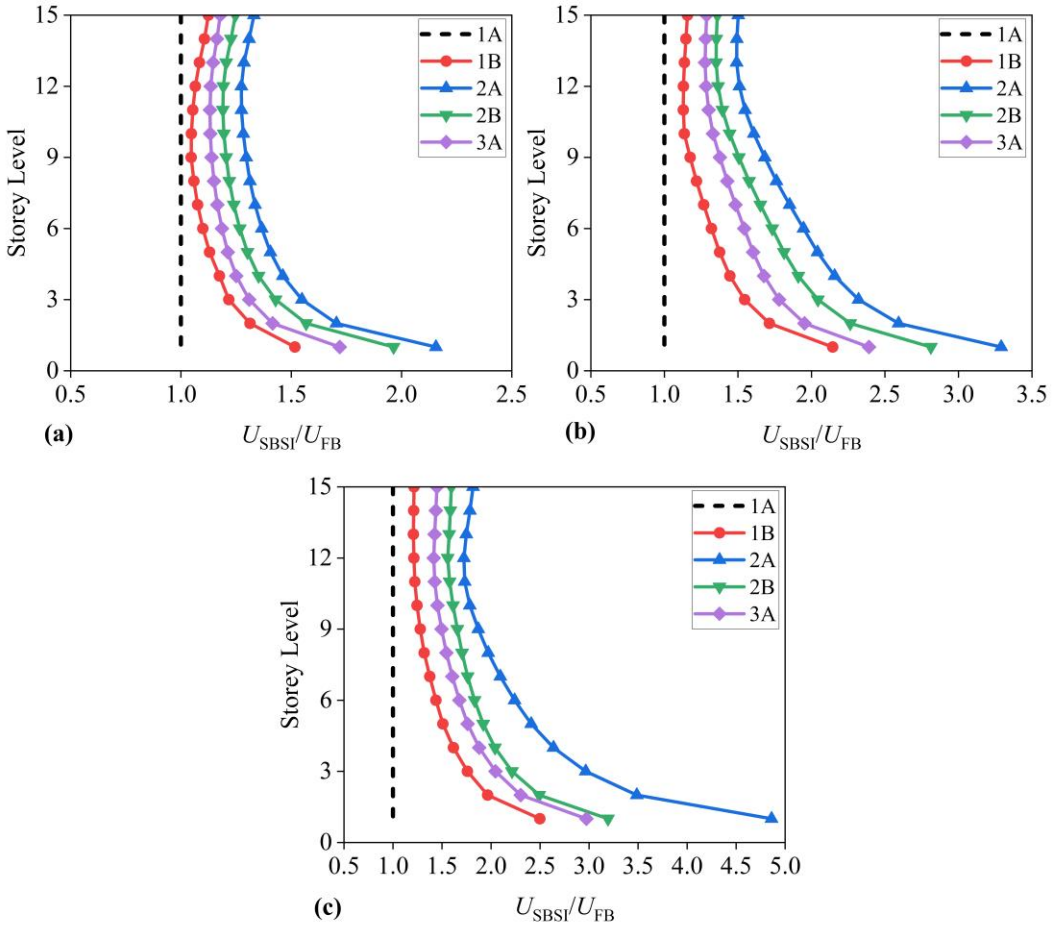

Figure 4.12 Normalized relative lateral displacement variation in comparison to fixed-base model without subterranean levels and SSI on soil type: (a) C, (b) D, and (c) E.

The maximum of U_{SBSI}/U_{FB} ratio is estimated and shown in Figure 4.13. The figure clearly reveals that the rate of increase for different soil stiffness is linear. As presented above in Figure 4.12c and clearly observed in this figure, furthermore, the higher values are occurred in soil type E particularly the flexible-base model denoted by model 2A. The results also show that as the stiffness of soil decreases, the maximum normalized relative storey displacement increases in comparison to fixed-base model (1A).

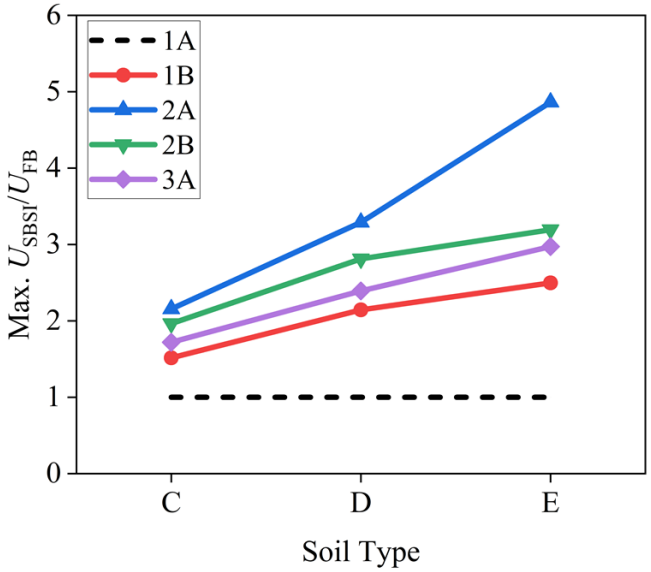

Figure 4.13 Maximum normalized relative storey lateral displacement in comparison to fixed-base (1A).

4.4.2.2 Effect of subsoil condition with the different base condition

Figure 4.14 presents the relative lateral storey displacement profile over the height of a 15-storey building on three different subsoils for five alternative models. It can be observed that the displacement profiles are varying nonlinearly over building heights. The results indicate that the lateral storey displacement increases as the stiffness of soil decrease for all alternative models (Figure 4.14a-e). The influences are more prevalent in structures simulated with soft soil (soil type E) and with flexible base models 2A, 2B and 3A as shown respectively in Figure 4.14c, d and e.

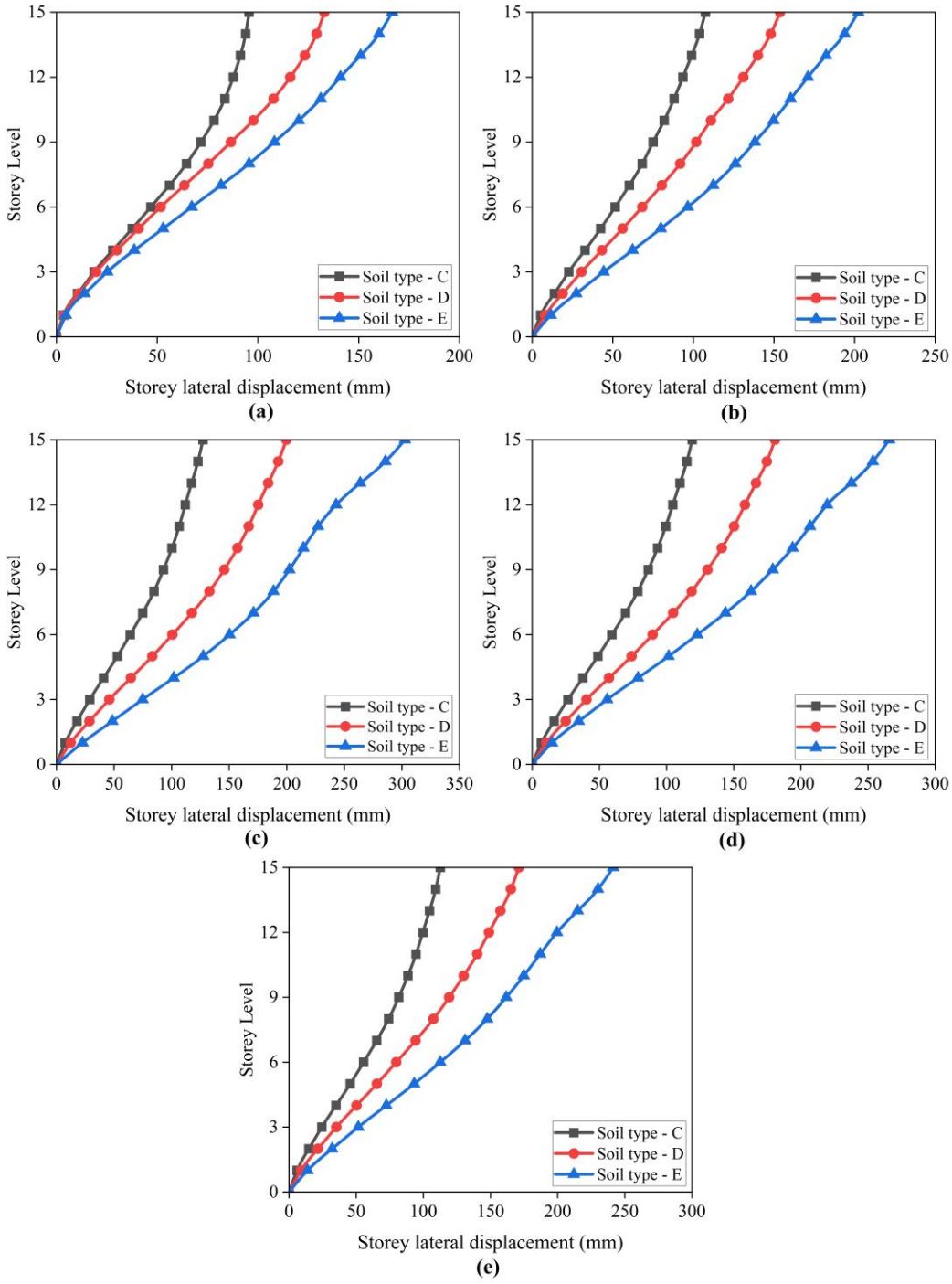

Figure 4.14 Average storey level lateral displacement results on three different subsoils for five foundation models: (a) 1A, (b) 1B, (c) 2A, (d) 2B, and (e) 3A.

Figure 4.15 shows the variation of maximum lateral displacement with the alternative models used in this study.

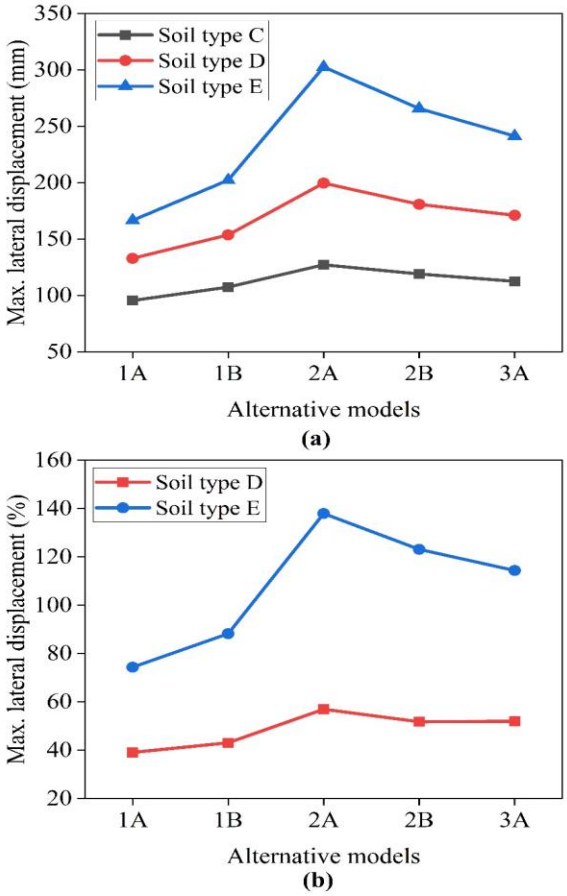

Figure 4.15 The maximum storey lateral displacement.

As presented in Figure 4.15a, the maximum lateral storey displacement response demands of the structure model in type C, D, and E soil profiles reach: for model 1A 96 mm, 133 mm, and 167 mm, respectively; for model 1B 107 mm, 154 mm and 202 mm, respectively; for model 2A 127 mm, 200 mm and 303 mm, respectively; for model 2B 119 mm, 181 mm and 266 mm, respectively and for model 3A 113 mm, 171 mm and 241 mm, respectively. The maximum relative lateral displacements of the building in comparison to the building on soil type C increase by 39% and 74% for model 1A, respectively (Figure 4.15b). Similarly, increased by 43% and 88% for model 1B, 57% and 138% for model 2A, 52% and 123% for model 2B, and 52% and 114% for model 3A, respectively, in comparison to building on soil type C. The results indicate that the lateral relative storey displacement of the building structure increases as the stiffness of the subsoil decrease. Lateral storey displacement for soil type E (soft) is higher than soil type D (medium) and C (dense), consecutively, for all alternative base models of the building.

Furthermore, Figure 4.16 show normalized relative storey lateral displacement of the building structure in comparison to soil type C with different alternative models.

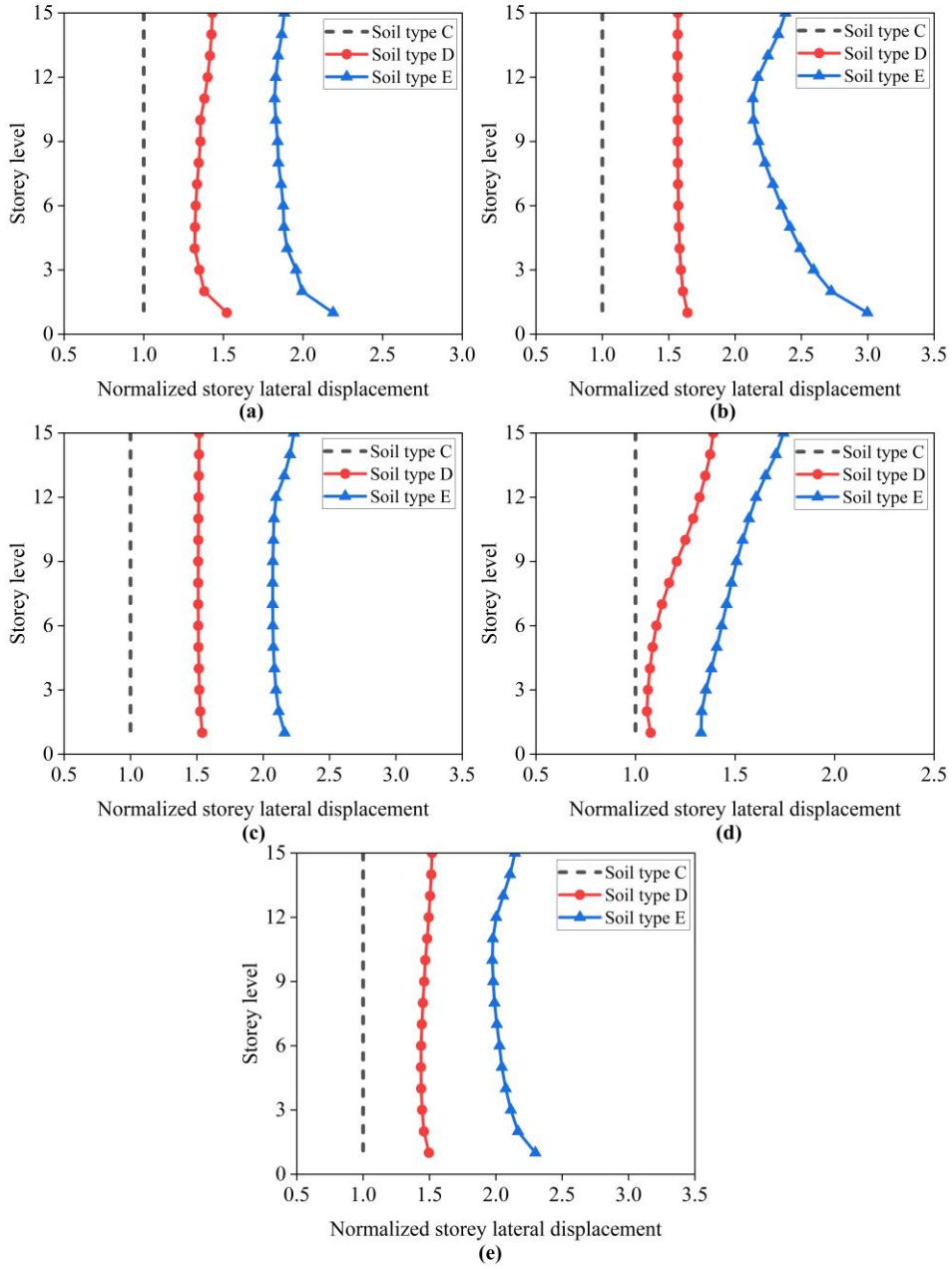

Figure 4.16 Variation of normalized relative story lateral displacement of the building structure with different alternative models in comparison to in soil type C: (a) 1A, (b) 1B, (c) 2A, (d) 2B, and (e) 3A.

From these figures, it can be observed that the normalized maximum response of building structure in a comparison of the building on soil type C of all models increased by 1.39 and 1.74 for model 1A (Figure 4.16a). Likewise, increased by 1.50 and 2.01 for model 1B (Figure 4.16b), 1.73 and 2.86 for model 2A (Figure 4.16c), 1.59 and 2.22 for model 2B (Figure 4.16d), and 1.54 and 2.35 for model 3A (Figure 4.16e), respectively, in comparison to building on soil type C. It is also confirmed that the lateral displacement increases as the stiffness of the soil decrease. Hence, the effect is more significant in soil types D and E.

It can be easily observed from the above results that the relative storey lateral displacement values are intensified by the effect of flexible-base condition and incorporation of subterranean levels, as well as the effect of subsoil condition. The higher relative storey lateral displacement was observed in flexible-base models, especially the building with subterranean modeled in relatively loose soil deposits (soil types D and E). Therefore, as the structure base flexibility increases, the governing relative storey lateral displacement increases. Likewise, in soils with less stiffness, the structural response is observed to be intensified.

In general, the detailed 3D finite element model represented by model 3A can predict more consistently taking into account the complex SSI problem, soil-structure nonlinearity, and subterranean levels effects. In a comparison of other models to model 3A (Figure 4.17), however, the flexible model represented by 2A highly amplified the storey lateral displacement, which is because the model failed to account for some important features such as soil nonlinearity and damping effects (i.e., In this case, the soil is only represented physically by springs). In contrast, the response results of fixed-base building structures represented by models 1A and 1B attenuated the response demands in comparison to flexible bases. It is because of disregarding the effect of subterranean levels in model 1A and the seismic SSI in both models.

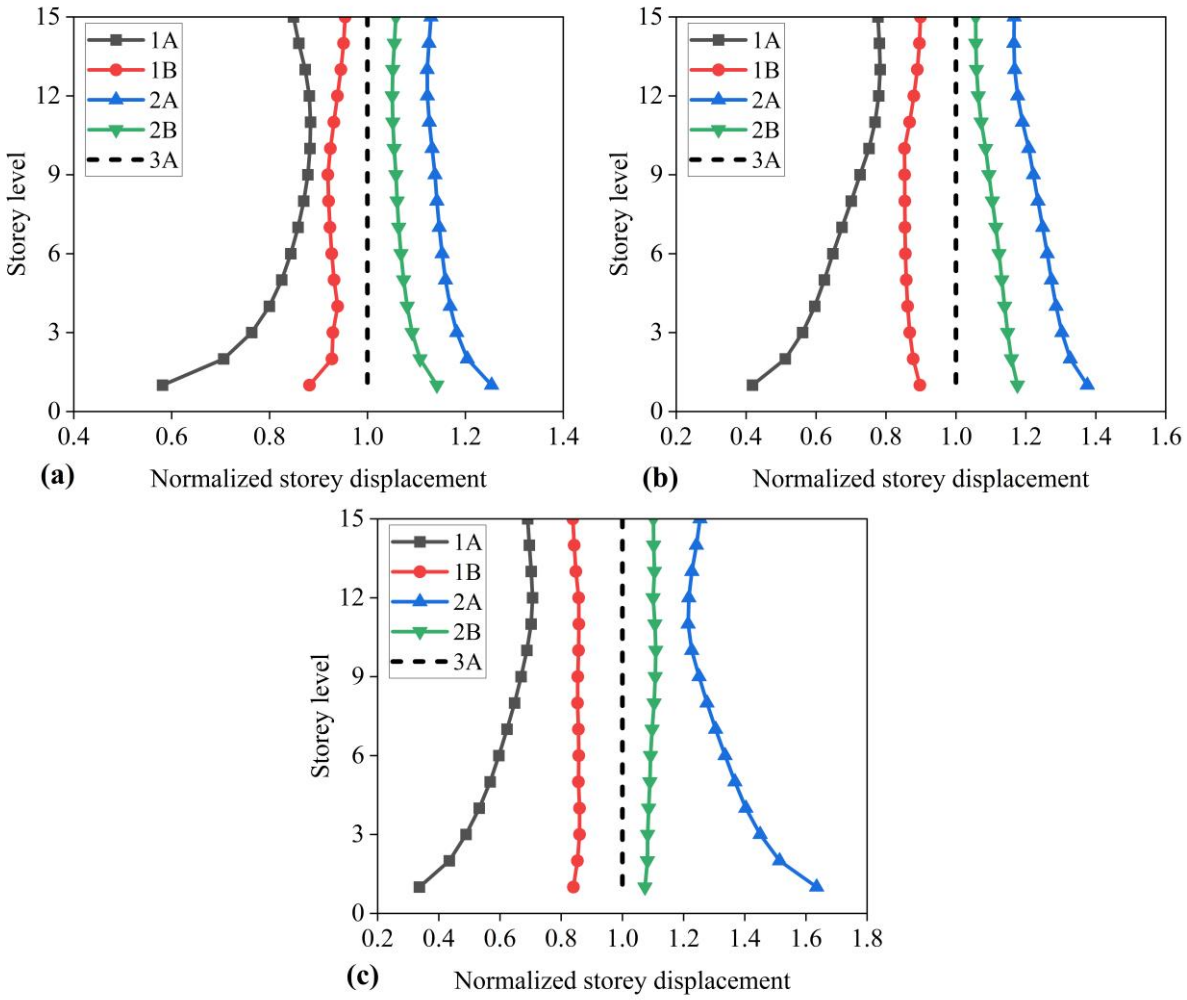

Figure 4.17 The normalized relative storey lateral displacement demands with respect to model 3A in soil type (a) C, (b) D, and (c) E.

4.4.3 Inter-storey drift ratio

In the analysis of the effects of lateral loads on the stability of vertical members, inter-storey drift ratio (DR) is one of the important parameters. It is a dimensionless parameter that characterizes the storey-level lateral displacements with respect to the corresponding storey height. The inter-storey drift can be utilized directly in the design and serviceability evaluation for beams and columns of the frame and can be associated to damage at the floor level (Ghobarah, 2004) as presents in Table 4.2. The DR values of the fixed-base and flexible-base models were evaluated using equation 4.1 as per IS 1893-1 (2016).

$$DR = \frac{(X_{i+1} - X_i)}{(H_{i+1} - H_i)} \tag{4.1}$$

where X_{i+1} is the lateral displacement at $(i+1)^{th}$ storey level, X_i is the lateral displacement at i^{th} storey level, and H_{i+1} and H_i are height at $(i+1)^{th}$ and i^{th} storey level, respectively.

Table 4.2 Drift ratio (%) limits associated with various damage levels (Ghobarah, 2004).

S. No	State of damage	Ductile MRF
1	No damage	< 0.2
2	Repairable damage	
	a) Light damage	0.4
	b) Moderate damage	< 1.0
3	Irreparable damage (> yield point)	> 1.0
4	Severe damage – Life safe – Partial collapse	1.8
5	Collapse	> 3.0

In this study, the minimum DR requirements of the fixed-base superstructure without subterranean levels were satisfied to be within the allowable limit (0.4%) during the analysis and design of the adopted building structure as per IS 1893-1 (2016). The DR values presented in the following sections were evaluated from the corresponding average values of the maximum storey lateral displacements for each base condition in different subsoil deposits.

4.4.3.1 Effect of different modeling strategies

The DR values of the 15-storey building structure with subterranean levels were evaluated and compared with various alternative models on different stiffness of soil deposits. Figure 4.18 shows the DR distribution of the building structure with different models for varying stiffness of soil.

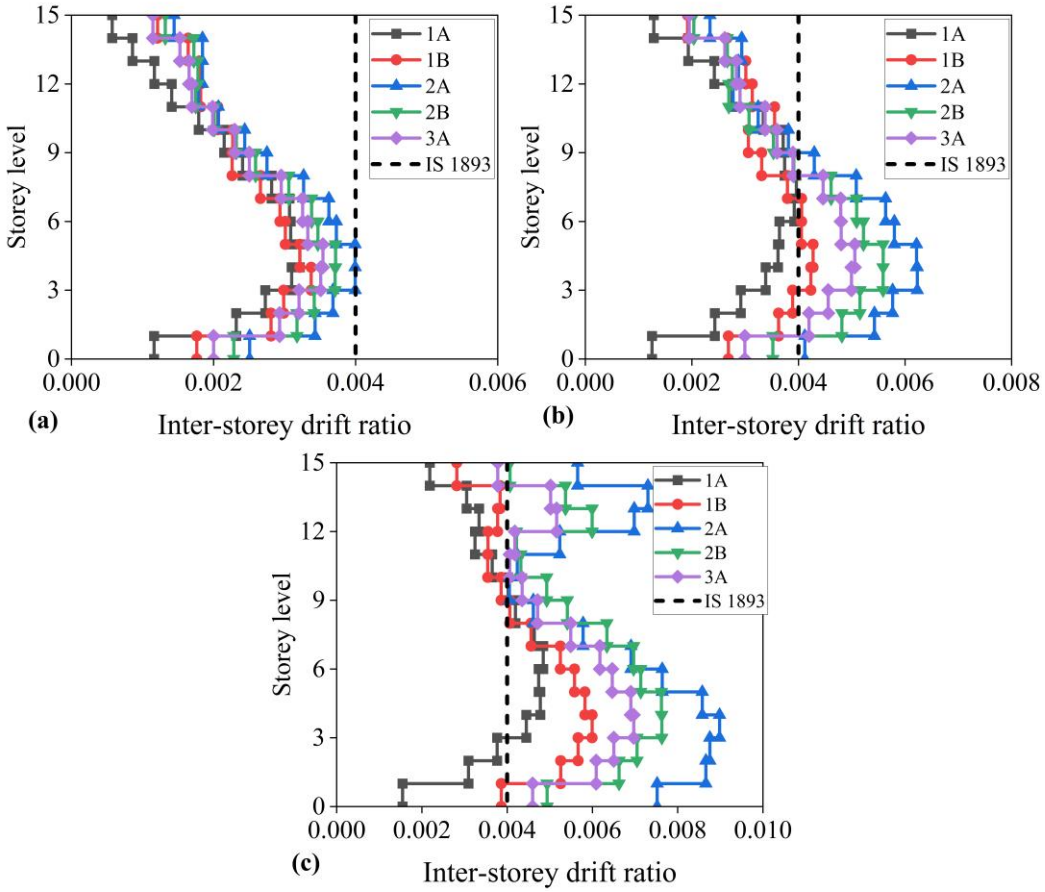

Figure 4.18 Average inter-storey drift ratio results for five different models on soil type: (a) C, (b) D, and (c) E.

As shown in Figure 4.18a, the DR value intensifies and reaches its maximum between the third and fifth storey levels on soil type C. The corresponding maximum DR values of the building with 1A, 1B, 2A, 2B, and 3A models are 0.0032, 0.0034, 0.0040, 0.0037, and 0.0035, respectively. The results reveal that, taking into account the interaction between the soil, subterranean levels, and superstructure, the DR values of the building on soil type C using the 2A model virtually reached the allowable value. Similarly, Figure 4.18b and c show the DR profile over the height of the building on soil types D and E, respectively. These values are 0.0040, 0.0043, 0.0062, 0.0056, and 0.0051 on soil type D, and 0.0048, 0.0060, 0.0090, 0.0076 and 0.0070 on soil type E for models 1A, 1B, 2A, 2B, and 3A, respectively. It is clearly observed from the results that the maximum values of the DR predominantly reached within the lower storeys (i.e., between third and seventh storey) of the building for both soil types and all alternative models and the DR value exceeded

the maximum permissible value (Figure 4.19). Furthermore, with reference to both Figures 4.18 and 4.19, the DR values are varying with different alternative models and soil stiffness. It is also observed from the figures that the DR values for all models in three soil types are higher than the fixed-base model represented by model 1A. The results prove that the incorporation of subterranean levels and SSI intensify the DR values of the building structure, particularly in soil types D and E.

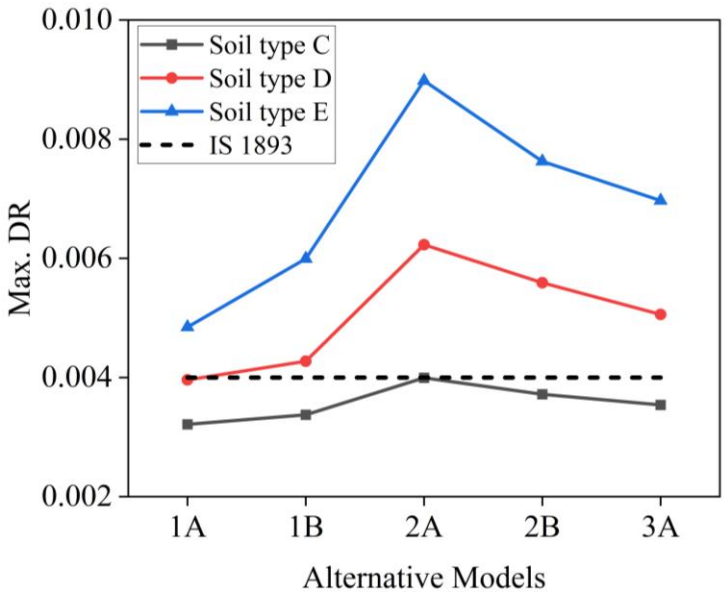

Figure 4.19 The maximum inter-storey drift ratio.

Figure 4.20 presents the normalized DR distribution of different alternative models in comparison to the fixed-base model without subterranean levels and SSI simulated in soil types C, D, and E. The normalized DR values increases as the stiffness of the soil changes from dense to soft. As revealed in these figures, these values are more pronounced in the lower (below third) and upper (above twelfth) storeys of all alternative models.

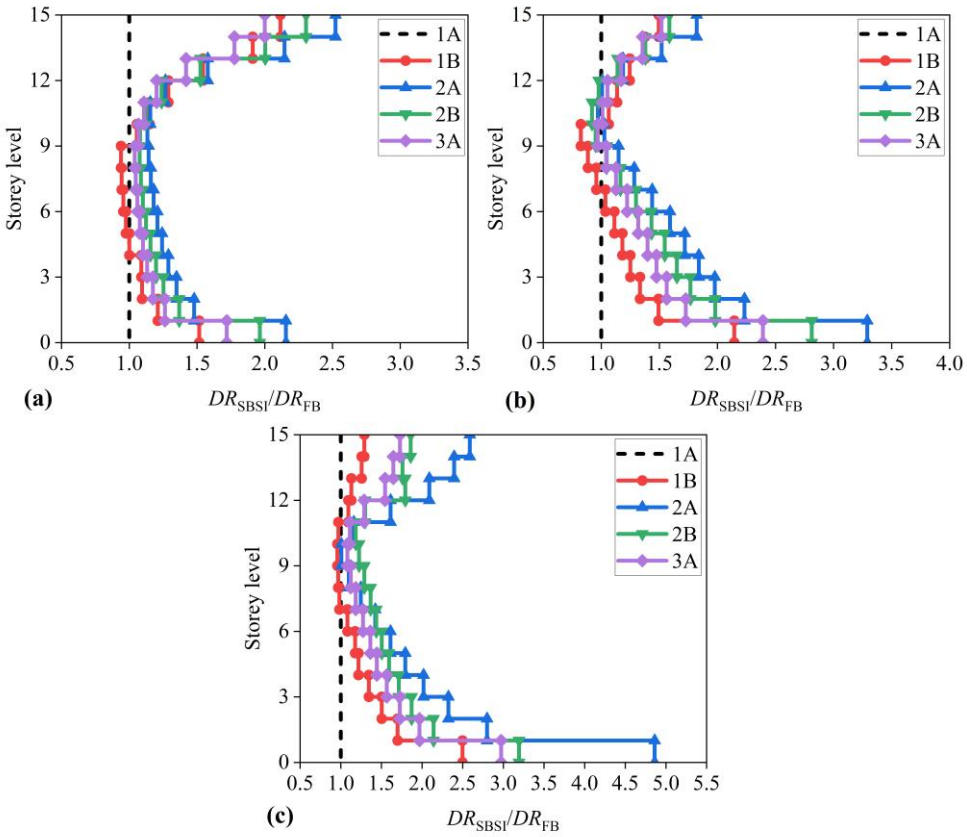

Figure 4.20 Normalized inter-storey drift ratio variation in comparison to fixed-base model without subterranean levels and SSI on soil type: (a) soil type C, (b) soil type D, and (c) soil type E.

The maximum normalized DR values are obtained to be 2.12, 2.52, 2.30 and 2.00, respectively on soil type C for 1B, 2A, 2B and 3A soil-structure system models. Also, the normalized DR values for 1B, 2A, 2B and 3A are 2.14, 3.29, 2.81 and 2.39 respectively simulated on soil type D. Similarly, these values are 2.50, 4.86, 3.19, and 2.97 respectively on soil type E. The highest normalized DR was observed in a SSS modeled with 2A followed by 2B, 3A, and 1B (Figure 4.21).

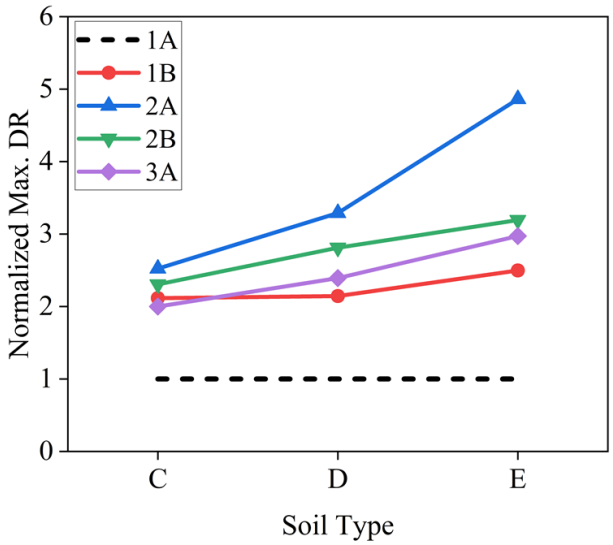

Figure 4.21 Normalized maximum inter-storey drift ratio.

4.4.3.2 Effect of subsoil conditions with different base conditions

As observed in the above sections, the stiffness variation of subsoil conditions induces a significant effect on the distribution of DR values over the height of the building structure having different base conditions. Figure 4.22 shows the average maximum DR results of nonlinear dynamic response analyses of the 15-storey model on three different subsoils for five alternative models.

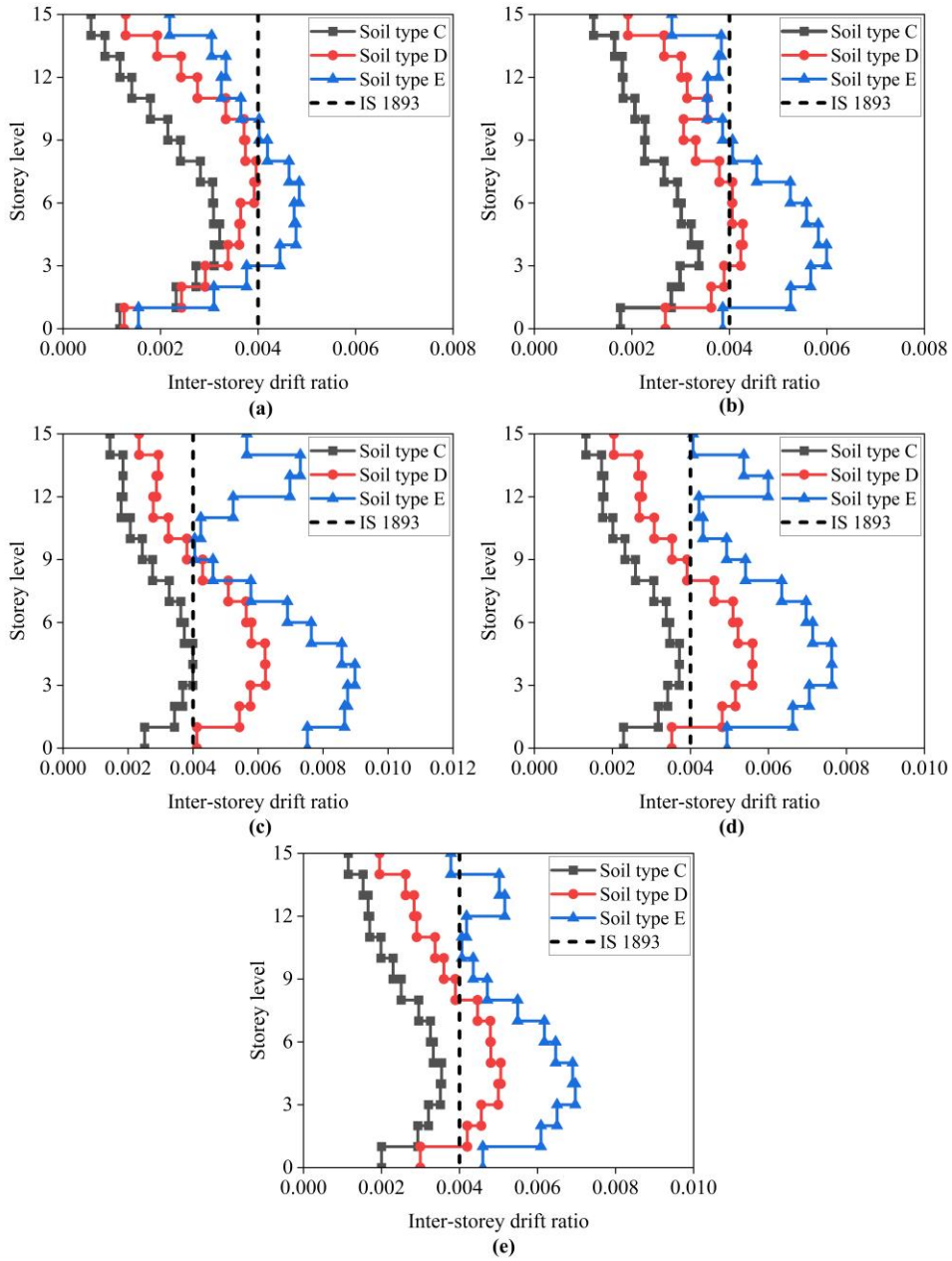

Figure 4.22 Average inter-storey drift ratio results on three different subsoils for five different models: (a) 1A, (b) 1B, (c) 2A, (d) 2B, and (e) 3A.

The maximum DR of the structure model in type C, D, and E soil types reach 0.0032, 0.0040, and 0.0048 respectively for model 1A (Figure 4.22a); 0.0034, 0.0043, and 0.0060 respectively for model 1B (Figure 4.22b); 0.0040, 0.0062 and 0.0090 respectively for model 2A (Figure 4.22c); 0.0037, 0.0056 and 0.0076 respectively for model 2B (Figure 4.22d), and 0.0035, 0.0051 and

0.0070 respectively for model 3A (Figure 4.22e). The results of the analysis show that the maximum DR value of the building structure exceeded the permissible limit, except in soil type C. In addition, the DR distribution of the building structure increases as the stiffness of the subsoil decrease. The higher values of DR occur within the lower story level of the building, between the third and seventh storey levels.

Furthermore, the building response demand in terms of normalized maximum DR is presented in Figure 4.23 in comparison to results obtained from building on soil type C simulated with different alternative models. The maximum normalized DR values for all the three types of soil and five model condition are given in Table 4.3. As can be seen from this table, the highest normalized DR was observed on the structure simulated in soil type E followed by soil type D and occurs within the upper storey level of the structure. It is clearly observed that as the soil stiffness decreased from stiff to soft the distribution of the normalized DR value with respect to soil type C (stiff soil) increased, predominantly in soil type E. Therefore, the analysis results confirm that the building response is found to be more intense in soils with low stiffness.

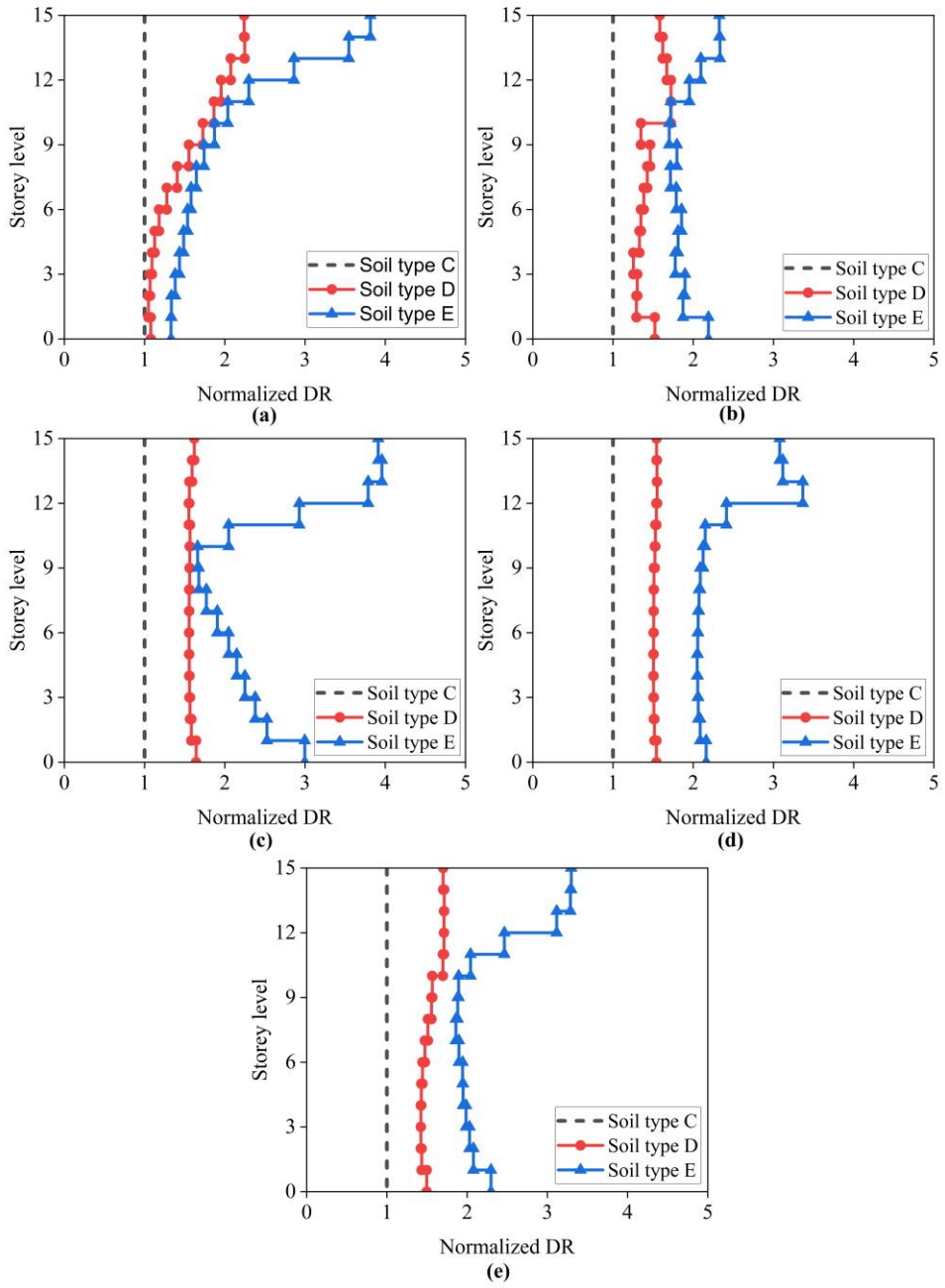

Figure 4.23 Variation of normalized inter-storey drift ratio of the building structure with different alternative models in comparison to in soil type C: (a) 1A, (b) 1B, (c) 2A, (d) 2B, and (e) 3A.

Table 4.3 Normalized maximum inter-storey drift ratio in comparison to soil type C.

Models	Soil type		
	C	D	E
1A	1.00	2.25	3.81
1B	1.00	1.72	2.33
2A	1.00	1.64	3.96
2B	1.00	1.55	3.37
3A	1.00	1.71	3.30

In summary, the results of the seismic response analysis of building structure with subterranean levels utilizing various alternative models in different soil deposits show that the response of the superstructure is affected significantly due to the incorporation of the subterranean levels and SSI with different approaches. As the flexibility of the base of the structure including subterranean levels increases, the lateral translational and rotational movement of the structure increases within subterranean levels and foundation level, which causes an intensification of storey level lateral displacement, as well as the corresponding DR of the superstructure. Likewise, as the stiffness of soil varies from dense to soft, these response parameters further increase.

4.4.4 Inference from Phase III

In this section, the results obtained from numerical studies on the influence of various alternative modeling strategies for seismic response history analysis of building frames with subterranean levels are presented. The conclusions obtained from phase III are as follows.

a) Storey level lateral displacement

i) The relative lateral storey level displacement profile over the height of a building with different alternative models varies nonlinearly with height.

ii) The horizontal storey level displacements of the flexible-base models for all soil types are higher than the corresponding fixed-base conditions. It is evident from the result that as the flexibility of the base increases, the relative storey lateral displacements increase.

iii) It is also found that the maximum storey lateral displacements of the building with different alternative models founded on soil type C have increased by 12%, 33%, 25%, and 18% respectively for models 1B, 2A, 2B, and 3A in comparison to fixed-base model (1A).

iv) Lateral displacement of the different alternative modes resting on soil type D increased by 16%, 50%, 36%, and 29% in comparison to the fixed-base model (1A) for 1B, 2A, 2B, and 3A, respectively.

v) In comparison to the fixed-base model (1A), the lateral displacements of the alternative models on soil type E increased by 21%, 82%, 60%, and 45%, respectively, for 1B, 2A, 2B, and 3A.

vi) It is found that a noticeable increase in displacement occurs in flexible-base models. The influences are more predominant in flexible-base supported structures modelled in soil type D (medium) and soil type E (soft) soil.

vii) The relative storey lateral displacement values were intensified by the effect of flexible-base conditions and incorporation of subterranean levels, as well as the effect of subsoil conditions. The higher relative storey lateral displacement was observed in flexible-base models, especially the building with subterranean levels simulated in relatively loose soil deposits (soil types D and E). In summary, as the structure base flexibility increases, the maximum relative storey lateral displacement increases. Similarly, in soils with less stiffness, the structural response was observed to be intensified by 16% - 82%.

viii) Furthermore, the flexible-base model represented by model 2A exhibits the highest relative lateral storey displacement in comparison to all other models, whereas models 2B and 3A show relatively the same values with a small difference.

b) Inter-storey drift ratio

i) The maximum DR values of the building with 1A, 1B, 2A, 2B, and 3A models are 0.0032, 0.0034, 0.0040, 0.0037, and 0.0035 respectively on soil type C. It is clear from the results that the DR values of the building on soil type C with the 2A model almost reached the permissible value considering the interaction between soil, subterranean levels, and superstructure.

ii) Similarly, the DR values are 0.0040, 0.0043, 0.0062, 0.0056, and 0.0051 on soil type D, and 0.0048, 0.0060, 0.0090, 0.0076 and 0.0070 on soil type E for models 1A, 1B, 2A, 2B, and 3A respectively. It is observed from the results that the maximum values of the DR

predominantly reached the lower storeys of the building and exceeded the permissible value for both soil types and all alternative models.

iii) The normalized DR distribution in comparison to the fixed-base model without subterranean levels and SSI simulated on soil types C, D, and E were evaluated (Figure 9b). The maximum normalized DR values are obtained to be 2.12, 2.52, 2.30, and 2.00, respectively, on soil type C for 1B, 2A, 2B, and 3A soil-structure system models. Also, the normalized DR values simulated on soil type D are 2.14, 3.29, 2.81, and 2.39 for models 1B, 2A, 2B, and 3A, respectively. Similarly, the DR values on soil type E are 2.50, 4.86, 3.19, and 2.97, respectively.

iv) The highest normalized DR was observed in a soil-structure system modelled with 2A followed by 2B, 3A, and 1B. Furthermore, the results reveal how the incorporation of subterranean levels and SSI significantly intensify the DR values of the building structure.

v) The highest DR was observed on the structure simulated in soil type E followed by soil type D and occurs within the lower storey level of the structure. It is observed that as the soil stiffness decreased from dense to soft the distribution of the DR value increased, predominantly in soil type E.

4.5 Phase IV – Influence of subterranean levels embedment depths on the seismic response of building frames

The influence of incorporating one or more subterranean levels on the seismic response of an RC-MRF building was analyzed. This was performed by comparing the results of nonlinear seismic response analysis of the mid-rise building with and without subterranean levels supported by various soil deposit subjected to strong earthquake ground motions. The results of the analyses have been compared and discussed in terms of structural displacements and drifts.

4.5.1 Modal analysis

Table 4.4 presents the results of the first mode analyses as period values. The fundamental period of vibration of models 0BS, 1BS, 3BS, and 5BS on soil type C increased by 51%, 34%, 19%, and 6%, respectively, in comparison to the fixed-base model (FB) without subterranean levels and SSI. Likewise, resting on soil type D increased by 83%, 63%, 41%, and 21%, and on soil type E increased by 103%, 80%, 57%, and 34%, respectively.

Table 4.4 Fundamental period of vibration (T_1) of the soil-structure system with different subterranean levels in various soil types.

Soil type	Alternative models				
	FB	0BS	1BS	3BS	5BS
C		2.74	2.43	2.16	1.93
D	1.82	3.33	2.96	2.57	2.21
E		3.69	3.27	2.86	2.43

4.5.2 Storey lateral displacement

4.5.2.1 Effect of subterranean levels and embedment depths

The average maximum lateral displacements along the storey level of the building frame with fixed-base, without and with subterranean levels have been plotted in Figure 4.24(i). The results reveal that the relative lateral storey displacement profile over the height of a building with different models varies nonlinearly with superstructure height. The maximum relative lateral displacement of the structure with FB, 0BS, 1BS, 3BS, and 5BS models in different soil profiles reach: for soil type C (Figure 4.24i-a) 96 mm, 131 mm, 122 mm, 113 mm, and 103 mm, respectively; for soil type D (Figure 4.24i-b) 133 mm, 206 mm, 184 mm, 171 mm, and 150 mm, respectively; and for soil type E (Figure 4.24i-c) 167 mm, 310 mm, 274 mm, 241 mm, 202 mm, respectively.

Comparing the results for average lateral displacements of the fixed-base model and flexible-base models without and with subterranean levels resting on subsoil types C, D, and E, the horizontal storey level displacements of the flexible-base conditions for all soil types are higher than corresponding fixed-base conditions (Figure 4.25a). It is evident from the result that as the flexibility of the base increases (i.e., as the subterranean levels decreases in this study), the relative storey lateral displacements increase.

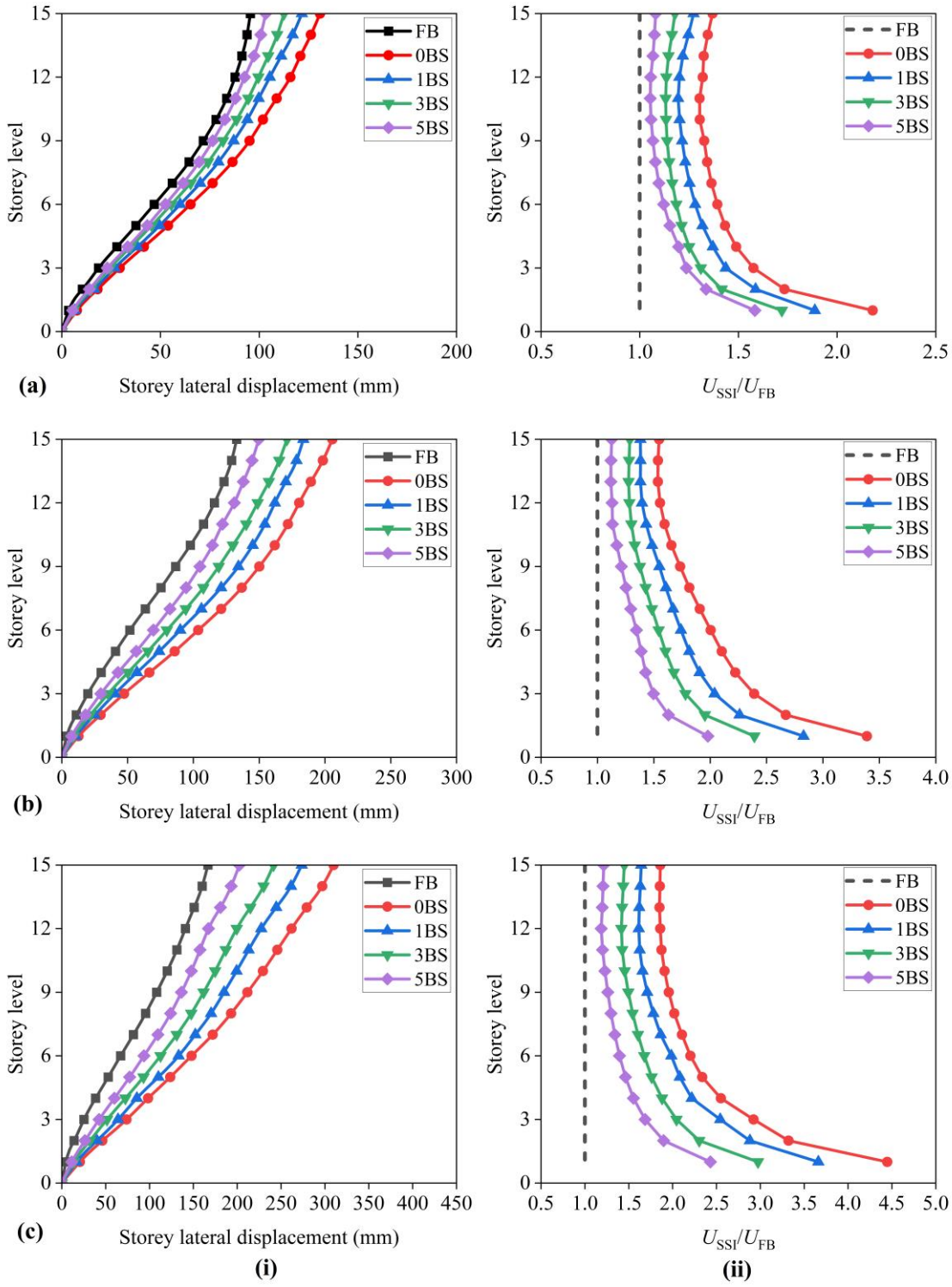

Figure 4.24 (i) Average storey level lateral displacement and (ii) normalized relative lateral displacement variation in comparison to fixed-base model on soil type: (a) C, (b) D, and (c) E.

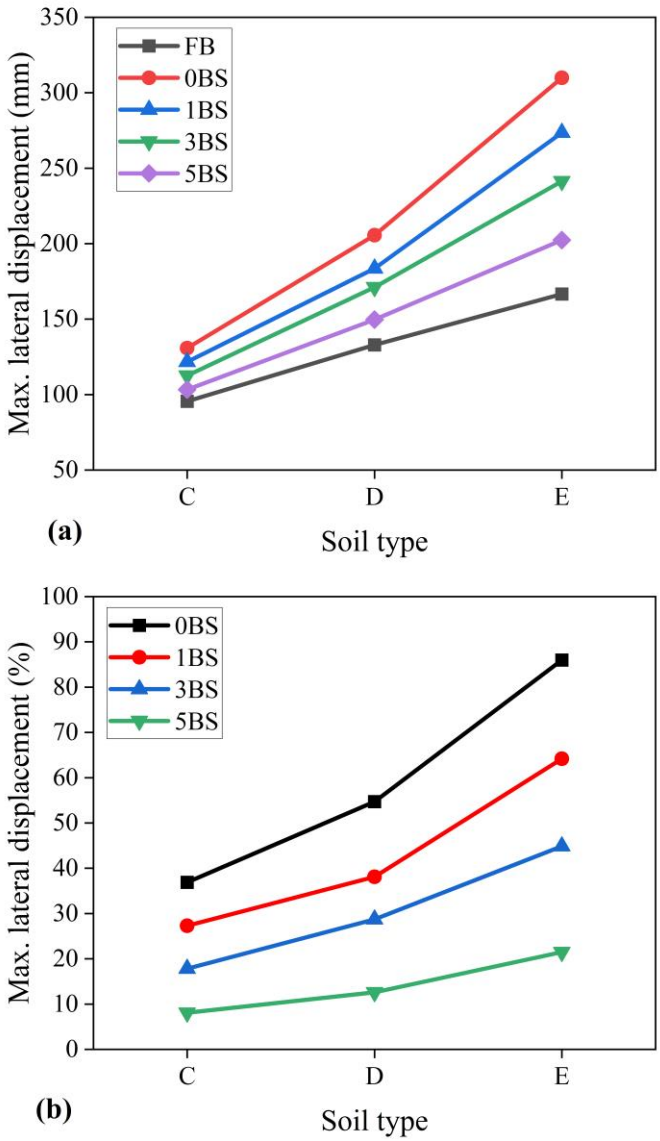

Figure 4.25 Maximum storey lateral displacement.

As shown in Figure 4.25b, the maximum lateral displacements of the building frame without and with subterranean levels resting on soil type C increase by 37%, 27%, 18%, and 8% for 0BS, 1BS, 3BS, and 5BS models, respectively, in comparison to fixed-base model (FB). For the models on soil type D, it is increased by 55%, 38%, 29%, and 13% for 0BS, 1BS, 3BS, and 5BS models, respectively, in comparison to the fixed-base model (FB). Similarly, it increased by 86%, 64%, 45%, and 21% for the models on soil type E. It has been shown that a noticeable increase in

displacement arises in flexible-base models and the effects are more prevalent in soil type D (medium) and soil type E (soft).

The ratio of (U_{SSI}/U_{FB}) relative lateral storey displacement of building frame having different subterranean levels incorporating soil-structure interaction (U_{SSI}) to relative lateral storey displacement of building frame with fixed-base at the ground surface (U_{FB}) was plotted. Figure 4.24(ii) shows the normalized relative lateral displacement variation in comparison to fixed-base building frames resting on three different soil types. From these results, it has been observed that the lower storeys are more influenced by the interaction between soil, foundation, subterranean levels, and superstructure, particularly in a soft soil medium. The normalized maximum response of the building frame in soil type C (Figure 4.24ii-a) with 0BS, 1BS, 3BS, and 5BS models are 2.18, 1.89, 1.72, and 1.58, respectively. Similarly, resting in soil type D (Figure 4.24ii-b) is 3.39, 2.83, 2.39, and 1.98, and in soil type E (Figure 4.24ii-c) 4.45, 3.66, 2.97, and 2.43, respectively. Additionally, the maximum value of U_{SSI}/U_{FB} ratio is shown in Figure 4.26. The flexible-base model represented by model 0BS exhibits the highest relative lateral storey displacement in comparison to all other models.

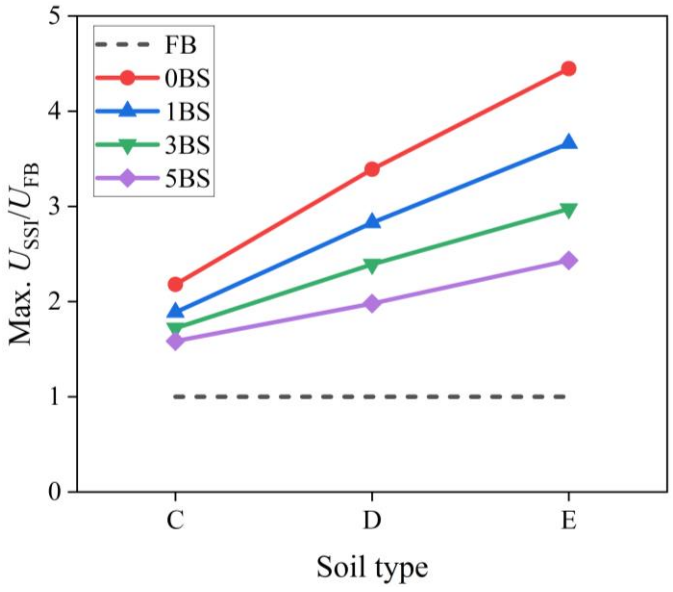

Figure 4.26 Maximum storey lateral displacement.

4.5.2.2 Effect of subsoil condition with different subterranean levels

Figure 4.27(i) presents the relative lateral storey displacement profile over the height of a 15-storey building on three different subsoils for five different models. The maximum lateral storey displacement response demands of the structure model in type C, D, and E soil profiles reach respectively: for model FB (Figure 4.27i-a) 96 mm, 133 mm, and 167 mm; for model 0BS (Figure 4.27i-b) 131 mm, 206 mm and 310 mm; for model 1BS (Figure 4.27i-c) 122 mm, 184 mm and 274 mm; for model 3BS (Figure 4.27i-d) 113 mm, 171 mm and 241 mm; and for model 5BS (Figure 4.27i-e) 103 mm, 150 mm and 202 mm.

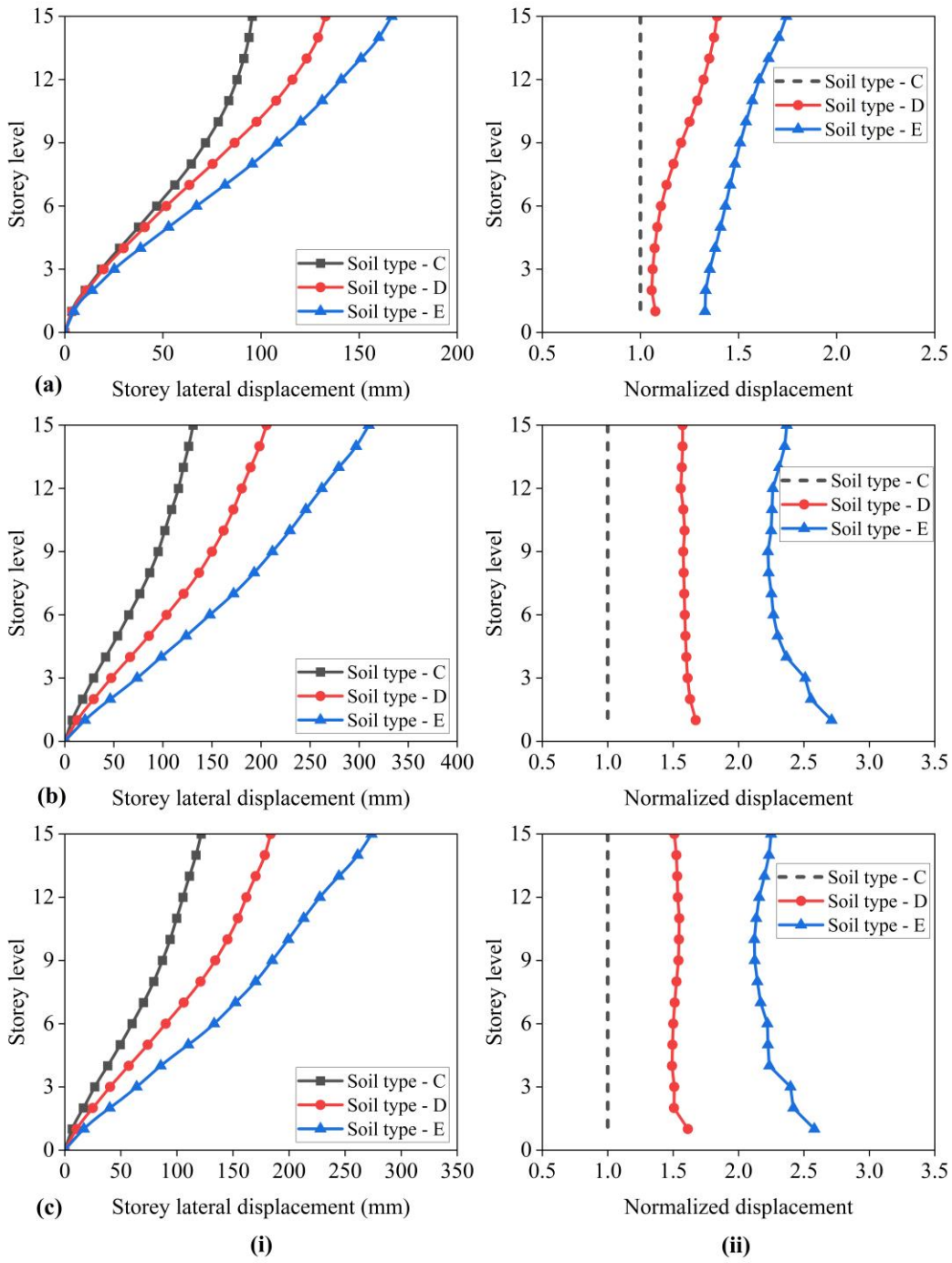

Figure 4.27 (i) Average storey level maximum lateral displacement, and (ii) variation of normalized relative storey lateral displacement of the building structure with different models in comparison to in soil type C: (a) FB, (b) 0BS, (c) 1BS, (d) 3BS, and (e) 5BS.

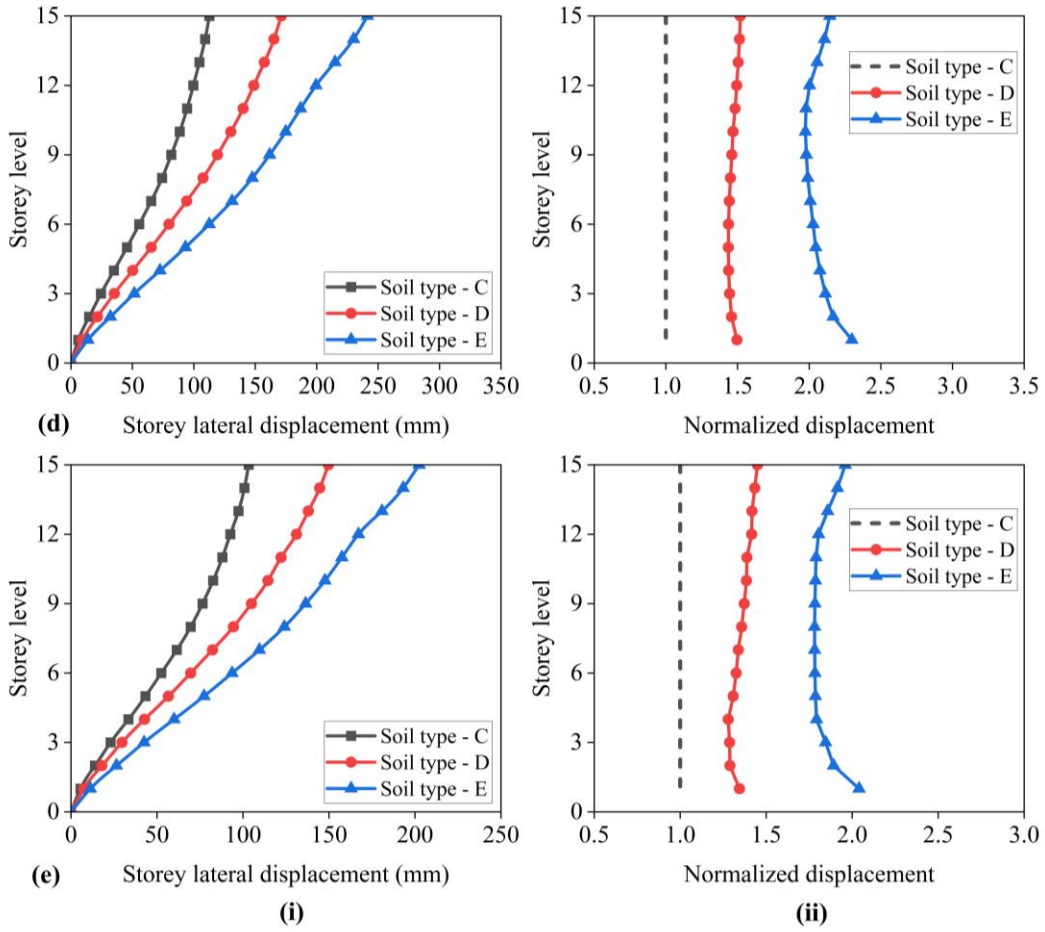

Figure 4.27 (Continued).

Furthermore, Figure 4.27(ii) shows the normalized relative storey level lateral displacement profile of the building structure with different models founded on soil type D and E in comparison to soil type C. Table 4.5 also presents the normalized maximum response of the building frame resting on soil type D and E in comparison to soil type C. Both figure and table are confirmed that the lateral displacement increases as the stiffness of the soil decrease.

Table 4.5 Maximum normalized relative storey lateral displacement in comparison to soil type C.

	Soil type		
Subterranean levels	C	D	E
FB	1.00	1.39	1.74
0BS	1.00	1.67	2.71
1BS	1.00	1.61	2.58
3BS	1.00	1.52	2.30
5BS	1.00	1.45	2.04

It can be observed from the above results and also as shown in Figure 4.28a, the maximum lateral storey displacement for soil type E (soft) is higher than soil type D (medium) and C (dense), consecutively, for all different models of the building without and with subterranean levels. As presented in Figure 4.28b, the maximum relative lateral displacements of the building structure simulated on soil type D and E increased by 39% and 74% for model FB respectively in comparison to the building on soil type C. Similarly, it is increased by 57% and 137% for model 0BS, 51% and 125% for model 1BS, 52% and 114% for model 3BS, and 45% and 96% for model 5BS. The results indicate that the lateral relative storey displacement of the building structure increases as the stiffness of the subsoil decrease.

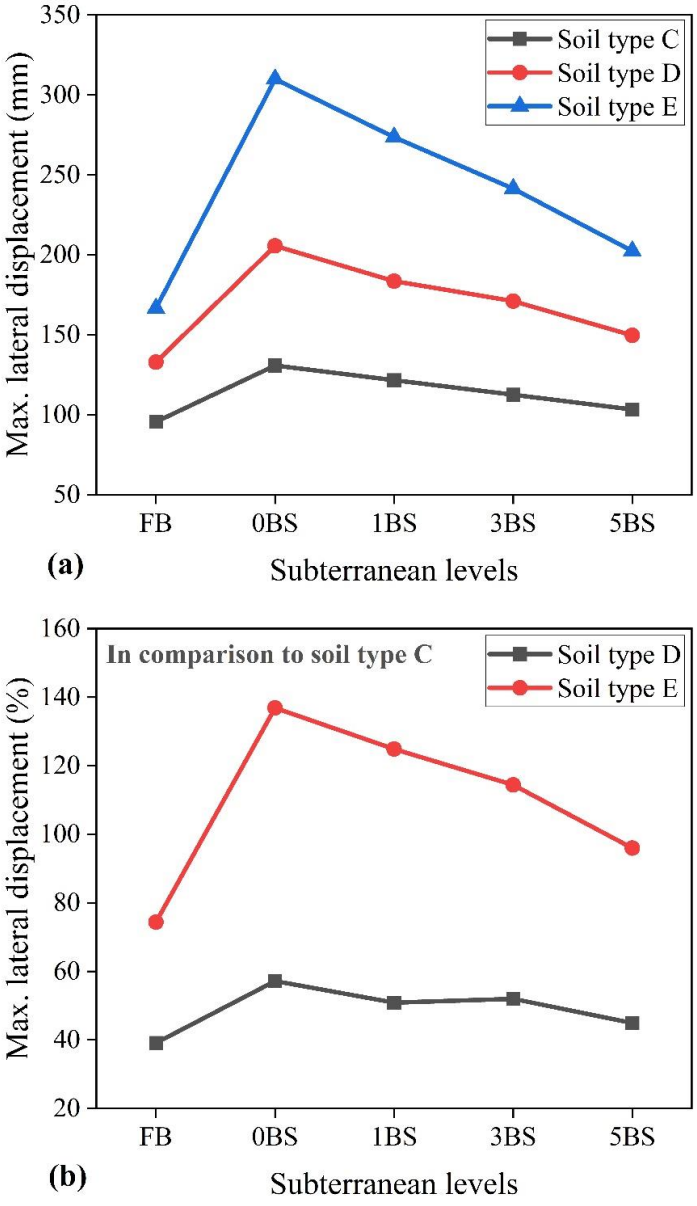

Figure 4.28 Maximum storey lateral displacement.

It can be easily observed from the results of Figures 4.24 and 4.27 that the relative storey lateral displacement values are intensified by the effect of flexible-base condition and incorporation of subterranean levels, as well as the effect of subsoil condition. The higher relative storey lateral displacement was observed in flexible-base models, especially the building without and with subterranean levels modeled in relatively loose soil deposits (soil types D and E). Therefore, as the structure base flexibility increases, the governing relative storey lateral

displacement increases. Likewise, in soils with less stiffness, the structural response is observed to be intensified.

As explained in the above sections, the results for lateral storey level displacements of the superstructure on all soil types with flexible-base models were higher than the corresponding fixed-base conditions. Also, the building with 0BS exhibits the highest relative lateral storey displacement in comparison to all other models. However, as shown in Figure 4.29 and in comparison to building with 0BS, the effects were reduced as the number of subterranean levels increased. It was observed that the buildings without subterranean levels are significantly affected by seismic SSI.

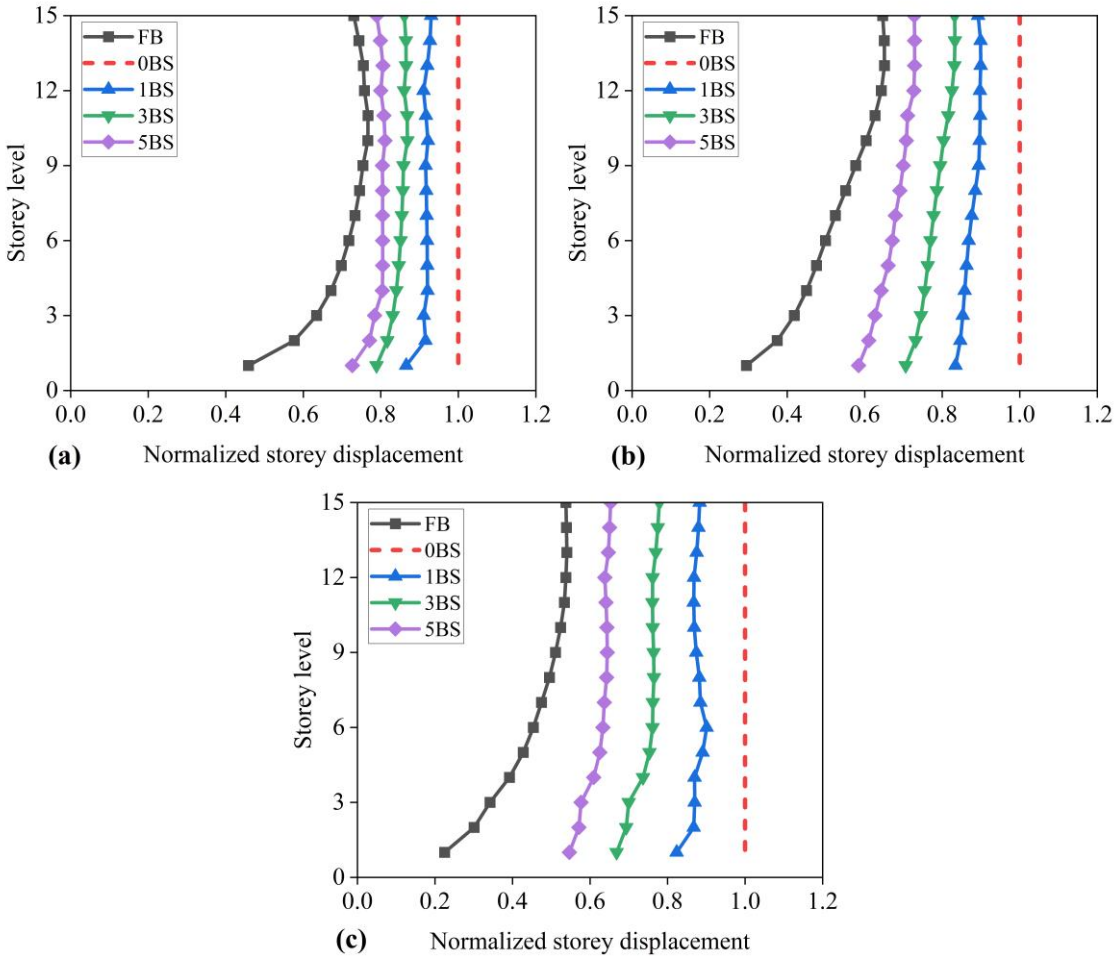

Figure 4.29 The normalized seismic response demands with respect to model 0BS in soil type (a) C, (b) D, and (c) E.

4.5.3 Inter-storey drift

4.5.3.1 Effect of subterranean levels and embedment depths

The DR values of the 15-storey building frame were evaluated and compared. Figure 4.30(i) shows the DR distribution of the building frame with different subterranean levels and embedment depths resting on soil with different stiffness. As revealed in Figure 4.30i-a, the DR value increases and reaches its maximum in the lower storey level of the building frame (i.e., between the third and fifth storey levels). For building simulated on soil type C, the corresponding maximum DR values of the building frame with FB, 0BS, 1BS, 3BS, and 5BS models are 0.0032, 0.0041, 0.0038, 0.0035, and 0.0035, respectively. The results of the analysis reveal that the DR value is lower than the allowable value, except for the flexible-base model without subterranean levels (0BS). Similarly, Figure 4.30i-b and c show the DR profile over the height of the building on soil types D and E, respectively. These values are 0.0040, 0.0064, 0.0056, 0.0051, and 0.0046 on soil type D, and 0.0048, 0.0092, 0.0082, 0.0070 and 0.0058 on soil type E for models FB, 0BS, 1BS, 3BS, and 5BS, respectively. The results show that for both soil types and all models the maximum values of the DR predominantly reached within the lower storey levels (i.e., between the second and seventh storey levels) of the building frame and exceeded the permissible value. Additionally, the incorporation of the foundation, subterranean levels, and SSI considerably intensifies the DR values of the building frame in comparison to the fixed-base model.

Figure 4.30(ii) present the normalized DR distribution in comparison to the fixed-base model without foundation, subterranean levels, and SSI simulated on soil types C, D, and E. For a soil-structure system with 0BS, 1BS, 3BS, and 5BS models on soil type C (Figure 4.30ii-a), the maximum normalized DR values are obtained to be 2.68, 2.71, 2.00, and 1.58, respectively. Also, in the system simulated on soil type D (Figure 4.30ii-b), the normalized DR values are 3.39, 2.83, 2.39, and 1.98, respectively. Similarly, these values are 4.45, 3.66, 2.97, and 2.43, respectively, on soil type E (Figure 4.30ii-c). The results of the analysis revealed that, in all models, the lower and upper storey levels of the building structure exhibit the major influence. The highest normalized DR was observed in a soil-structure system simulated on soil types D and E with 0BS.

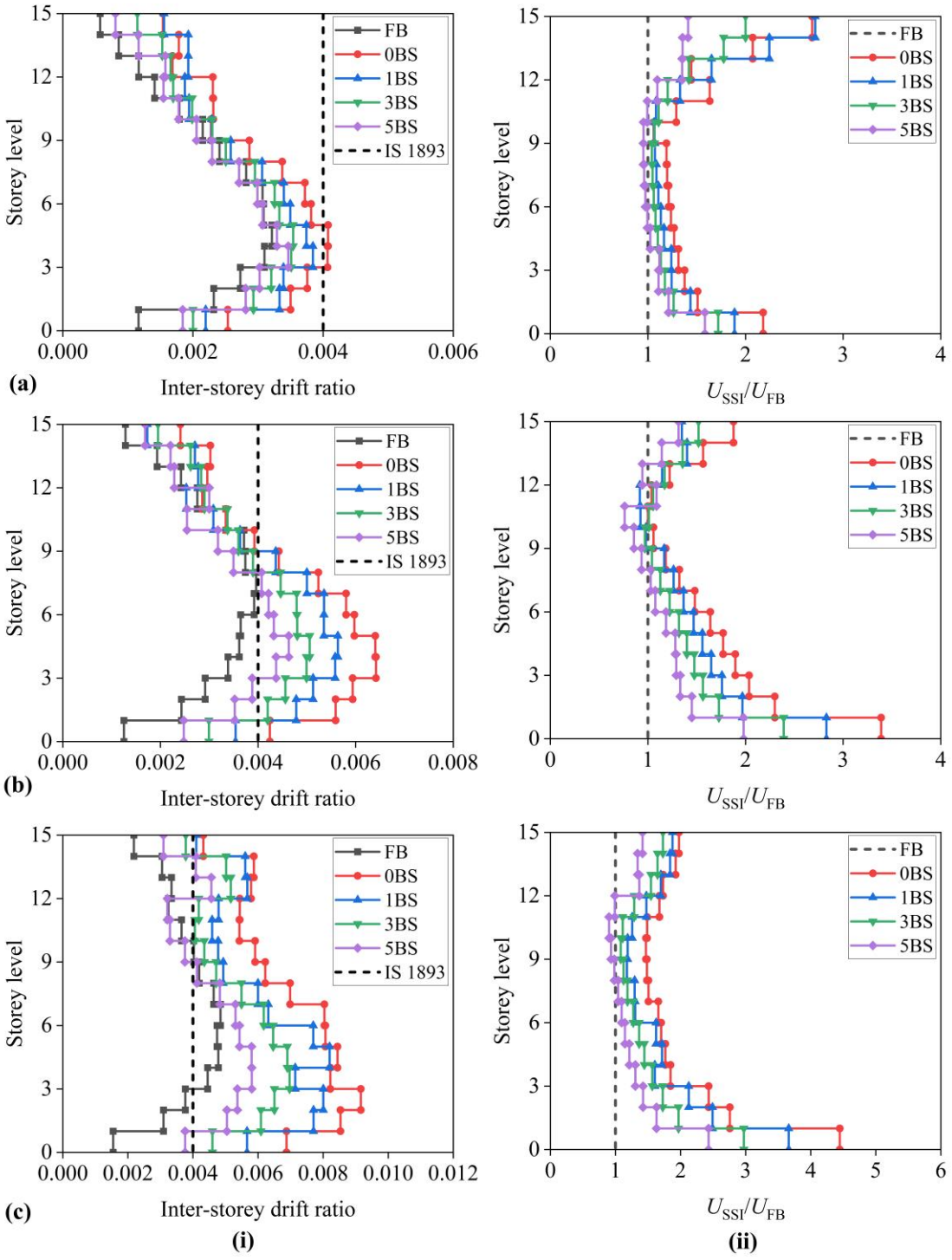

Figure 4.30 (i) Average inter-storey drift ratio and (ii) normalized inter-storey drift ratio variation in comparison to fixed-base model on soil type: (a) C, (b) D, and (c) E.

4.5.3.2 Effect of subsoil condition with different subterranean levels

The stiffness variation of subsoil conditions could alter the distribution of DR values over the height of the building frame. Figure 4.31(i) presents the results of an average maximum DR obtained from the nonlinear seismic response analyses of the 15-storey model resting on three different subsoils with different subterranean levels.

The maximum DR of the building frame simulated in soil types C, D, and E reach respectively 0.0032, 0.0040 and 0.0048 for model FB (Figure 4.31i-a); 0.0041, 0.0064 and 0.0092 for model 0BS (Figure 4.31i-b); 0.0038, 0.0056 and 0.0082 for model 1BS (Figure 4.31i-c); 0.0035, 0.0051 and 0.0070 for model 3BS (Figure 4.31i-d); and 0.0035, 0.0046 and 0.0058 for model 5BS (Figure 4.31i-e). The results of the analysis show that the maximum DR value of the building structure exceeded the permissible limit, except in soil type C. In addition, the DR distribution of the building structure increases as the stiffness of the subsoil decrease. The higher values of DR occur within the lower story level of the building.

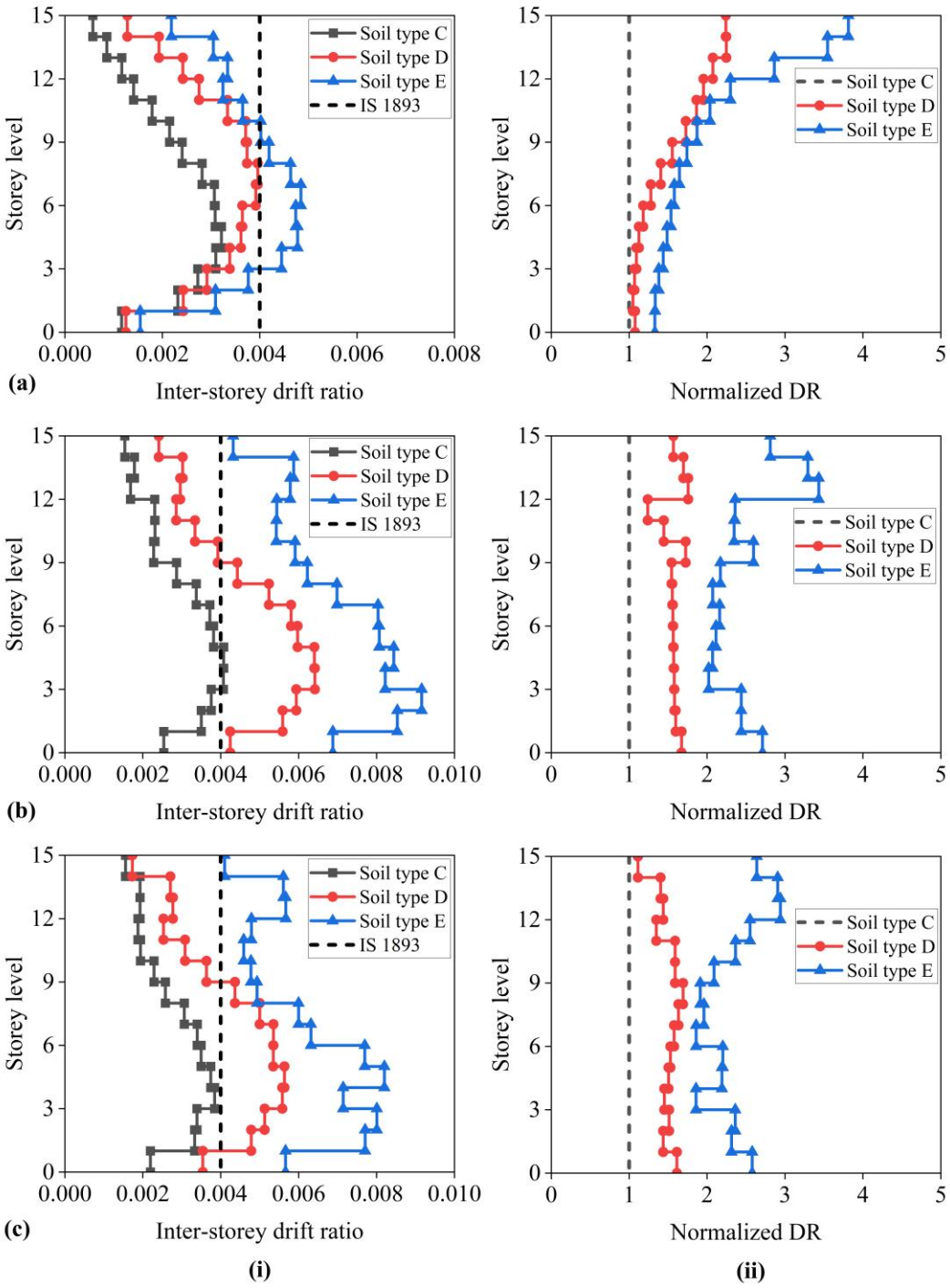

Figure 4.31 (i) Average inter-storey drift ratio and (ii) variation of normalized inter-storey drift ratio of the building structure with different models in comparison to in soil type C: (a) FB, (b) 0BS, (c) 1BS, (d) 3BS, and (e) 5BS.

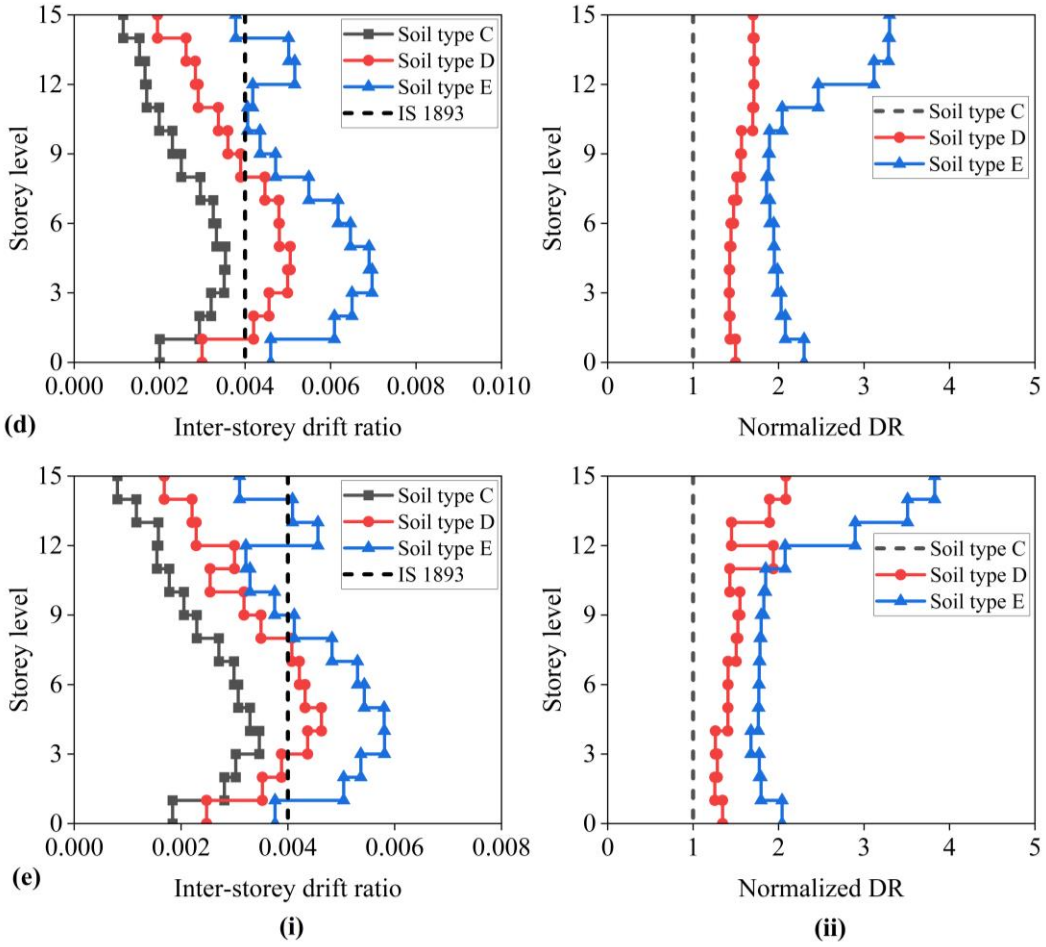

Figure 4.31 (Continued).

Additionally, the building response demand in terms of normalized maximum DR is presented in Figure 4.31(ii) in comparison to results obtained from building on soil type C simulated with different subterranean levels. The maximum normalized DR values are 2.25 and 3.81 on soil types D and E, respectively, for model FB (Figure 4.31ii-a). Similarly, the values are to be 1.76 and 3.43 for model 0BS (Figure 4.31ii-b), 1.69 and 2.94 for model 1BS (Figure 4.31ii-c), 1.71 and 3.30 for model 3BS (Figure 4.31ii-d), and 2.08 and 3.83 for model 5BS (Figure 4.31ii-e) of soil-structure system. The highest normalized DR was observed on the structure simulated in soil type E followed by soil type D and occurs within the upper story level of the structure. It is clearly observed that as the soil stiffness decreased from stiff to soft the distribution of the normalized DR value with respect to soil type C (stiff soil) increased, predominantly in soil type E.

4.5.4 Inference from Phase IV

In this section, the results obtained from numerical studies on the influence of subterranean levels and embedment depths on the seismic response of building frames resting on different soil profiles under seismic loads are presented. The conclusions obtained from Phase IV are as follows.

a) Storey lateral displacement

i) The maximum relative displacement response demands of the structure with a fixed-base (FB) model and zero to five subterranean levels (0BS, 1BS, 3BS, and 5BS) flexible-base models resting on soil types C, D, and E were evaluated. Comparing the results of the seismic response analyses, the horizontal storey level displacements of the flexible-base models for all soil types are higher than the corresponding fixed-base conditions.

ii) The maximum lateral displacements of the building resting on soil type C increase by 37%, 27%, 18%, and 8% in comparison to the fixed-base model for 0BS, 1BS, 3BS, and 5BS models, respectively. For the models resting on soil type D, it increases by 55%, 38%, 29%, and 13% in comparison to the fixed-base model for 0BS, 1BS, 3BS, and 5BS models, respectively. Similarly, it increases by 86%, 64%, 45%, and 21% for the models resting on soil type E in comparison to the fixed-base model. It is found that a noticeable increase in displacement occurs in building with 0, 1, and 3 subterranean levels. The effects are more prevalent in soil type D (medium) and soil type E (soft) soil.

iii) The ratio (U_{SSI}/U_{FB}) of relative lateral storey displacement of soil-structure interaction (U_{SSI}) to relative lateral storey displacement of fixed-base (U_{FB}) was evaluated. The normalized maximum response of building structure in soil type C with 0BS, 1BS, 3BS, and 5BS models are 2.18, 1.89, 1.72, and 1.58, respectively. Similarly, resting in soil type D are 3.39, 2.83, 2.39, and 1.98, as well as in soil type E 4.45, 3.66, 2.97, and 2.43, respectively.

iv) The results more relevant to reveal that as the lateral inter-storey displacement reduces as the number of subterranean levels increases from zero (i.e., no subterranean level) to one, three, and five.

v) Furthermore, the flexible-base model with 0BS exhibits the highest relative lateral storey displacement in comparison to all other models, whereas the storey lateral displacement reduces as the subterranean level embedment depth increases.

vi) The results indicate that the lateral relative storey displacement of the building structure increases as the stiffness of the subsoil decrease. Lateral storey displacement for soil type E (soft) is higher than soil type D (medium) and C (dense), consecutively, for all models of the building.

b) Inter-storey drift ratio

i) The DR values of the 15-storey building structure with various subterranean levels were evaluated and compared with fixed-base models on different soil deposits. The maximum DR values of the building with FB, 0BS, 1BS, 3BS, and 5BS models are 0.0032, 0.0041, 0.0038, 0.0035, and 0.0035, respectively. It is clear from the results that the DR values of the building on soil type C with a 0BS model exceeded the permissible value.

ii) Similarly, these values are 0.0040, 0.0064, 0.0056, 0.0051, and 0.0046 on soil type D, and 0.0048, 0.0092, 0.0082, 0.0070 and 0.0058 on soil type E for models FB, 0BS, 1BS, 3BS, and 5BS, respectively. It is observed from the results that the maximum values of the DR predominantly reached within the lower storeys of the building for both soil types and exceeded the permissible value for all models.

iii) The normalized DR distribution in comparison to the fixed-base model without subterranean levels and SSI simulated on soil types C, D, and E were evaluated. The maximum normalized DR values are obtained to be 2.68, 2.71, 2.00, and 1.58, respectively, on soil type C for 0BS, 1BS, 3BS, and 5BS soil-structure system models. Also, the normalized DR values for 0BS, 1BS, 3BS, and 5BS are 3.39, 2.83, 2.39, and 1.98, respectively, simulated on soil type D. Similarly, these values are 4.45, 3.66, 2.97, and 2.43, respectively, on soil type E. The highest normalized DR has been observed in a soil-structure system modelled with 0BS followed by 1BS, 3BS, and 5BS.

4.6 Summary

Numerous issues concerning the influence of subterranean levels with raft foundations on the seismic response performance of a fifteen-storey medium-rise RC-MRF building located on dense, medium, and soft soil profiles under earthquake loading were investigated in this Chapter. A large number of nonlinear seismic response history analyses were carried out by using various approaches SSI model to study the response of building frames with subterranean levels. The subterranean levels, subsoil conditions, input earthquake ground motion, and modeling strategies

were varied in the numerical analysis. The influences of these various parameters on the foundation-level motion of the structure, storey level lateral displacements, and inter-storey drifts with different subterranean levels were evaluated in this study. Based on the results, the conclusions that can be drawn from the present numerical study are listed below.

- Due to the presence of a subterranean system and the stiffness difference between soil and an embedded component of the structure the foundation level motion of the building structure the characteristics and value of the FIM are considerably varied with respect to the FFM.
- For seven foundation level motions recorded on medium and soft soil deposits, it was observed that the horizontal foundation level motion or FIM of the building structure decreases compared to the FFM with an increase in the subterranean levels.
- In comparison to close-form solutions, the numerical method is more consistent as it can incorporate various combinations such as the influences of deeply embedded subterranean levels along with their flexibility, the nonlinearity behavior of subsoil deposit, as well as the frequency-dependent attenuation or intensification of the subterranean level motion, especially in lower periods and higher subterranean levels.
- The seismic response characteristic and demands of the superstructure are considerably altered by the various modelling strategies often used for the analysis of the seismic response of building structures.
- The storey level lateral displacement value increases by 12% - 82% and the corresponding DR value exceeds the permissible 0.4% as the flexibility of the base increases. It is essentially because of the increase in translational and rotational movement of the underground structural system in comparison to the fixed-base model.
- The lateral inter-storey displacement and DR are reduced as the number of subterranean levels increases, whereas the model without subterranean level (0BS) exhibits the highest response value in comparison to all other models.
- The seismic response demands are also intensified as the degree of compressibility of soil changes from dense to soft. It is a result of the degradation of soil stiffness in soft soil deposits which in turn causes additional movements in the substructure systems.

According to the investigation in this study, however, the incorporation of the influence of kinematic SSI, subterranean levels, and seismic SSI is required to predict accurately the dynamic response characteristics and demands of the superstructure with great rigor. Therefore, the inelastic seismic design of an RC-MRF building structure excluding the substructure level and SSI is not adequate to assure structural safety, especially the building structure resting on medium and soft soil deposits.

CHAPTER - 5

SUMMARY AND CONCLUSIONS

5.1 Summary

The aim of this study was to assess the influence of subterranean levels, subsurface site conditions, and SSI modelling approach on the seismic response of RC-MRF building frame under seismic loads. This chapter summarizes the major findings of the research as well as recommendations for future research.

Major Findings of the Work

Effect of subterranean on FIM and applicability of theoretical models

1) From the numerical and theoretical studies undertaken in this thesis of the influence of subterranean levels on FIM, it is observed that the foundation level motions of the building structure were altered due to the presence of a subterranean system and the stiffness difference between soil and an embedded component of the structure, as well as embedment depths.
2) The numerical models results reveal that as the subterranean levels increases the characteristics and value of the FIM are considerably varied with respect to the FFM. These results demonstrate clearly how the embedded stiff subterranean level existence in different subsoil conditions causes the high frequencies to be filtered or the reduction of FIM with respect to FFM.
3) The numerical method is more consistent as it can incorporate various combination of effects and nonlinearity behaviour, especially in lower periods and higher subterranean levels.
4) Theoretical models, however, do not take into account the influences of deeply embedded subterranean levels along with their flexibility, the nonlinearity behavior of subsoil deposit, as well as the frequency-dependent attenuation or intensification of the subterranean level motion.
5) As a result, even if building codes used simplified approaches where FFM was assumed to represent the base excitation and may often be correct enough, the influence of kinematic SSI must be taken into account with reference to a variety of substructure systems which is required to accurately predict the base motion of a structure (FIM).

Effect of different modelling strategies

1) The seismic response demand of the superstructure in terms of storey level relative lateral displacement and DR values were intensified while incorporating the subterranean levels and SSI, as well as due to the variation of soil density. The influence is more considerable predominantly in the case of flexible-base models resting in medium and soft soil.
2) As the flexibility of the base increases, the average storey level lateral displacement and the corresponding DR value increases. It is essentially because of the increase in translational and rotational movement of the underground structural system in comparison to the fixed-base model. In addition, as the soil's degree of compressibility changes from dense to soft, the dynamic response demands are also intensified. It is a result of the degradation of soil stiffness in soft soil deposits which in turn causes additional movements in the substructure systems.
3) Different modeling strategies often used for the analysis of the seismic response of building structures considerably alter the seismic response characteristic and demand of the superstructure. The detailed 3D finite element model represented by model 3A can predict more consistently taking into account the complex SSI problem, soil-structure nonlinearity, and subterranean levels effects.
4) However, the flexible model represented by 2A has amplified the storey lateral displacement and DR values, as the model failed to account for some important features such as soil nonlinearity and damping effects.
5) In contrast, the response results of fixed-base building structures represented by models 1A and 1B attenuated the response demands in comparison to flexible bases. It is because of disregarding the effect of subterranean levels in model 1A and the seismic SSI in both models.
6) According to the investigation in this study, the incorporation of the influence of subterranean levels and seismic SSI is required to predict accurately the dynamic response characteristics and demands of the superstructure, especially the building structure resting on medium and soft soil deposits. Therefore, the inelastic seismic design of an RC-MRF building structure excluding the substructure level and SSI is not adequate to assure structural safety.

Effect of subterranean levels and embedment depths

1) The flexibility of the superstructure was increased by the subterranean levels and soil. Comparing the results for average lateral storey level displacements and inter-storey drifts of

the superstructure on all soil types were higher than the corresponding fixed-base conditions. However, the effects were reduced as the number of subterranean levels increased.

2) On the other hand, the results indicate that the lateral relative storey displacement of the building structure increases as the stiffness of the soil decrease from dense to soft. The building with 0BS exhibits the highest relative lateral storey displacement in comparison to all other models.
3) The results also indicated that the buildings without subterranean levels are significantly affected by seismic SSI. But, buildings with subterranean levels are less prone to damage. Based on the above findings, therefore, it is recommended to incorporate the subterranean levels in the seismic response analysis.

5.2 Recommendation for further research

Findings presented in this work have illustrated the influence and importance of incorporating subterranean levels for the seismic response analysis of building frames. The incorporation of subterranean levels and nonlinear SSI effects can contribute to a better understanding and lead to a more reliable seismic design of structures. This study has a restricted scope, thus further investigation could be done in the following areas:

- This study has focused only on 15-storey medium-rise reinforced concrete moment-resisting building frames in a high-risk earthquake-prone zone. Further comparative study should be conducted considering different heights of buildings and seismic zones for different response reduction values.
- For simplicity and to reduce computational time, a regular building structure with subterranean levels resting on a mat foundation in a uniform dense to soft soil profile under several unidirectional earthquake loads was investigated in this study. Future work should propose irregular building structures resting on different foundation types in layered soil profiles subjected to three-directional earthquake loadings, which provides a comprehensive observation to understand the effect of building irregularity, the role of different foundation types, possible local layered soil effects, and multi-directional earthquake loadings on the seismic response of building frames with subterranean levels.

- To simulate the nonlinear behavior of soil under the influence of earthquake loadings a Mohr-Coulomb constitutive model was used to reduce the number of soil parameters. In this study, a built-in tool of ABAQUS software was also applied to model the soil-structure system. It is proposed for future research to utilize custom subroutines in ABAQUS to develop an innovative auto-modeling system for the rapid generation of integrated structural and soil domain systems. The subroutine of the modified various constitutive models can be applied to consider the nonlinearity of the soil in the computational process, especially for medium and soft soils. This advancement could further enhance the novelty and the seismic response analysis.
- Although there exists a handful of techniques related to the incorporation of SSI and the extent of the inclusion of subterranean levels for code-based seismic resistance analysis and design of buildings. Many regional seismic resistance design codes, on the other hand, provide insufficient procedures and require that SSI effect and subterranean levels be considered in the design process. Of course, the development of code-based analysis and design needs an extensive parametric investigation of various soils, structures, and foundations. There is a need to develop formulated design guidelines and advanced code-based design procedures for practical applications in real projects.

5.3 Limitations of the Present Study

The following are the limitations of the present study

- The present work is limited to studying the influence of subterranean levels on the foundation level input motion and the behaviour of the superstructure.
- The present investigation is limited to numerical model studies only and is validated based on numerical study only.
- The work has been confined to studying the structural behaviour of the superstructure.
- The water table is considered to be below the bedrock, the soil profile is uniform, and the shear-wave velocity is consistent with depth.

LIST OF PUBLICATIONS

Journals:

1. Tadesse, Z.L., Padavala, H.K. & Koteswara, V.R.P., (2022), "Seismic response assessment of building structures with underground stories: a state-of-the-art review", Innovative Infrastructure Solutions, Springer International Publishing, Volume 7, issue 6, pp 1-18. DOI: https://doi.org/10.1007/s41062-022-00942-5 [Scopus and ESCI Indexed].
2. Tadesse, Z.L., Padavala, H.K. & Koteswara, V.R.P., (2022), "Effect of Subterranean Levels on the Foundation Input Motions for Dynamic response analysis of Building Structure", Asian Journal of Civil Engineering, Springer International Publishing. DOI: https://doi.org/10.1007/s42107-022-00531-y [Indexed in Scopus].
3. Z L Tadesse, H K Padavala & V R P Koteswara, (2023), "Effect of subterranean levels on the dynamic response of RC-MRF buildings", IOP Conf. Series: Materials Science and Engineering, 1273 (012014). DOI: https://doi.org/10.1088/1757-899X/1273/1/012014 [Indexed in Scopus].
4. Tadesse, Z.L., & Padavala, H.K. (2023), "The Influence of Soil-Structure Interaction Modeling Approaches on the Seismic Response of Building Frame with Subterranean Levels" Arabian Journal for Science and Engineering, Springer International Publishing, [SCI and Scopus Indexed]. Under review.

National and International Conferences:

1. Zeleke Lulayehu Tadesse, Hari Krishna Padavala, & Venkata R. P. Koteswara, (2022), "Assessment of the transfer function models application for seismic SFSI response analysis of building with subterranean levels", Proceedings of International Conference on Advancement in Structural & Geotechnical Engineering, ASGE'22, 25th – 27th August 2022, IITE, Indus University, Ahmedabad, India, page No: 13-20.
2. Tadesse, Z.L., Padavala, H.K. & Koteswara, V.R.P., (2022), "Effect of subterranean levels on the dynamic response of RC-MRF buildings", National Conference on Structural and Geotechnical Engineering, NCSGE-2022, 11th – 12th November, 2022, NIT Jamshedpur.

3. Zeleke Lulayehu Tadesse, Hari Krishna Padavala, & Venkata R. P. Koteswara, 2022, “Kinematic SSI effect on foundation input motions for building with subterranean levels”, GEOLEAP - Geotechnics: Learning, Evaluation, Analysis and Practice, Indian Geotechnical Conference, IGC 2022, 15th – 17th December, 2022, Kochi, India.

BIBLIOGRAPHY

Abdel Raheem, S. E., Ahmed, M. M., & Alazrak, T. M. A. (2015). Evaluation of soil–foundation–structure interaction effects on seismic response demands of multi-story MRF buildings on raft foundations. *International Journal of Advanced Structural Engineering*, *7*(1), 11–30. https://doi.org/10.1007/s40091-014-0078-x

Adamidis, O., Gazetas, G., Anastasopoulos, I., & Argyrou, C. (2014). Equivalent-linear stiffness and damping in rocking of circular and strip foundations. *Bulletin of Earthquake Engineering*, *12*(3), 1177–1200. https://doi.org/10.1007/s10518-013-9554-0

Al Agha, W., Alozzo Almorad, W., Umamaheswari, N., & Alhelwani, A. (2020). Study the seismic response of reinforced concrete high-rise building with dual framed-shear wall system considering the effect of soil structure interaction. *Materials Today: Proceedings*, *43*(February), 2182–2188. https://doi.org/10.1016/j.matpr.2020.12.111

Ali, T., Eldin, M. N., & Haider, W. (2023). The Effect of Soil-Structure Interaction on the Seismic Response of Structures Using Machine Learning, Finite Element Modeling and ASCE 7-16 Methods. *Sensors*, *23*(4). https://doi.org/10.3390/s23042047

Amendola, C., de Silva, F., Vratsikidis, A., Pitilakis, D., Anastasiadis, A., & Silvestri, F. (2021). Foundation impedance functions from full-scale soil-structure interaction tests. *Soil Dynamics and Earthquake Engineering*, *141*, 106523. https://doi.org/10.1016/j.soildyn.2020.106523

Amorosi, A., Boldini, D., & di Lernia, A. (2017). Dynamic soil-structure interaction: A three-dimensional numerical approach and its application to the Lotung case study. *Computers and Geotechnics*, *90*, 34–54. https://doi.org/10.1016/j.compgeo.2017.05.016

Anwar, N., Uthayakumar, A., & Najam, F. A. (2019). Significance of Soil-Structure Interaction in Seismic Response of Buildings. *NED University Journal of Research*, *1*, 43–54. https://doi.org/10.35453/nedjr-stmech-2019-0004

Apsel, R. J., & Luco, J. E. (1987). Impedance functions for foundations embedded in a layered medium: An integral equation approach. *Earthquake Engineering & Structural Dynamics*, *15*(2), 213–231. https://doi.org/10.1002/eqe.4290150205

ASCE/SEI 4-16. (2017). Seismic analysis of safety-related nuclear structures. In *In. American Society of Civil Engineers, Reston, Virginia* (Vol. 4). https://doi.org/10.1061/9780784413937

ASCE/SEI 4-98. (1998). Seismic analysis of safety-related nuclear structures. In *In. American Society of Civil Engineers, Reston, Virginia* (Vol. 4).

ASCE/SEI 7-10. (2010). Minimum design loads for buildings and other structures. In *American Society of Civil Engineers, Virginia*.

ASCE/SEI 7-16. (2018). Minimum Design Loads for Buildings and Other Structures. In *American Society of Civil Engineers (ASCE)*.

ATC-40. (1996). Seismic evaluation and retrofit of concrete buildings. *Applied Technology Council*, *1*, 334.

ATC 40. (1996). Seismic evaluation and retrofit of concrete buildings (Report No. ATC-40). *Applied Technology Council, Redwood City, California, USA*.

Badry, P., & Satyam, N. (2017). Seismic soil structure interaction analysis for asymmetrical buildings supported on piled raft for the 2015 Nepal earthquake. *Journal of Asian Earth Sciences*, *133*, 102–113. https://doi.org/10.1016/j.jseaes.2016.03.014

Bahuguna, A., & Firoj, M. (2022). Nonlinear Seismic Performance of Nuclear Structure with Soil–Structure Interaction. *Iranian Journal of Science and Technology - Transactions of Civil Engineering*, *46*(4), 2975–2988. https://doi.org/10.1007/s40996-021-00728-2

Baker, A. L. L. (1957). Raft Foundations: The Soil-Line Method of Design. In *London: Concrete Publications Ltd* (3rd ed.).

Bapir, B., Abrahamczyk, L., Wichtmann, T., & Prada-Sarmiento, L. F. (2023). Soil-structure interaction: A state-of-the-art review of modeling techniques and studies on seismic response of building structures. *Frontiers in Built Environment*, *9*, 1–17. https://doi.org/10.3389/fbuil.2023.1120351

Bielak, J. (1974). Dynamic behaviour of structures with embedded foundations. *Earthquake Engineering & Structural Dynamics*, *3*(3), 259–274. https://doi.org/10.1002/eqe.4290030305

Bilotta, E., De Sanctis, L., Di Laora, R., D'Onofrio, A., & Silvestri, F. (2015). Importance of seismic site response and soil-structure interaction in the dynamic behaviour of a tall building founded on piles. *Geotechnical Earthquake Engineering - Geotechnique Symposium in Print 2015*, *5*, 125–134. https://doi.org/10.1680/gee.61491.125

Bolisetti, C., & Whittaker, A. S. (2015). Site response, soil-structure interaction and structure-soil-structure interaction for performance assessment of buildings and nuclear structures. *University at Buffalo, State University of New York 212 Ketter Hall, Buffalo, NY 14260*, 388.

Bolisetti, C., Whittaker, A. S., Mason, H. B., Almufti, I., & Willford, M. (2014). Equivalent linear and nonlinear site response analysis for design and risk assessment of safety-related nuclear structures. *Nuclear Engineering and Design*, *275*, 107–121. https://doi.org/10.1016/j.nucengdes.2014.04.033

Boore, D. M. (2001). Effect of Baseline Correction on Response Spectra for Two Recordings of the 1999 Chi-Chi, Taiwan, Earthquake. *Bulletin of the Seismological Society of America*, *91*(October), 1119–1211. internal-pdf://118.89.57.152/boore_99_chichi_baseline.pdf

Boore, D. M., & Bommer, J. J. (2005). Processing of strong-motion accelerograms: Needs, options and consequences. *Soil Dynamics and Earthquake Engineering*, *25*(2), 93–115. https://doi.org/10.1016/j.soildyn.2004.10.007

Bowles, J. E. (1997). *Foundation Analysis and Design*.

Brandenberg, S. J., Mylonakis, G., & Stewart, J. P. (2015). Kinematic Framework for Evaluating Seismic Earth Pressures on Retaining Walls. *Journal of Geotechnical and Geoenvironmental Engineering*, *141*(7), 04015031. https://doi.org/10.1061/(asce)gt.1943-5606.0001312

Brown, C. B., Laurent, J. M., & Tilton, J. R. (1977). Beam-plate system on Winkler foundation. *Journal of the Engineering Mechanics Division*, *103*, 589–600.

Cai, Y. X., Gould, P. L., & Desai, C. S. (2000). Nonlinear analysis of 3D seismic interaction of soil-pile-structure systems and application. *Engineering Structures*, *22*(2), 191–199. https://doi.org/10.1016/S0141-0296(98)00108-4

Casciati, S., & Borja, R. I. (2004). Dynamic FE analysis of South Memnon Colossus including 3D soil-foundation-structure interaction. *Computers and Structures*, *82*(20–21), 1719–1736. https://doi.org/10.1016/j.compstruc.2004.02.026

Cavalieri, F., Correia, A. A., Crowley, H., & Pinho, R. (2020). Dynamic soil-structure interaction models for fragility characterisation of buildings with shallow foundations. *Soil Dynamics and Earthquake Engineering*, *132*(November). https://doi.org/10.1016/j.soildyn.2019.106004

Celebi M. and Safak E. (1991). Seismic response of transamerica building. I: data and preliminary analysis. *J. Struct. Eng.*, *117*(8), 2389–2404.

Chopra, A. K. (2007). Dynamics of structures. In *Prentice Hall*. https://doi.org/10.1193/1.1586188

Colasanti, R. J., & Horvath, J. S. (2010). Practical Subgrade Model for Improved Soil-Structure Interaction Analysis : Software Implementation. *Practice Periodical on Structural Design*

and Construction, *15*(4), 278–286.

Conti, R., Morigi, M., Rovithis, E., Theodoulidis, N., & Karakostas, C. (2018). Filtering action of embedded massive foundations: New analytical expressions and evidence from 2 instrumented buildings. *Earthquake Engineering and Structural Dynamics*, *47*(5), 1229–1249. https://doi.org/10.1002/eqe.3014

Conti, R., Morigi, M., & Viggiani, G. M. B. (2017). Filtering effect induced by rigid massless embedded foundations. *Bulletin of Earthquake Engineering*, *15*(3), 1019–1035. https://doi.org/10.1007/s10518-016-9983-7

Cook, R. D., Malkus, D. S., & Plesha, M. E. (1989). *Concepts and Applications of Finite Element Analysis*. Wiley, New York.

Crouse, C. B., Hushmand, B., & Martin, G. R. (1987). Dynamic soil-structure interaction of a single-span bridge. *Earthquake Engineering & Structural Dynamics*, *15*, 711–729.

CSI. (2020). SAP2000 Integrated Software for Structural Analysis and Design. *Computers and Structures Inc., Berkeley, California*.

Day, S. M. (1978). Seismic response of embedded foundations. *Preprints of Conference Proceedings of ASCE Convention and Exposition, Chicago, IL, Preprint No. 3450, American Society of Civil Engineers, New York, New York*.

de Silva, F., Pitilakis, D., Ceroni, F., Sica, S., & Silvestri, F. (2018). Experimental and numerical dynamic identification of a historic masonry bell tower accounting for different types of interaction. *Soil Dynamics and Earthquake Engineering*, *109*, 235–250. https://doi.org/10.1016/j.soildyn.2018.03.012

Dobry, R., & Gazetas, G. (1986). Dynamic response of arbitrarily shaped foundations. *Journal of Geotechnical Engineering*, *112*(2), 109–135.

Dominguez, J., & Roesset, J. M. (1978). Response of embedded foundations to travelling waves. In *Massachusetts Institute of Technology, Department of Civil Engineering, Constructed Facilities Division*.

Dutta, S. C., Bhattacharya, K., & Roy, R. (2004). Response of low-rise buildings under seismic ground excitation incorporating soil-structure interaction. *Soil Dynamics and Earthquake Engineering*, *24*(12), 893–914. https://doi.org/10.1016/j.soildyn.2004.07.001

Dutta, S. C., & Roy, R. (2002). A critical review on idealization and modeling for interaction among soil-foundation-structure system. *Computers and Structures*, *80*(20–21), 1579–1594.

https://doi.org/10.1016/S0045-7949(02)00115-3

Duval, A., Al-akhras, H., Maurin, F., Elguedj, T., Duval, A., Al-akhras, H., Maurin, F., & Elguedj, T. (2014). Abaqus/CAE 6.14 User's Manual. *Dassault Systémes Inc. Providence, RI, USA*.

Ehlers, G. (1942). The effect of soil flexibility on vibrating systems. *Beton Und Eisen*, *41*(21/22), 197–203.

El Hoseny, M., Ma, J., Dawoud, W., & Forcellini, D. (2023). The role of soil structure interaction (SSI) on seismic response of tall buildings with variable embedded depths by experimental and numerical approaches. *Soil Dynamics and Earthquake Engineering*, *164*, 107583. https://doi.org/10.1016/j.soildyn.2022.107583

El Hoseny, M., Ma, J., & Josephine, M. (2022). Effect of Embedded Basement Stories on Seismic Response of Low-Rise Building Frames Considering SSI via Small Shaking Table Tests. *Sustainability (Switzerland)*, *14*(3). https://doi.org/10.3390/su14031275

Elsabee, F., & Morray, J. P. (1977). Dynamic Behavior of Embedded Foundations. *Massachusetts Institute of Technology, Department of Civil Engineering, Constructed Facilities Division.*

EN 1998-5. (2004). *Eurocode 8: Design of structures for earthquake resistance-Part 5: Foundations, retaining structures and geotechnical aspects. 1*(2005).

Far, H. (2019). Advanced computation methods for soil-structure interaction analysis of structures resting on soft soils. *International Journal of Geotechnical Engineering*, *13*(4), 352–359.

Fatahi, B., & Tabatabaiefar, S. H. R. (2014). Fully Nonlinear versus Equivalent Linear Computation Method for Seismic Analysis of Midrise Buildings on Soft Soils. *International Journal of Geomechanics*, *14*(4), 04014016. https://doi.org/10.1061/(asce)gm.1943-5622.0000354

Fatahi, B., Van Nguyen, Q., & Hokmabadi, A. S. (2016). The effects of foundation size on the seismic performance of buildings considering the soil-foundation-structure interaction. *Structural Engineering and Mechanics*, *58*(6), 1045–1075. https://doi.org/10.12989/sem.2016.58.6.1045

Feldgun, V. R., Karinski, Y. S., Yankelevsky, D. Z., & Kochetkov, A. V. (2016). A new analytical approach to reconstruct the acceleration time history at the bedrock base from the free surface signal records. *Soil Dynamics and Earthquake Engineering*, *85*, 19–30. https://doi.org/10.1016/j.soildyn.2016.03.003

FEMA 356. (2000). Prestandard and Commentary the Seismic Rehabilitation of Buildings.

Federal Emergency Management Agency, Washington, DC, USA.

FEMA 440. (2005). Improvement of Nonlinear Static Seismic Analysis Procedures. *Federal Emergency Management Agency, Washington DC, 440*, 392.

FEMA 450. (2003). NEHRP Recommended Provisions for Seismic Regulations for New Buildings and Other Structures. *Part 1*, 338.

Ganainy, H. El, & Naggar, M. H. El. (2009). Seismic performance of three-dimensional frame structures with underground stories. *Soil Dynamics and Earthquake Engineering*, *29*(9), 1249–1261. https://doi.org/10.1016/j.soildyn.2009.02.003

Gazetas, G. (1991). Foundation vibrations. *Foundation Engineering Handbook*, 553–593.

Gerolymos, N., & Gazetas, G. (2006). Winkler model for lateral response of rigid caisson foundations in linear soil. *Soil Dynamics and Earthquake Engineering*, *26*, 347–361.

Ghandil, M., & Behnamfar, F. (2015). The near-field method for dynamic analysis of structures on soft soils including inelastic soil-structure interaction. *Soil Dynamics and Earthquake Engineering*, *75*, 1–17. https://doi.org/10.1016/j.soildyn.2015.03.018

Ghandil, M., & Behnamfar, F. (2017). Ductility demands of MRF structures on soft soils considering soil-structure interaction. *Soil Dynamics and Earthquake Engineering*, *92*(January 2016), 203–214. https://doi.org/10.1016/j.soildyn.2016.09.051

Ghobarah, A. (2004). On drift limits associated with different damage levels. *In International Workshop on Performance-Based Seismic Design (Vol. 28). Ontario, Canada: Department of Civil Engineering, McMaster University*. http://peer.berkeley.edu/publications/peer_reports/reports_2004/reports_2004.html

Goktepe, F., Celebi, E., & Omid, A. J. (2019). Numerical and experimental study on scaled soil-structure model for small shaking table tests. *Soil Dynamics and Earthquake Engineering*, *119*(January), 308–319. https://doi.org/10.1016/j.soildyn.2019.01.016

Gorbunov-Pasadov, M. I. (1949). *Beams and plates on an elastic base*.

Gueguen, P., & Bard, P. Y. (2005). Soil-structure and soil-structure-soil interaction: Experimental evidence at the volvt test site. *Journal of Earthquake Engineering*, *9*(5), 657–693. https://doi.org/10.1080/13632460509350561

Güllü, H., & Jaf, H. S. (2016). Full 3D nonlinear time history analysis of dynamic soil–structure interaction for a historical masonry arch bridge. *Environmental Earth Sciences*, *75*(21). https://doi.org/10.1007/s12665-016-6230-0

Hardin, B. O., & Drnevich, V. P. (1972). Shear Modulus and Damping in Soils: Measurement and Parameter Effects (Terzaghi Leture). *Journal of the Soil Mechanics and Foundations Division*, *98*(6), 603–624. https://doi.org/10.1061/jsfeaq.0001756

Harr, M. E. (1966). *Foundation of Theoretical Soil Mechanics* (2nd printi). McGraw Hill.

Hashash, Y. M. A., Musgrove, M. I., Harmon, J. A., Ilhan, O., Xing, G., Numanoglu, O., Groholski, D. R., Phillips, C. A., & Park, D. (2020). DEEPSOIL 7.0, User Manual. *Urbana, IL, Board of Trustees of University of Illinois at Urbana-Champaign*, *2020*, 1–170.

Hassani, N., Bararnia, M., & Ghodrati Amiri, G. (2018). Effect of soil-structure interaction on inelastic displacement ratios of degrading structures. *Soil Dynamics and Earthquake Engineering*, *104*(September 2016), 75–87. https://doi.org/10.1016/j.soildyn.2017.10.004

Hetényi, M., & Hetbenyi, M. I. (1946). Beams on elastic foundation: theory with applications in the fields of civil and mechanical engineering. *Ann Arbor, MI: University of Michigan Press*, *16*.

Hokmabadi, A. S., Fatahi, B., & Samali, B. (2014). Assessment of soil-pile-structure interaction influencing seismic response of mid-rise buildings sitting on floating pile foundations. *Computers and Geotechnics*, *55*, 172–186. https://doi.org/10.1016/j.compgeo.2013.08.011

Horvath, J. S. (1993). Beam-column-analogy model for soil-structure interaction analysis. *Journal of Geotechnical Engineering*, *119*(2), 358–364. https://doi.org/10.1061/(ASCE)0733-9410(1993)119:2(358)

Horvath, J. S., & Regis J. Colasanti, P. E. (2011). Practical Subgrade Model for Improved Soil-Structure Interaction Analysis : Model Development. *International Journal of Geomechanics*, *11*(1), 59–64.

Iguchi, M., & Luco, J. E. (1982). VIBRATION OF FLEXIBLE PLATE ON VISCOELASTIC MEDIUM. *Journal of the Engineering Mechanics Division*, *108*(EM6), 1103–1120. https://doi.org/10.1061/jmcea3.0002893

IS 16700. (2017). Indian Standard Criteria for Structural Safety of Tall Concrete Buildings. *Bureau of Indian Standards, New Dehli*.

IS 1893 (Part 1). (2016). Criteria for Earthquake resistant design of structures,Part 1:General Provisions and buildings. *Bureau of Indian Standards, New Delhi*, *1893*, 1–44.

IS 1893 (Part 2). (2014). Criteria for Earthquake Resistance Design of Structures, Part 2: Liquid Retaining Tanks. *Bureau of Indian Standards, New Delhi*, 22.

IS 1893 (Part 3). (2014). Criteria for Earthquake Resistant for Design of Structures, Part 3: Bridges and Retaining Walls. *Bureau of Indian Standards, New Delhi*.

IS 1893 (Part 4). (2015). Criteria for Earthquake Resistant Design of Structures, Part 4: Industrial Structures Including Stack-Like Structures. *Bureau of Indian Standards, New Delhi*.

IS 456. (2000). Code of practice for plain and reinforced concrete (third revision). *Bureau of Indian Standards, New Dehli*, 1–114.

IS 875 (Part 1). (1997). CODE OF PRACTICE FOR DESIGN LOADS (OTHER THAN EARTHQUAKE) FOR BUILDINGS AND STRUCTURES, PART 1: DEAD LOADS-UNIT WEIGHTS OF BUILDING MATERIALS AND STORED MATERIALS. *Bureau of Indian Standards, New Dehli*.

IS 875 (Part 2). (1987). Code of Practice for Design Loads (Other than Earthquake) for Buildings and Structures, Part 2: Imposed Loads. *Bureau of Indian Standards, New Dehli*.

IS 875 (Part 3). (2015). Design loads (other than earthquake) for buildings and structures—code of practice for wind loads. In *Bureau of Indian Standards, New Delhi, India*.

Ishibashi, I., & Zhang, X. (1993). Unified dynamic shear moduli and damping ratios of sand and clay. *Soils and Foundations*, *33*(1), 182–191. http://www.mendeley.com/research/geology-volcanic-history-eruptive-style-yakedake-volcano-group-central-japan/

Izzuddin, B. A., Jahromi, H. Z., & Zdravkovic, L. (2007). Partitioned analysis of nonlinear soil-structure interaction using iterative coupling. *Interaction and Multiscale Mechanics*, *1*(1), 33–51.

Jakrapiyanun, W. (2002). Physical Modeling of Dynamic Soil-Foundation-Structure-Interaction Using a Lammar Container [University of California Sandiego]. In *Ph.D. Thesis*. http://dx.doi.org/10.1016/j.jaci.2012.05.050

JSCE 15. (2007). *Standard Specifications for Concrete Structures - design JSCE 15. Tokyo: Japan Society of Civil Engineers*.

Karabalis, D. L., & Beskos, D. E. (1986). Dynamic response of 3-D embedded foundations by the boundary element method. *Computer Methods in Applied Mechanics and Engineering*, *56*(1), 91–119. https://doi.org/10.1016/0045-7825(86)90138-6

Kassas, K., Adamidis, O., & Anastasopoulos, I. (2022). Structure–soil–structure interaction (SSSI) of adjacent buildings with shallow foundations on liquefiable soil. *Earthquake Engineering and Structural Dynamics*, *51*(10), 2315–2334. https://doi.org/10.1002/eqe.3665

Kausel, E. (1974). Forced vibrations of circular foundations on layered media. In *Department of Civil Engineering, MIT*.

Kausel, E. (2010). Early history of soil-structure interaction. *Soil Dynamics and Earthquake Engineering*, *30*(9), 822–832. https://doi.org/10.1016/j.soildyn.2009.11.001

Kausel, E., Whitman, R. V., Morray, J. P., & Elsabee, F. (1978). The spring method for embedded foundations. *Nuclear Engineering and Design*, *48*(2–3), 377–392. https://doi.org/10.1016/0029-5493(78)90085-7

Kerr, A. D. (1965). A study of a new foundation model. *Acta Mech.*, *1*(2), 135–147.

Khazaei, J., Amiri, A., & Khalilpour, M. (2017). Seismic evaluation of soil-foundation-structure interaction: Direct and Cone model. *Earthquake and Structures*, *12*(2), 251–262. https://doi.org/10.12989/eas.2017.12.2.251

Kim, D.-S., Ha, J. G., Lee, S.-H., & Choo, Y. W. (2014). Simulation of soil-foundation-structure interaction of Hualien large-scale seismic test using dynamic centrifuge test. *Soil Dynamics and Earthquake Engineering*, *61–62*, 176–187. https://doi.org/10.1016/j.soildyn.2014.01.008

Kramer, S. L., & Stewart, J. P. (2004). "Geotechnical aspects of seismic hazards", Earthquake Engineering: from Engineering Seismology to Performance-based Engineering. *Edited ByYousef Bozorgnia, Vitelmo V. Bertero, CRC Press*.

Kramrisch, F., & Rogers, P. (1961). Simplified Design of Combined Footings. *Journal of the Soil Mechanics and Foundations Division*, *87*, 19–44.

Krawinkler, H., Medina, R., & Alavi, B. (2003). Seismic drift and ductility demands and their dependence on ground motions. *Engineering Structures*, *25*(5), 637–653. https://doi.org/10.1016/S0141-0296(02)00174-8

Kuhlemeyer, R. L., & Lysmer, J. (1973). Finite Element Method Accuracy for Wave Propagation Problems. In *Journal of the Soil Mechanics and Foundations Division* (Vol. 99, Issue 5, pp. 421–427). https://doi.org/10.1061/jsfeaq.0001885

Kutanis, M., & Elmas, M. (2001). Non-Linear Seismic Soil-Structure Interaction Analysis Based on Sismik Y ¨ sımı C. *Turk J Engin Environ Sci*, *25*, 617–626.

lagaguine, M., & Sbartai, B. (2023). Non-linear soil-structure interaction effect on the seismic response of a building. *Arabian Journal of Geosciences*, *16*(6). https://doi.org/10.1007/s12517-023-11455-5

Lee, J., Park, D., & Park, D. (2016). Analyzing load response and load sharing behavior of piled

rafts installed with driven piles in sands. *Computers and Geotechnics*, *78*, 62–71. https://doi.org/10.1016/j.compgeo.2016.05.008

Lee, M. K. D. (1978). DESRA-2: Dynamic effective stress response analysis of soil deposits with energy transmitting boundary including assessment of liquefaction potential. *Research Report, University of British Columbia*.

Leoni, G., Carbonari, S., & Dezi, F. (2012). Nonlinear seismic behaviour of wall-frame dual systems accounting for soil–structure interaction. *Earthquake Eng.& Structural Dynamics*, *41*, 1651–1672. https://doi.org/10.1002/eqe.1195

Lindman, E. L. (1975). "Free-space" boundary conditions for the time dependent wave equation. *Journal of Computational Physics*, *18*(1), 66–78. https://doi.org/10.1016/0021-9991(75)90102-3

Liou, G., & Huang, P. (1994). Effect of Flexibility on Impedance Functions for Circular Foundation. *Journal of Engineering Mechanics*, *120*(7), 1429–1446. https://doi.org/10.1061/(asce)0733-9399(1994)120:7(1429)

Lu, X., Chen, B., Li, P., & Chen, Y. (2004). Numerical analysis of tall buildings considering dynamic soil-structure interaction. *Journal of Earthquake Engineering and Engineering Vibration*, *24*(3), 130–138.

Lu, Y. (2016). Seismic Soil-Structure Interaction In Performance-Based Design. *Doctoral Dissertation, Faculty of Engineering Department of Civil Engineering, University of Nottingham*.

Luco, J. E., Trifunac, M. D., & Wong, H. L. (1988). Isolation of soil-structure interaction effects by full-scale forced vibration tests. In *Earthquake Engineering & Structural Dynamics* (Vol. 16, Issue 1, pp. 1–21). https://doi.org/10.1002/eqe.4290160102

Luco, J. E., & Westmann, R. A. (1971). Dynamic response of circular footings. *Journal of the Engineering Mechanics Division*, *97*(5), 1381–1395. https://doi.org/10.1061/jmcea3.0001467

Luco, J. E., & Wong, H. L. (1987). Seismic response of foundations embedded in a layered half-space. *Earthquake Engineering & Structural Dynamics*, *15*(2), 233–247. https://doi.org/10.1002/eqe.4290150206

Luo, C., Yang, X., Zhan, C., Jin, X., & Ding, Z. (2016). Nonlinear 3D finite element analysis of soil-pile-structure interaction system subjected to horizontal earthquake excitation. *Soil*

Dynamics and Earthquake Engineering, *84*, 145–156. https://doi.org/10.1016/j.soildyn.2016.02.005

Lysmer, J., & Kuhlemeyer, R. L. (1969). Finite dynamic model for infinite media. *Journal of the Engineering Mechanics Division*, *95*(4), 859–877. https://doi.org/10.1061/jmcea3.0001339

Maheshwari, B. K., Truman, K. Z., El Naggar, M. H., & Gould, P. L. (2004). Three-dimensional nonlinear analysis for seismic soil-pile-structure interaction. *Soil Dynamics and Earthquake Engineering*, *24*(4), 343–356. https://doi.org/10.1016/j.soildyn.2004.01.001

Manolis, G. D., & Markou, A. (2012). A distributed mass structural system for soil-structureinteraction and base isolation studies. *Archive of Applied Mechanics*, *82*(10–11), 1513–1529. https://doi.org/10.1007/s00419-012-0659-8

Maravas, A., Mylonakis, G., & Karabalis, D. L. (2014). Simplified discrete systems for dynamic analysis of structures on footings and piles. *Soil Dynamics and Earthquake Engineering*, *61–62*, 29–39. https://doi.org/10.1016/j.soildyn.2014.01.016

Massumi, A., & Tabatabaiefar, H. R. (2007). Effects of Soil-Structure Interaction on Seismic Behaviour of Ductile Reinforced Concrete Moment Resisting Frames. *In Proceedings of World Housing Congress on Affordable Quality Housing (WHC2007)*.

Matinmanesh, H., & Asheghabadi, M. S. (2011). Seismic analysis on soil-structure interaction of buildings over sandy soil. *Procedia Engineering*, *14*, 1737–1743. https://doi.org/10.1016/j.proeng.2011.07.218

MCBC. (2004). Complementary Technical Norms for Earthquake Resistant Design. *Mexico City Building Code, Mexico City, Mexico*.

Medina, C., Aznárez, J. J., Padrón, L. A., & Maeso, O. (2013). Effects of soil-structure interaction on the dynamic properties and seismic response of piled structures. *Soil Dynamics and Earthquake Engineering*, *53*, 160–175. https://doi.org/10.1016/j.soildyn.2013.07.004

Meek, J., & Veletsos, A. S. (1974). Simple models for foundations in lateral and rocking motion. *Proceedings of the 5th World Conf. on Earthquake Engineering*, 2610–2631.

Meek, J. W., & Wolf, J. P. (1992a). Cone models for homogeneous soil. I. *Journal of Geotechnical Engineering*, *118*(5), 667–685. https://doi.org/10.1061/(ASCE)0733-9410(1992)118:5(667)

Meek, J. W., & Wolf, J. P. (1992b). Cone models for soil layer on rigid rock. II. *Journal of Geotechnical Engineering*, *118*(5), 686–703. https://doi.org/10.1061/(ASCE)0733-9410(1992)118:5(686)

Meek, J. W., & Wolf, J. P. (1994a). Cone Models For Embedded Foundation. *Journal of Geotechnical Engineering*, *120*(1), 60–80. https://doi.org/10.1061/(ASCE)0733-9410(1994)120:1(60)

Meek, J. W., & Wolf, J. P. (1994b). Material damping for lumped-parameter models of foundations. *Earthquake Engineering & Structural Dynamics*, *23*(4), 349–362. https://doi.org/10.1002/eqe.4290230402

Meli, R., Faccioli, E., Muria-Vila, D., Quaas, R., & Paolucci, R. (1998). A study of site effects and seismic response of an instrumented building in mexico city. *Journal of Earthquake Engineering*, *2*(1), 89–111. https://doi.org/10.1080/13632469809350315

Meymand, P. J. (1998). Shaking table scale model tests of nonlinear soil-pile-superstructure interaction in soft clay. *PhD Thesis, Department of Civil Engineering, University of California, Berkeley, California, USA*. http://nisee.berkeley.edu/meymand/files/intro.pdf

Miao, Y., Zhong, Y., Ruan, B., Cheng, K., & Wang, G. (2020). Seismic response of a subway station in soft soil considering the structure-soil-structure interaction. *Tunnelling and Underground Space Technology*, *106*(September), 103629. https://doi.org/10.1016/j.tust.2020.103629

Mikami, A., Stewart, J. P., & Kamiyama, M. (2008). Effects of time series analysis protocols on transfer functions calculated from earthquake accelerograms. *Soil Dynamics and Earthquake Engineering*, *28*(9), 695–706. https://doi.org/10.1016/j.soildyn.2007.10.018

Mita, A., & Luco, J. E. (1989). Impedance functions and input motions for embedded square foundations. *Journal of Geotechnical Engineering*, *115*(4), 491–503. https://doi.org/10.1061/(ASCE)0733-9410(1989)115:4(491)

Mohammadyar, M. A., & Akhtarpour, A. (2023). A study on the seismic soil − structure interaction of a concrete shear wall − steel frame building system with underground stories. *Asian Journal of Civil Engineering*, *0123456789*. https://doi.org/10.1007/s42107-023-00667-5

Mohasseb, S., & Abdollahi, B. (2009). *Soil-Structure Interaction Analyses Using Cone Models*. *10*(4). http://www.iiees.ac.ir/jsee

Moss, R. E. S., Crosariol, V., & Kuo, S. (2010). Shake Table Testing To Quantify Seismic Soil-Structure-Interaction of Underground Structures. *Proceedings of the 5th International Conference on Recent Advances in Geotechnical Earthquake Engineering and Soil Dynamics, San Diego, California, USA*, *1*, 1–5.

Mourlas, C., Khabele, N., Bark, H. A., Karamitros, D., Taddei, F., Markou, G., & Papadrakakis, M. (2020). Effect of Soil-Structure Interaction on Nonlinear Dynamic Response of Reinforced Concrete Structures. *International Journal of Structural Stability and Dynamics*, *20*(13), 1–39. https://doi.org/10.1142/S0219455420410138

Murià-Vila, D., Taborda-Rios, R., & Zapata-Escobar, A. (2004). Soil-Structure Interaction Effects in Two Instrumented Tall Buildings. *13th World Conference on Earthquake Engineering*, 1911.

Mylonakis, G., Nikolaou, S., & Gazetas, G. (2006). Footings under seismic loading: Analysis and design issues with emphasis on bridge foundations. *Soil Dynamics and Earthquake Engineering*, *26*(9), 824–853. https://doi.org/10.1016/j.soildyn.2005.12.005

Naeim, F., Tileylioglu, S., Alimoradi, A., & Stewart, J. P. (2008). Impact of foundation modeling on the accuracy of response analysis for a tall building. *In Seminar on Utilization of Strong Motion Data*, 19–55.

Nguyen, D. Van, Kim, D., & Nguyen, D. D. (2020). Nonlinear seismic soil-structure interaction analysis of nuclear reactor building considering the effect of earthquake frequency content. *Structures*, *26*, 901–914. https://doi.org/10.1016/j.istruc.2020.05.013

Nguyen, Q. Van, Fatahi, B., & Hokmabad, A. S. (2017). Influence of Size and Load-Bearing Mechanism of Piles on Seismic Performance of Buildings Considering Soil–Pile–Structure Interaction. *International Journal of Geomechanics*, *17*(7), 04017007. https://doi.org/10.1061/(asce)gm.1943-5622.0000869

NIST. (2012). Soil-Structure Interaction for Building Structures. In *Department of Commerce, Washington, DC*.

Oz, I., Senel, S. M., Palanci, M., & Kalkan, A. (2020). Effect of soil-structure interaction on the seismic response of existing low and mid-rise RC buildings. *Applied Sciences (Switzerland)*, *10*(23), 1–21. https://doi.org/10.3390/app10238357

Oztoprak, S., & Bolton, M. D. (2013). Stiffness of sands through a laboratory test database. *Geotechnique*, *63*(1), 54–70. https://doi.org/10.1680/geot.10.P.078

Pais, A., & Kausel, E. (1988). Approximate formulas for dynamic stiffnesses of rigid foundations. *Soil Dynamics and Earthquake Engineering*, *7*(4), 213–227. https://doi.org/10.1016/S0267-7261(88)80005-8

PEER. (n.d.). *PEER Ground Motion Database, Pacific Earthquake Engineering Research Centre,*

University of California, Berkeley, CA. http://peer.berkeley.edu/peer_ground_motion_database

PEER. (2017). Guidelines for Performance-Based Seismic Design of Tall Buildings (PEER Report No. 2017/06). *Pacific Earthquake Engineering Center Headquarters at the University of California, Berkeley*.

Piro, A., de Silva, F., Parisi, F., Scotto di Santolo, A., & Silvestri, F. (2020). Effects of soil-foundation-structure interaction on fundamental frequency and radiation damping ratio of historical masonry building sub-structures. *Bulletin of Earthquake Engineering*, *18*(4), 1187–1212. https://doi.org/https://doi.org/10.1007/s10518-019-00748-4

Poulos, H. G., & Davis, E. H. (1974). Elastic solutions for soil and rock mechanics. Textbook. Figs, Tabls, Refs. *New York: Wiley*, *582*. https://doi.org/10.1016/0148-9062(74)91768-9

Rahmani, A., Taiebat, M., Liam Finn, W. D., & Ventura, C. E. (2016). Evaluation of substructuring method for seismic soil-structure interaction analysis of bridges. *Soil Dynamics and Earthquake Engineering*, *90*, 112–127. https://doi.org/10.1016/j.soildyn.2016.08.013

Raychowdhury, P. (2011). Seismic response of low-rise steel moment-resisting frame (SMRF) buildings incorporating nonlinear soil-structure interaction (SSI). *Engineering Structures*, *33*(3), 958–967. https://doi.org/10.1016/j.engstruct.2010.12.017

Rayhani, M. H., & El Naggar, M. H. (2008). Numerical Modeling of Seismic Response of Rigid Foundation on Soft Soil. *International Journal of Geomechanics*, *8*(6), 336–346. https://doi.org/10.1061/(asce)1532-3641(2008)8:6(336)

Rayhani, M. H. T., & El Naggar, M. H. (2007). Centrifuge modeling of seismic response of layered soft clay. *Bulletin of Earthquake Engineering*, *5*(4), 571–589. https://doi.org/10.1007/s10518-007-9047-0

Requena-Garcia-Cruz, M. V., Romero-Sánchez, E., & Morales-Esteban, A. (2022). Numerical investigation of the contribution of the soil-structure interaction effects to the seismic performance and the losses of RC buildings. *Developments in the Built Environment*, *12*(October), 1–10. https://doi.org/10.1016/j.dibe.2022.100096

RezaTabatabaiefar, S. H., Fatahia, B., & Samali, B. (2013). Lateral seismic response of building frames considering dynamic soil-structure interaction effects. *Structural Engineering and Mechanics*, *45*(3), 307–317. https://doi.org/10.12989/sem.2013.45.3.311

Robert, E. S. (2009). *Dynamic nonlinear soil-structure interaction (Doctoral dissertation, Ecole*

Centrale Paris).

Roesset, J. M. (2013). Soil structure interaction the early stages. *Journal of Applied Science and Engineering*, *16*(1), 1–8.

Roesset, J. M., & Ettouney, M. M. (1977). Transmitting boundaries: A comparison. *International Journal for Numerical and Analytical Methods in Geomechanics*, *1*(2), 151–176. https://doi.org/10.1002/nag.1610010204

Ryan, K. L., & Polanco, J. (2008). Problems with Rayleigh Damping in Base-Isolated Buildings. *Journal of Structural Engineering*, *134*(11), 1780–1784. https://doi.org/10.1061/(asce)0733-9445(2008)134:11(1780)

Saad, G., Saddik, F., & Najjar, S. (2012). Impact of Soil Structure Interaction on the Seismic Design of Reinforced Concrete Buildings with Underground Stories. *Proceedings of the Fifthteenth World Conference on Earthquake Engineering*, 4935.

Sawada, K., & Takemura, J. (2014). Centrifuge model tests on piled raft foundation in sand subjected to lateral and moment loads. *Soils and Foundations*, *54*(2), 126–140. https://doi.org/10.1016/j.sandf.2014.02.005

Scarfone, R., Morigi, M., & Conti, R. (2020). Assessment of dynamic soil-structure interaction effects for tall buildings: A 3D numerical approach. *Soil Dynamics and Earthquake Engineering*, *128*, 105864. https://doi.org/10.1016/j.soildyn.2019.105864

Seed, H. B., & Idriss, I. M. (1970). *`Soil moduli and damping factors for dynamic response analyses', UCB/EERC-70/10, Earthquake Engineering Research Center, University of California, Berkeley*.

Seed, H. B., Wong, R. T., Idriss, I. M., & Tokimatsu, K. (1986). Moduli and damping factors for dynamic analyses of cohesionless soils. *Journal of Geotechnical Engineering*, *112*(11), 1016–1032. https://doi.org/10.1061/(ASCE)0733-9410(1988)114:8(958)

SeismoMatch. (2018). *A Computer Program for Spectrum Matching of Earthquake Records*. http://www.seismosoft.com.

Sextos, A. G., Manolis, G. D., Athanasiou, A., & Ioannidis, N. (2017). Seismically induced uplift effects on nuclear power plants. Part 1: Containment building rocking spectra. *Nuclear Engineering and Design*, *318*, 276–287. https://doi.org/10.1016/j.nucengdes.2016.12.035

Sharma, N., Dasgupta, K., & Dey, A. (2018). A state-of-the-art review on seismic SSI studies on building structures. In *Innovative Infrastructure Solutions* (Vol. 3, Issue 1).

https://doi.org/10.1007/s41062-017-0118-z

Shen, C., & Qian, D. (2019). Dynamic characteristics and seismic response of frame–core tube structures, considering soil–structure interactions. *Structural Design of Tall and Special Buildings*, *28*(3), 1–20. https://doi.org/10.1002/tal.1575

Smith, W. D. (1974). A nonreflecting plane boundary for wave propagation problems. *Journal of Computational Physics*, *15*(4), 492–503. https://doi.org/10.1016/0021-9991(74)90075-8

Sobhi, P., & Far, H. (2022). Impact of structural pounding on structural behaviour of adjacent buildings considering dynamic soil-structure interaction. In *Bulletin of Earthquake Engineering* (Vol. 20, Issue 7). Springer Netherlands. https://doi.org/10.1007/s10518-021-01195-w

Sotiriadis, D., Klimis, N., Margaris, B., & Sextos, A. (2019). Influence of structure – foundation – soil interaction on ground motions recorded within buildings. *Bulletin of Earthquake Engineering*, *17*(11), 5867–5895. https://doi.org/10.1007/s10518-019-00700-6

Sotiriadis, D., Klimis, N., Margaris, B., & Sextos, A. (2020). Analytical expressions relating free-field and foundation ground motions in buildings with basement, considering soil-structure interaction. *Engineering Structures*, *216*, 110757.

Steven L. Kramer. (1996). *Geotechnical earthquake engineering*. Prentice Hall Civil Engineering and Engineering Mechanics Series. University of Washington.

Stewart, J. P. (2000). Variation between foundation-level and free-field earthquake ground motions. *Earthquake Spectra*, *16*(2), 511–532.

Stewart, J. P., Fenves, G. L., & Seed, R. B. (1999). Seismic Soil-Structure Interaction in Buildings. I: Analytical Methods. *Journal of Geotechnical and Geoenvironmental Engineering*, *125*(1), 26–37. https://doi.org/10.1061/(asce)1090-0241(1999)125:1(26)

Stewart, J. P., & Tileylioglu, S. (2007). Input ground motions for tall buildings with subterranean levels. *Structural Design of Tall and Special Buildings*, *16*(5), 543–557. https://doi.org/10.1002/tal.429

Sun, J. I., Golesorkhi, R., & Seed, H. B. (1988). *`Dynamic moduli and damping ratios for cohesive soils', UCB/EERC-88/15, Earthquake Engineering Research Center, University of California, Berkeley.*

Tabatabaiefar, H. R., & Fatahi, B. (2014a). Idealisation of soil-structure system to determine inelastic seismic response of mid-rise building frames. *Soil Dynamics and Earthquake*

Engineering, *66*, 339–351. https://doi.org/10.1016/j.soildyn.2014.08.007

Tabatabaiefar, H. R., & Fatahi, B. (2014b). Idealisation of soil – structure system to determine inelastic seismic response of mid-rise building frames. *Soil Dynamics and Earthquake Engineering*, *66*, 339–351. https://doi.org/10.1016/j.soildyn.2014.08.007

Tabatabaiefar, H. R., Fatahi, B., Ghabraie, K., & Zhou, W. H. (2015). Evaluation of numerical procedures to determine seismic response of structures under influence of soil-structure interaction. *Structural Engineering and Mechanics*, *56*(1), 27–47. https://doi.org/10.12989/sem.2015.56.1.027

Tabatabaiefar, H. R., & Massumi, A. (2010). A simplified method to determine seismic responses of reinforced concrete moment resisting building frames under influence of soil-structure interaction. *Soil Dynamics and Earthquake Engineering*, *30*(11), 1259–1267. https://doi.org/10.1016/j.soildyn.2010.05.008

Tabatabaiefar, S., Fatahi, B., & Samali, B. (2014). Numerical and experimental investigations on seismic response of building frames under influence of soil-structure interaction. *Advances in Structural Engineering*, *17*(1), 109–130. https://doi.org/10.1260/1369-4332.17.1.109

Tadesse, Z. L., Krishna, H., & Venkata, P. (2022). Effect of subterranean levels on the foundation input motions for dynamic response analysis of building structure. *Asian Journal of Civil Engineering*, 1–16. https://doi.org/10.1007/s42107-022-00531-y

Tahghighi, H., & Mohammadi, A. (2020a). Numerical evaluation of soil–structure interaction effects on the seismic performance and vulnerability of reinforced concrete buildings. *International Journal of Geomechanics*, *20*(6), 04020072.

Tahghighi, H., & Mohammadi, A. (2020b). Numerical Evaluation of Soil–Structure Interaction Effects on the Seismic Performance and Vulnerability of Reinforced Concrete Buildings. *International Journal of Geomechanics*, *20*(6). https://doi.org/10.1061/(asce)gm.1943-5622.0001651

Tehranizadeh, M., & Barkhordari, M. S. (2018). Effect of Peripheral Wall Openings in Basement and Number of Basement Floors on the Base level of Braced Framed Tube System. *International Journal of Civil Engineering*, *16*(9), 1157–1173. https://doi.org/10.1007/s40999-017-0270-z

Tileylioglu, S., Stewart, J. P., & Nigbor, R. L. (2011). Dynamic Stiffness and Damping of a Shallow Foundation from Forced Vibration of a Field Test Structure. *Journal of Geotechnical*

and Geoenvironmental Engineering, *137*(4), 344–353. https://doi.org/10.1061/(asce)gt.1943-5606.0000430

Torabi, H., & Rayhani, M. T. (2014). Three dimensional Finite Element modeling of seismic soil-structure interaction in soft soil. *Computers and Geotechnics*, *60*, 9–19. https://doi.org/10.1016/j.compgeo.2014.03.014

Triantafyllidis, T. (1986). Dynamic stiffness of rigid rectangular foundations on the half-space. *Earthquake Engineering & Structural Dynamics*, *14*, 391–411. https://doi.org/10.1002/eqe.4290140307

Turan, A., Hinchberger, S. D., & El Naggar, H. (2009). Design and commissioning of a laminar soil container for use on small shaking tables. *Soil Dynamics and Earthquake Engineering*, *29*(2), 404–414. https://doi.org/10.1016/j.soildyn.2008.04.003

Turan, A., Hinchberger, S. D., & El Naggar, M. H. (2013). Seismic soil-structure interaction in buildings on stiff clay with embedded basement stories. *Canadian Geotechnical Journal*, *50*(8), 858–873. https://doi.org/10.1139/cgj-2011-0083

Varun, Assimaki, D., & Gazetas, G. (2009). A simplified model for lateral response of large diameter caisson foundations—Linear elastic formulation. *Soil Dynamics and Earthquake Engineering*, *29*, 268–291.

Vega, J., Aznárez, J. J., Santana, A., Alarcón, E., Padrón, L. A., Pérez, J. J., & Maeso, O. (2013). On soil-structure interaction in large non-slender. *Bull Earthquake Engineering*, *11*, 1403–1421. https://doi.org/10.1007/s10518-013-9433-8

Veletsos, A. S., & Meek, J. W. (1974). Dynamic behaviour of building-foundation systems. *Earthquake Engineering & Structural Dynamics*, *3*(2), 121–138. https://doi.org/10.1002/eqe.4290030203

Veletsos, A. S., & Parsad, A. M. (1988). *Seismic Interaction of Structures and Soils: Stochastic Approach, Technical Report NCEER-88-0021*.

Veletsos, A. S., & Wei, Y. T. (1971). Lateral and rocking vibration of footings. *Journal of the Soil Mechanics and Foundations Division*, *97*(9), 1227–1248.

Vesic, A. B. (1961). Bending of Beams Resting on Isotropic Elastic Solid. *Journal of Engineering Mechanics-Asce*, *87*, 35–54.

Visuvasam, J., & Chandrasekaran, S. S. (2019). Effect of soil–pile–structure interaction on seismic behaviour of RC building frames. *Innovative Infrastructure Solutions*, *4*(1).

https://doi.org/10.1007/s41062-019-0233-0

Vrettos, C. (1999). Vertical and rocking impedances for rigid rectangular foundations on soils with bounded non-homogeneity. *Earthquake Engineering and Structural Dynamics*, *28*(12), 1525–1540. https://doi.org/10.1002/(SICI)1096-9845(199912)28:12<1525::AID-EQE879>3.0.CO;2-S

Vucetic, M. (1994). Cyclic threshold shear strains in soils. *Journal of Geotechnical Engineering*, *120*(12), 2208–2228. https://doi.org/10.1016/0148-9062(95)92388-x

Vucetic, M., & Dobry, R. (1991). Effect of soil plasticity on cyclic response. *Journal of Geotechnical Engineering*, *117*(1), 89–107.

Wani, F. M., Vemuri, J., Rajaram, C., & R, D. V. B. (2022). Effect of soil structure interaction on the dynamic response of reinforced concrete structures. *Natural Hazards Research*, *2*(4), 304–315. https://doi.org/10.1016/j.nhres.2022.11.002

Wei, H., Zhang, Z., & Qin, X. (2017). Experimental study on damping characteristics of soil-structure interaction system based on shaking table test. *Soil Dynamics and Earthquake Engineering*, *98*, 183–190. https://doi.org/10.1016/j.soildyn.2017.04.002

Winkler E. (1867). Die Lehre von der Elasticitaet und Festigkeit. *Prag, Dominicus*.

Wolf, J. P. (1985). Dynamic soil-structure interaction. In *Dynamic soil-structure interaction.*

Wolf, J. P. (1986). A comparison of time-domain transmitting boundaries. *Earthquake Engineering & Structural Dynamics*, *14*(4), 655–673. https://doi.org/10.1002/eqe.4290140412

Wolf, J. P. (1994a). Foundation vibration analysis using simple physical models. In *Pearson Education*. https://doi.org/10.1016/b978-0-7506-6164-5.x5000-x

Wolf, J. P. (1994b). *Foundation Vibration Analysis Using Simple Physical Models*. Englewood Cliffs, NJ: Prentice-Hall.

X.M.Yang, Y.Chen, & B.P.Yang. (2008). Three-Dimension Dynamic Soil-Structure Interaction Analysis Using The Substructure Method In The Time Domain. *14th World Conference on Earthquake Engineering (14WCEE).*

Yamahara, H. (1970). Ground motions during earthquakes and the input loss of earthquake power to an excitation of buildings. In *Soils and Foundations* (Vol. 10, Issue 2).

Yeganeh, N., & Fatahi, B. (2019). Effects of choice of soil constitutive model on seismic performance of moment-resisting frames experiencing foundation rocking subjected to near-

field earthquakes. *Soil Dynamics and Earthquake Engineering*, *121*, 442–459. https://doi.org/10.1016/j.soildyn.2019.03.027

Zhang, J., Andrus, R. D., & Juang, C. H. (2005). Normalized Shear Modulus and Material Damping Ratio Relationships. *Journal of Geotechnical and Geoenvironmental Engineering*, *131*(4), 453–464. https://doi.org/10.1061/(asce)1090-0241(2005)131:4(453)

Zhang, X., & Far, H. (2022a). Effects of dynamic soil-structure interaction on seismic behaviour of high-rise buildings. *Bulletin of Earthquake Engineering*, *20*(7), 3443–3467. https://doi.org/10.1007/s10518-021-01176-z

Zhang, X., & Far, H. (2022b). Seismic behaviour of high-rise frame-core tube structures considering dynamic soil–structure interaction. In *Bulletin of Earthquake Engineering* (Vol. 20, Issue 10). Springer Netherlands. https://doi.org/10.1007/s10518-022-01398-9

Zienkiewicz, O. C., Emson, C., & Bettess, P. (1983). A novel boundary infinite element. *International Journal for Numerical Methods in Engineering*, *19*(3), 393–404. https://doi.org/10.1002/nme.1620190307